DESIGN EXPLORATION & ENHANCEMENTS FOR LOW COMPLEXITY MASSIVE MIMO DETECTORS WITH HIGH MODULATION ORDER

A Thesis

by

VISHNU PRANEETH REDDY POTHIREDDY

Submitted to the Office of Graduate and Professional Studies of
Texas A&M University
in partial fulfillment of the requirements for the degree of

MASTER OF SCIENCE

Chair of Committee,	Gwan Seong Choi
Committee Members,	Jiang Hu
	Duncan H. Walker
Head of Department,	Miroslav M. Begovic

May 2019

Major Subject: Computer Engineering

ABSTRACT

Global energy consumed by communication and information technologies is expected to increase rapidly due to continuous usage of wireless standards and the expansion for their requirements [1]. In the next generation wireless communications, Multi Input and Multi Output (MIMO) systems are most promising technology to achieve high spectral efficiencies, while going past various challenges like resource and energy constraints [2]. There exists many detection algorithms like Maximum Likelihood (ML), Zero Forcing (ZF), Minimum Mean Square Error (MMSE) which have low silicon complexity but consume significant power for high-end MIMO systems, due to their high computational complexity.

And then there are certain low power detection algorithms like real domain breadth first search K-best, with either conventional enumeration or Schnorr Euchner (SE) based enumeration. This improvement through either, comes with cost of comparatively high silicon complexity and sacrifices the performance in terms of detection bit error rate (BER). The complex domain equivalent may improve the BER performance but it's dedicated algorithm ensures even higher silicon complexity. Several modifications have been performed on original complex domain K-best algorithm to decrease its high silicon complexity, retaining the better performance of the system.

This work focuses on study and implementation of original real SE based K-best algorithm [3]. It also features my attempt to perform theoretical analysis of original complex domain detection algorithm, and to implement modified [4] and improved versions of complex domain to decrease its high silicon complexity, retaining BER performance. This work also focuses on exploration and implementation of past attempts on design modifications of complex domain algorithms and compare them across different attributes such as performance, computational and silicon complexity.

Few system level and algorithmic level enhancements have been proposed and implemented for low complexity detectors explored. Dynamic fixed point iterative version of original real domain detector [3] has been studied and implemented, along with possible enhancements for complex domain detector. Pipelined hardware architecture of real domain SE based K-best detector [5] has

also been studied as part of this work, with the intention of extending this to dynamic fixed point version and also complex domain detector.

DEDICATION

To my mother, my father, my grandmother, and my grandfather, who have loved, supported and encouraged me unconditionally.

ACKNOWLEDGMENTS

Though this work carries my name as sole author, this endeavour would have been surely impossible in such short period of time, without support of numerous altruistic people.

Foremost, I would like to express my profound gratitude to my advisor, Dr Gwan Seong Choi, for his support, motivation, perceptive teaching methods and most importantly, his valuable time. I also would like to sincerely thank my thesis committee members Dr. Jiang Hu and Dr. Duncan Hank Walker, for their insightful comments, valuable time and feedback. I would like to thank my colleague Pravir Singh Gupta for his patience, constant guidance, and Dr Ehsan Rohani for his technical suggestions, with regard to my thesis work, especially at the initial stages of my research, and also for providing career counsel. Last but not least, I am grateful to all my friends at Texas A&M University who played a crucial part in maintaining positive energy, that ultimately led to the completion of this effort.

CONTRIBUTORS AND FUNDING SOURCES

All research work conducted for this thesis and the generation of data was completed by the student independently. Existing algorithms used for design exploration and implementation, have been cited accordingly and all the data that may have been used for performance comparison with proposed algorithms, has been properly cited throughout this report.

NOMENCLATURE

ML	Maximum Likelihood
ZF	Zero Forcing
MMSE	Minimum Mean Square Error
MIMO	Multi Input and Multi Output
BER	Bit Error Rate
WLAN	Wireless Local Area Network
WiMAX	Worldwide interoperability for Microwave Access
QoS	Quality of Service
SNR	Signal to Noise Ratio
OFDM	Orthogonal Division Frequency Multiplexing
MU-MIMO	Multi User Multi Input Multi Output
QAM	Quadrature Amplitude Modulation
ASK	Amplitude Shift Keying
PSK	Phase Shift Keying
SISO	Single Input Single Output
LOS	Line of sight
SM-MIMO	Spatial Modulation Multi Input Multi Output
MU-MIMO	Multi User Multi Input Multi Output
LDPC	Low Density Parity Check
LLR	Log Likelihood Ratio
RVD	Real Value Decomposition
ECC	Error Correction Code

FEC	Forward Error Correction
RVD	Real Value Decomposition
PED	Partial Euclidean Distance
DFS	Depth First Search
SD	Sphere Decoding
BFS	Breadth First Search

TABLE OF CONTENTS

Page

LIST OF FIGURES

FIGURE Page

LIST OF TABLES

TABLE Page

1. INTRODUCTION

The demand for high spectral Wireless Communications have been increasing rapidly in many applications and also plays a crucial role in many technological advancements. The exploration of spatial dimension can increase the throughput of the wireless communication system and can meet the bandwidth requirements of modern day applications and customers. This technology termed as Multi Input Multi Output (MIMO) systems is the most promising technology to build next generation wireless systems because of their diversity gain and spatial multiplexing capabilities. The vast usage of various networking devices clearly defines the importance of such technologies and the need for their development and implementation in practical usages. Various emerging applications resulted in many wireless standard protocols and bandwidth specifications. However the increasing demand for certain bandwidth and high data rates may degrade the quality of data transmission. The available spectrum of bandwidth should be utilized efficiently which can be state of the art wireless communication algorithms and their power efficient VLSI implementations. [6]

1.1 MIMO Systems & Technology

Multi-path signal propagation by usage of more than single antenna at transmitting and receiving end of the wireless communication is referred to as Multi input Multi output systems. The channel throughput of over 480 Mbps used in IEEE 802.11n wireless LAN standard was achieved using MIMO technology. Due of their higher spectral efficiency, they can easily satisfy high throughput requirements compared to single antenna aided communication systems. MIMO systems exploit the usage of spatial dimension which helps in tackling resource constraint and impairment problems in wireless communications.

The spatial dimension along with time and frequency division multiplexing defines MIMO systems as most promising technology for various important applications like Worldwide Interoperability for Microwave Access (WiMAX) [7], Wireless Local Area Network (WLAN) [8]. The antennas at source and receiver ends can be used together to minimize BER or to increase data

bandwidth. Hence a Trade off between Quality of Service (QoS) and spectral efficiency can be achieved by varying the diversity gain and multiplexing gain, displayed by MIMO systems. The channel reliability can be increased by beam-forming and space time coding techniques. This is referred to as diversity gain and the corresponding diversity order is mathematically represented as slope of BER graphical representation of the channel reliability with respect to its Signal to Noise Ratio (SNR) value. Such high reliability of transmission can be achieved by transmitting redundant information across different propagation paths in the system. Thus channel interference and independent fading can be overcome with redundant information received at the other end, decreasing the co-channel interference value significantly.

The different propagation paths can also be used to transmit different sources of information thus increasing the bandwidth and degrees of freedom in the system. This is possible at cost of lower reliability and possibly high amount of bit errors across the transmission channel. The spatial multiplexing MIMO systems can be compared to Orthogonal Frequency Division Multiplexing (OFDM) systems where sub-channels of different adjacent frequencies transmit independent modulated data but with the advantage and possibility of creating various sub-channels within same bandwidth. As the name suggests, each transmitted signal is multiplexed onto different number of spatial channels, which is equal to number of receiver antennas. This possibility leads to Multi User MIMO (MU-MIMO), where different independent spatial information can be transmitted to multiple users at the receiver end.

Spatial multiplexing MIMO systems showcase their advantage in high data bandwidth with the cost of channel transmission reliability and special attention needs to be given to the design of antenna at receiver end to improve reliability of multiplexed transmission. Moreover designing energy efficient MIMO receiver antennas with high reliability is one of the most challenging tasks due to spatial interference in the channel and resulting complex implementation of signal detectors, to be integrated on each receiver antenna [1]. This has motivated me to explore various low complexity detection algorithms for spatially multiplexed MIMO systems and the possible enhancements that can be made to either, decrease silicon or computational complexity, or to decrease BER of

MIMO detectors. To define the importance of such low complexity detection algorithms and to display impact of enhancements made to them, I have decided to implement the low complexity detection algorithms and their enhancements made, on High M-QAM constellations and then advance our exploration onto massive MIMO systems.

1.2 Quadrature Amplitude Modulation

When two carriers with phase difference of 90 degrees are modulated, two dimensional bit to symbol mapping can be achieved due to combination of amplitude and phase variations. The amplitude variation of each symbol refers to distance of symbol from the center, and the phase variation contributes to angular direction of symbol. This results in Quadrature Amplitude Modulation (QAM), which is combination of Amplitude Shift Keying (ASK) and Phase Shift Keying (PSK). QAM modulation is widely applied in digital transmission of radio communications ranging from cellular technology to various wireless applications, due to its higher data bandwidth. Since it is derived from independent double side-band suppressed carries, the possible data bandwidth is twice the bandwidth of ordinary modulation techniques, when compared across same number of symbols.

For an M-Ary QAM modulation, each symbol is composed of $\log_2$(M) bits and the corresponding constellation diagram consists of $\sqrt{M}$ rows and $\sqrt{M}$ columns with total number of M symbols in constellation diagram. All symbols along same row have identical second half number of bits and all symbols along same column have identical first half number of bits. This observation gives rise to the concept of real domain and complex domain part of complex symbol representations in the constellation diagram.

Let us take an example of 64-QAM and try to understand its constellation diagram and its organization, from mathematical point of view. Figure 1.1 represents constellation diagram of 64-QAM which was directly generated from MATLAB.

A 64-QAM constellation diagram, as shown above, has 64 symbols in total, spread across 8 rows and 8 columns. Each constellation symbol has been constructed from 6 bits, before transmitting them across wireless medium. It can be deduced that all six symbols across same row have

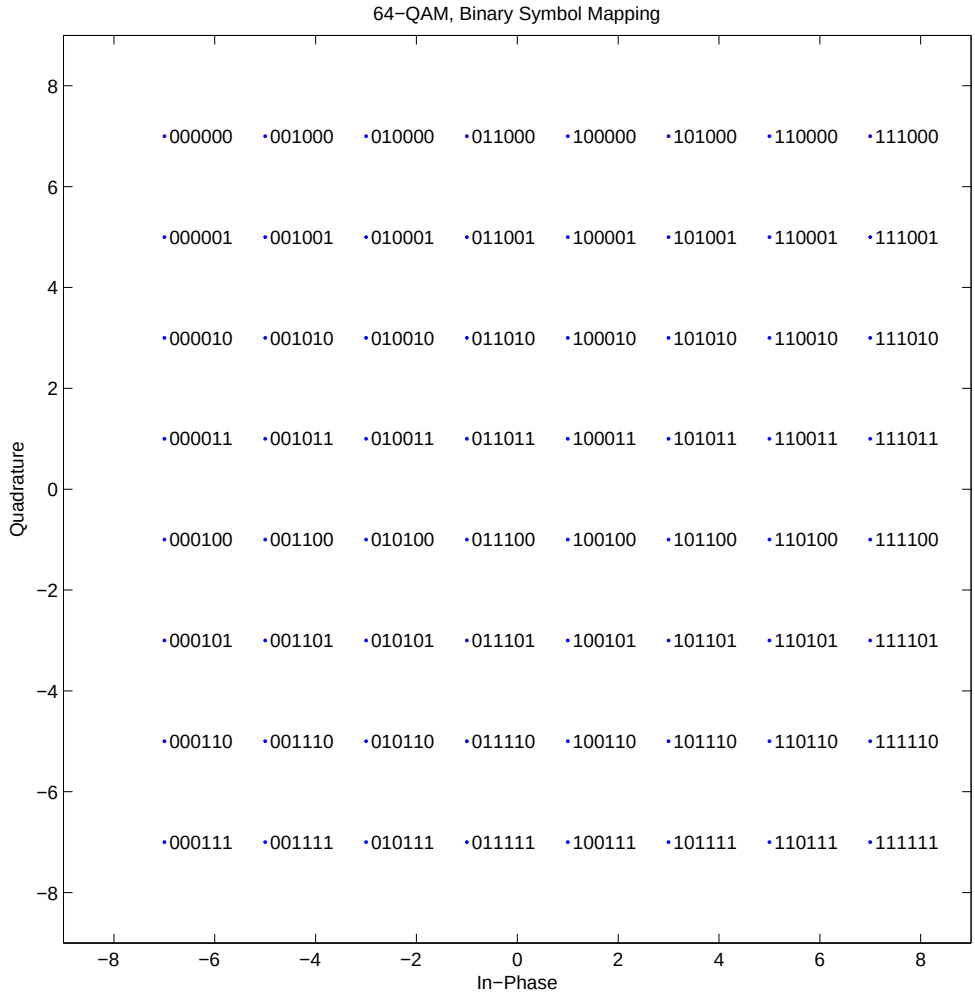

Figure 1.1: 64-QAM Constellation Diagram

identical second three bits, and different last three bits, resulting in real domain part of complex representation and all six symbols across same column have identical first three bits and different last three bits resulting in complex domain part of complex representation. Hence one complex symbol can be split into two real domain symbols for computational processing for detection. This representation concept has been used to implement two different low complex detection algorithms as we see later in this research work.

As we increase the modulation order, we can achieve higher levels of spectral efficiency and

can transmit data at faster rates. More information can be transmitted across the channel, with same amount of power consumption as one symbol of high modulation order consists of more number of bits. But as we increase modulation order, their symbols become more susceptible towards noise and channel interference. Currently, due to lack of cutting-edge low power MIMO detectors, wireless communication systems have been using dynamic modulation orders to transmit data through wireless medium. The modulation order is adapted based on channel characteristics observed at receiver antennas. Lower modulation techniques can be used to perform reliable transmission of data with lower bandwidth, and higher modulation techniques can be used to increase data transmission rates, sacrificing performance, thus ultimately leading to redundant transmission of data.

Therefore, in this work, I have focused on high order constellations like 64-QAM, 256-QAM and 1024-QAM. The susceptible behaviour of symbols at high modulation order, makes it harder to design low complexity MIMO detector, that consumes low power and can concurrently achieve BER performance comparable to Maximum Likelihood (ML) detection algorithm. I have focused on exploring such existing algorithms which have previously displayed decent BER performance on high modulation orders, and I have made my attempt, to make enhancements to existing algorithms where ever it seemed necessary and possible, aiming to either improve BER performance or to further decrease power consumption.

1.3 Shannon Hartley Theorem

Shannon Hartley defines the theoretical limit for information transmission rate through the channel. With specified noise interference and bandwidth, it gives an upper limit for amount of error free digital information that can be transmitted over a communication channel [9]. The Shannon Hartley equation for channel capacity of Single Input Single Output (SISO) system is defined in (1.1) below.

$$C = B \times log_2(1 + SNR) \tag{1.1}$$

where C is Channel Capacity, B is Channel Bandwidth, SNR is Signal Noise Ratio.

The channel capacity can be increasing by increasing channel bandwidth. But this also increases vulnerability of transmission due to faster modulation carrier and multiple path fading, as expected. But introducing multiple signal paths by expanding along spatial dimension, condition of transmission channel can be accurately interpreted at receiver antennas. Usage of multiple signal paths increases reliability of transmission, along with information rate. Assuming we have N number of spatial streams corresponding to $N \times N$ MIMO system, the improved Shannon Hartley equation can be represented as in (1.2) below, approximately increasing the maximum channel capacity by N times, making MIMO systems promising technology for high throughput communications.

$$C = N \times B \times log_2(1 + SNR) \tag{1.2}$$

where N is spatial order of MIMO system, C is Channel Capacity, B is Channel Bandwidth, SNR is Signal Noise Ratio.

1.4 Massive MIMO Systems

The capability of spatial multiplexing MIMO Systems to serve multiple subscribers or multiple devices can be scalable with respect to number of antennas used on transmitting base stations and also on the receiving end. In simple words, any MIMO system with high antenna count on either transmitting end can be referred to as massive MIMO system. To successfully handle the multi fold data transmission increase in upcoming communication era, massive MIMO systems are one of the most promising technology, especially in close range or Line of Sight (LOS) wireless communication systems. They are most effective in compact areas where performance reliability and faster data transmission rates are mandatory requirements of consumers. Massive MIMO systems provide higher spectral efficiency and reliability due to large number of signal paths, compared to conventional MIMO systems. They also provide reduction in transmission latency and comprehensive detection power when perceived from standpoint of power consumed per frame. Such potential of massive MIMO systems, when integrated with ability of high quadrature amplitude

modulation orders substantially increases spectral efficiency and transmission data rates of future fifth generation wireless communication systems (5G).

However to make use of these attractive advantages, provided by massive MIMO systems and high QAM orders, there are more challenges to overcome, compared to conventional MIMO systems, especially in low SNR channel regions. Most significant are increased spatial interference, computational complexity, silicon complexity and performance of MIMO detector. Large scale Spatial Modulation Multi User MIMO (SM-MIMO) is another sought after technology, capable of providing similar performance requirements, but has its own drawbacks [10]. As part of this thesis, I have focused on exploring various low power detection algorithms, which can provide acceptable level of performance, on massive MIMO systems. Such algorithms were analysed, implemented and possible algorithm enhancements have been proposed theoretically and also have been implemented during this research. Hardware architecture design enhancements of such detection algorithms have also been theoretically reported.

1.5 Low Density Parity Check Decoding Systems & their Importance

The received signals at MIMO detector are transformed into symbols which are combination of bits and corresponding Likelihood Ratio (LLR) values. The LLR values represent the likeliness of particular bit, to have been transmitted as a '1' or '0', at base end transmitting antennas. But the detection by itself doesn't provide lowest bit error rate performance possible, and thus need powerful decoding mechanism like low density parity check decoder, which can flip incorrectly detected bits and thus significantly decrease bit error rate, sometimes even to its one tenth order.

All bits of each LDPC codeword that was transmitted may have been flipped due to noise interference and variable channel conditions. There are various well-known algorithms that LDPC codes can be decoded. Belief propagation, message passing and the iterative algorithms are few to mention. Soft LDPC decoding system iteratively check the bit probabilities which were referred to as LLR values earlier. An LDPC system is organized as variable nodes which contain message information bits and check nodes which update bit probabilities based on each message information bit received from variable nodes, which are connected to it. If a variable node is connected to check

node, it is referred to as '1' in parity check matrix. Each parity check matrix represents spatial bipartite graph with connections between variable nodes and check nodes. They are referred to as 'low density' due to very low number of connections between them thus reducing computational power consumption by its nature. Along with simple computational operations like update, LDPC decoder also provide an advantage of parallelism leading to various types of LDPC decoders in terms of their functionality, performance, speed depending on user requirements.

Let us assume check nodes, C_i, $i \in (1, 2, ..., r)$ and variable nodes V_j, $j \in (1, 2, ..., n)$ and also a connection between variable node V_k and check node C_q. For this connection, the check node C_q is updated by using all the message bit information from variable nodes connected to it, except message bit from variable node V_k. This update is performed based on equation used to construct LDPC codewords at the transmission such as even number of '1' bits in every codeword etc. The bit probabilities for '1' and '0' are updated accordingly and transmitted to variable node V_k for its update, by using all bit probabilities of check nodes connected to it, except LLR values received from check node C_q. At same time, all the high bit probability message bits on variable nodes are gathered to form codeword and to perform parity check, for its validation. The iteration between variable nodes and check nodes is continued as explained above, until parity check equation is satisfied.

Both MIMO detection and LDPC decoding systems together achieve significantly better BER performance compared to their individual capabilities. Belief propagation with double bipartite or single tripartite graphs can be used to simultaneously process MIMO detection and iterative soft LDPC decoding as proposed in [11]. But complexity of using concurrent bipartite or tripartite graphs may increase linearly with massive MIMO systems. In this thesis work, I have generated results with BER performance, by independently implementing massive MIMO detector as a standalone. For future work, we plan to integrate the performance achieved by this independent MIMO detector, with fully parallel LDPC decoding system to achieve even better BER performance.

1.6 Thesis Outline

The structure of this thesis is organized as follows: Chapter I gives an brief introduction about MIMO technology and its significance. It conveys my motivation for this research work. Chapter II describes about configuration and simulation framework of system models used to derive experimental results. It also gives a brief touch on existing detection algorithms, to make this work, self-explanatory. Chapter III is emphasized about design exploration of various low complex detection algorithms, compares implementation results for fixed point iteration and floating point versions. It also defines an outline for challenges and possible enhancements for explored algorithms. Chapter IV is focused on potential enhancements that can lead to lower silicon complexity or power consumption of massive MIMO detection algorithms. It juxtaposes implementation results of existing algorithms with their enhanced versions, to acknowledge better performance in the latter. Chapter V eventually gives summary of this thesis work and presents possible future work that can be developed on top of this research.

2. EXPERIMENTAL FRAMEWORK FOR DESIGN EXPLORATION AND ENHANCEMENT

This chapter has been divided into five major sub-chapters. The first sub-chapter describes about basic MIMO system model and other attributes involved in defining model such as noise interference, transmitted and received vectors, channel matrix relating to observed wireless channel conditions. The second sub-chapter showcases the configurations and dimensions of system models that have been used for this research work. The third part describes about the simulation tools and framework of MIMO libraries that have been used to generate base stations for transmission, and gives details of modulation orders, dimensions of MIMO systems and coding type. The fourth sub-chapter gives a very brief implementation outline and describes plan of action that was used for Chapter III and Chapter IV. The final sub-chapter introduces existing and very well-known detection algorithms for making this work, self explanatory.

2.1 Basic MIMO System Model

An equivalent baseband complex MIMO system, where number of transmit antennas is denoted by N_T and number of receiving antennas is denoted by N_R ($\geq N_T$), can be modelled as shown in (2.1).

$$\tilde{Y} = \tilde{H}\tilde{x} + \tilde{n} \tag{2.1}$$

where $\tilde{Y} \in C^{N_R \times 1}$ represents complex received signal vector, $\tilde{H} \in C^{N_R \times N_T}$ is randomly generated complex channel matrix imitating Rayleigh fading channel model, $\tilde{x} \in C^{N_T \times 1}$ represents complex transmitted vector with symbol modulation order and $\tilde{n} \in C^{N_R \times 1}$ represents randomly generated additive white Gaussian noise complex vector with zero mean and co-variance of $\sigma^2 \times I_{N_R}$. The Signal to Noise ratio (SNR) is represented by σ, which is mathematically represented as shown in (2.2)

$$SNR = 1/\sigma^2 \tag{2.2}$$

At each base station antenna, bits to be transmitted are mapped onto 'Q' possible complex symbols, taken from complex constellation ($S_k \in \Omega$) derived with respect to quadrature amplitude modulation, where each complex symbols or constellation point is comprised of $log_2(Q)$ distinct transmission bits. Each frame can be referred to as N_T such constellation points which are transmitted from N_T base station antennas. Assuming the basic system model described above, at any given time t, N_T complex symbols each with bit sequence of length $log_2(Q)$ are concurrently transmitted into wireless channel. Hence transmission rate of defined MIMO system in spatial multiplexing mode is given by $N_T \times log_2(Q)$ distinct bits per channel use or per frame.

As discussed above, each complex constellation symbol from QAM order 'Q' can be represented as shown in (2.3).

$$S_k = S_k^{\,r} + S_k^{\,i} \tag{2.3}$$

where $S_k^{\,r},\ S_k^{\,i} \in (-\sqrt{Q}+1), (-\sqrt{Q}), ..., -1, +1, ..., (\sqrt{Q}-2), (\sqrt{Q}-1)$. There are $\sqrt{Q}$ possible real valued entries for building in-phase and quadrature parts of constellation diagram. Also if we refer to each constellation point from 1.1, the first half bits can be connected to real part of constellation symbol ($S_k^{\,r}$) and second half can be attributed to complex part ($S_k^{\,i}$). Hence each complex constellation point can be split into two real domain constellation points for detection processing, to reduce constellation search space Ω for detecting symbol, closer to received vector. The following table 2.1 provides concise conversion of complex domain MIMO equation to real domain equivalent.

And the corresponding real domain basic MIMO equation can be represented as shown in (2.4) below.

$$Y = Hx + n \tag{2.4}$$

Table 2.1: Conversion of Complex domain MIMO system to Real domain MIMO system

Attribute	**Complex Domain**	**Real Domain Equivalent**
Received Vector	$\mathbb{C}^{N_R \times 1}$	$\mathbb{R}^{2N_R \times 1}$
Channel Matrix	$\mathbb{C}^{N_R \times N_T}$	$\mathbb{R}^{2N_R \times 2N_T}$
Transmitted Vector	$\mathbb{C}^{N_T \times 1}$	$\mathbb{R}^{2N_T \times 1}$
Noise	$\mathbb{C}^{N_R \times 1}$	$\mathbb{R}^{2N_R \times 1}$
Constellation	Ω	ω
Possible Entries	Q	$\sqrt{Q}$
Symbol bit length	$log_2(Q)$	$(1/2) \times log_2(Q)$

where $Y \in C^{2N_R \times 1}$ represents real domain received signal vector, $H \in C^{2N_R \times 2N_T}$ is real domain channel matrix, $x \in C^{2N_T \times 1}$ represents real domain transmitted vector with symbol modulation order 'Q' and $n \in C^{2N_R \times 1}$ represents real domain noise equivalent. This implies that detecting $2 \times N_T$ real domain symbols from $C^{2N_R \times 1}$ received vector is equivalent to detecting N_T complex symbols from $C^{N_R \times 1}$ complex vector. This can also be perceived from (2.5). It is assumed that MIMO detector is provided accurate estimate of channel condition matrix $\tilde{H}$ which can be achieved through training of pilot symbols.

$$|\omega|^{\,2 \times N_T} = |\Omega|^{\,N_T} \tag{2.5}$$

Let us assume this basic MIMO system model to derive main objective of any MIMO detection algorithm. The original MIMO problem is to derive best possible estimate of transmitted complex symbol vector $\tilde{z}$, from complex vector received from channel $\tilde{Y}$, after transmitting through its noise interference by minimizing euclidean noise equivalent. This can be defined as shown in 2.6

$$\hat{\tilde{z}} = \underset{\tilde{s} \in \Omega^{\,N_T}}{\operatorname{argmin}} \; || \, \tilde{Y} - \tilde{H} \, \tilde{s} \, ||^{\,2} \tag{2.6}$$

Typical MIMO detector checks every constellation symbol to find best estimate for corresponding transmitted symbol, minimizing the euclidean distance as shown in (2.6). The correctness of estimate depends on various characteristics like detection algorithm being used, dimensions of MIMO systems, modulation order, channel conditions and noise interference in wireless medium.

The complex MIMO detection problem can be transformed to real domain MIMO detection problem using real value decomposition (RVD) as described in (2.1). Hence real domain equivalent can be represented as shown in (2.7) below.

$$\hat{z} = \underset{s^r \in \omega^{2N_T}}{\operatorname{argmin}} \; || \, Y - H \, s^r \, ||^2 \tag{2.7}$$

Hence it can be deduced that $N_T \times N_R$ complex MIMO problem can be solved as $2N_T \times 2N_R$ real domain MIMO problem. Once all $2N_T$ levels of detection in real domain, the symbols are de-mapped back into their bit sequence representation. The Log Likelihood ratio values of each of these bits is calculated and they are dispatched to LDPC decoding system for further processing, to improve bit error rate. Before reaching MIMO detector, the received vector has to go through pre-processing, which includes channel estimator to extract channel matrix from previously known transmitted pilot symbols, representing wireless medium conditions and then QR decomposition and Lattice Reduction (LR) for better detection performance. Lattice Reduction (LR) increases orthogonality of channel matrix and its new basis vectors are less correlated with better properties for symbol estimation and detection [12]. In this research work, MIMO detector is assumed to have knowledge of channel matrix, since this work has been focused on detection algorithms and their enhancements.

2.1.1 QR Decomposition

The CORDIC algorithm using Given's rotation [13] has been used to perform QR decomposition on channel matrix. The channel matrix $\tilde{H} \in C^{N_R \times N_T}$ is transformed into unitary matrix $\tilde{Q} \in C^{N_R \times N_T}$ and upper triangular matrix $\tilde{R} \in C^{N_R \times N_T}$, using equation shown in (2.8) below. Since Q is an unitary matrix, $\tilde{Q}^{\,H}$ = $\tilde{Q}^{\,-1}$, it's conjugate transpose is equal to matrix inverse.

$$H = Q \times R \tag{2.8}$$

The basic MIMO equation defined in (2.1) is multiplied with $Q^{\,H}$ to perform nullify operation. This updates basic MIMO equation as shown in (2.9, 2.10) for complex domain and (2.11, 2.12).

$$\tilde{Y}\tilde{Q}^{H} = (\tilde{H}\tilde{x} + \tilde{n})\ \tilde{Q}^{H} \tag{2.9}$$

$$\bar{Y} = \tilde{Y}\tilde{Q}^{H} = \tilde{R}\tilde{x} + \bar{n} \tag{2.10}$$

$$YQ^{H} = (Hx + n)\ Q^{H} \tag{2.11}$$

$$\check{Y} = YQ^{H} = Rx + \check{n} \tag{2.12}$$

where $\tilde{R}$ is an upper triangular matrix derived from QR decomposition of channel matrix and $\bar{n}$ = $\tilde{n}\tilde{Q}^{H}$. The resultant noise vector $\bar{n}$ retains the properties of $\tilde{n}$, which is white Gaussian noise. Hence the MIMO problem equation, defined in 2.6 can re-defined as shown in (2.13).

$$\hat{\tilde{z}} = \underset{\tilde{s} \in \Omega^{N_T}}{\operatorname{argmin}} \ || \bar{Y} - \tilde{R}\,\tilde{s} \,||^{2} \tag{2.13}$$

and the corresponding real domain equivalent of MIMO problem, defined in 2.7 can re-defined as shown in (2.14)

$$\check{z} = \underset{s^{r} \in \omega^{2N_T}}{\operatorname{argmin}} \ || \check{Y} - R\,s^{r} \,||^{2} \tag{2.14}$$

This transformation allows us to solve complex MIMO problem, one antenna level at a time, due to nature of upper triangular channel matrix, formed from QR decomposition.

2.2 System Model Experimental Configurations

This section describes all the experimental configurations and antenna dimensions of MIMO system model, defined in (2.4), that have been used to evaluate low complexity algorithms that were explored and upon which enhancements were made. The configurations of all models used, for generating implementation results, are displayed in Table 2.2 below.

Table 2.2: System Model Experimental Configuration Table

System Models	Antenna Configurations Used $(N_{\mathrm{T}} \times N_{\mathrm{R}})$	Transmission Order of 'Q' QAM order	K
Configuration 1	$(8 \times 8), (25 \times 25)$, $(40 \times 40), (50 \times 50)$, $(60 \times 60), (80 \times 80)$, (100×100) and (120×120) complex MIMO systems	64-QAM 256-QAM 1024-QAM	5
Configuration 2	(8×8) Conventional MIMO System, for different K-Best possible estimations	64-QAM 256-QAM 1024-QAM	5,10,15 20,100
Configuration 3	(100×100) Massive MIMO System, for different K-Best possible estimations	64-QAM 256-QAM 1024-QAM	5,10 15,20
Configuration 4	(8×8) Conventional MIMO System	4-QAM, 16-QAM 64-QAM, 256-QAM 1024-QAM, 4096-QAM	5
Configuration 5	(100×100) Massive MIMO System	4-QAM, 16-QAM 64-QAM, 256-QAM 1024-QAM, 4096-QAM	5

Where 'Q' is constellation order, N_T represents number of transmit antennas at base station, 'K' represent number of K-Best estimates at each antenna level

The system models defined as per first configuration in Table 2.2 were used to evaluate detection algorithms behaviour with respect to antenna dimensions of MIMO system. I have implemented real domain K-Best, complex domain K-Best, enhanced complex domain K-Best MIMO detectors to observe their performance as we advance from conventional MIMO systems to massive MIMO systems with higher antenna dimensions. The second configuration was used to evaluate performance transition of K-Best possible estimates in conventional MIMO systems, as we increase number of estimates, allowed per antenna level. The third configuration was used to perform similar evaluations, but on massive MIMO systems. I have used high modulation order values **Q = 64, 256, 1024** in all configurations. Using high modulation order constellations further increases spectral efficiency and comprehensive throughput of system as a whole, with reduced power consumption. Massive MIMO systems with high modulation orders as described in first configuration also decreases overall communication latency by transmitting same amount of information, with less number of frames than conventional MIMO systems.

However powerful MIMO detection algorithms and hence, extensive computational power are essential to derive accurate estimation of symbols, in massive MIMO systems with high modulation order. This accounts for exponential increase in energy consumption at receiver antenna, causing it one of the significant factor, while designing massive MIMO detectors. As part of this thesis work, detection algorithms which are capable of achieving good trade-off between spectral efficiency and energy consumption, depending on application requirements for bit error rate or communication latency, have been explored and their possible enhancements were implemented.

2.3 Simulation Framework & Tools

I have used features of MATLAB MIMO toolbox to set up N_T base antennas to transmit complex modulation symbols, and to design MIMO multipath fading channel. This set up imitates Rayleigh fading channel, filters complex baseband input frames through it and generates complex received vector. These were used to evaluate performance of detections algorithms explored and to present bit error rate implementation results in this thesis work, for both floating point and fixed point iterations. As mentioned earlier, the MIMO detectors are expected to have knowledge of

channel conditions and channel estimation matrix $\tilde{H}$. This simulation framework is valid in high noise interference and obstacle rich scattering environments.

The implementation results for all configurations described in Table 2.2 are presented in this thesis work, using simulation framework elucidated before. I have presented results for high modulation orders **Q = 64, 256, 1024** for significant reasons explained below. Due to high power requirements and design challenges, majority of to-date literature results reported on performance of low power K-Best detection algorithms explored in this work, were limited to lower modulation orders **Q = 4, 16, 64**. High QAM orders, especially **Q = 64, 256** are standardized constellations for various IEEE global standards.

2.4 Implementation Outline

This is summary of implementation outline that I followed throughout the stretch of my thesis work. Initially I have evaluated floating point versions of existing low power MIMO detection algorithms - Real domain Schnorr Euchner (SE) based K-Best MIMO detector and Complex domain SE based K-Best MIMO detector, which can provide extremely low computational complexity. I have implemented fixed point iterative versions of those, by calculating minimum number of fractional bits for each variable used for simulations. I have evaluated performance of above detectors on massive MIMO systems with high modulation order, thus fortifying their reliability and compatibility towards such system configurations. I have performed these simulations for $N \times N$ MIMO system, **N = 8, 25, 40, 50, 60, 80, 100, 120** with modulation orders as per latest 3GPP standards, defined for 5G communication systems.

Later, I have implemented possible enhancements for Complex domain K-Best detector, which I have elucidated in Chapter IV, in floating point and fixed point iterative versions. I have also implemented fractional bit width varying fixed point arithmetic Real domain K-Best detector in MATLAB, which can be integrated with clock gating power optimization technique to further reduce power consumption at higher antenna levels of massive MIMO systems.

2.5 Traditional MIMO Detection Algorithms

As discussed in 2.6, main objective of any MIMO detector is to extract best estimate of transmitted complex symbol vector $\tilde{z}$, from received complex vector $\tilde{Y}$ after transmitting through channel conditions and noise interference, defined by $\tilde{H}$ and $\tilde{n}$ respectively. MIMO detectors are fundamentally categorized into hard and soft decision MIMO detectors. Soft detectors reach at their final decision to extract best possible estimate, after exchanging information with decoding systems. They are used in error correction coded MIMO detectors where detector has to exchange soft information iteratively with decoding system like Fully parallel LDPC decoder. The Log Likelihood ratio values of bits, de-mapped from detected symbols are used as basis for soft information. Hard decision detectors are mainly used for uncoded or coded communication systems, where final decision is reached without iterative exchange of information.

Since LDPC codes or other potential error correction codes (ECC) is standardized usage for any modern wireless communication systems, soft decision MIMO detectors have most practical applications with forward error correction (FEC) capability and provide better performance for high end MIMO system models.

Based on performance, MIMO detectors are fundamentally categorized into optimal, sub-optimal and near-optimal algorithms [3]. And each of these algorithms bring their inherent trade-off between performance, computational complexity, silicon complexity and power requirements. Exhaustive search Maximum Likelihood detector is well-known algorithm for achieving optimal performance but displays exponential increase in complexity with number of transmit antennas N_T and modulation order 'Q' and thus an incorrect option for practical applications. Various sub-optimal and near-optimal algorithms with low power requirements and complexity are being developed or improved to achieve enough bit error rate performance, required for practical applications.

Sub-optimal detectors are further categorized into linear and non-linear detectors, based on presence of additional non-linear interference cancellation logic embedded into them. Various sub-optimal linear detectors like Zero Forcing (ZF) and Minimum Mean Square Estimation (MMSE)

algorithms significantly decrease complexity problem associated with ML detector, with price of significant drop in bit error rate performance. Non-linear detectors also fail to improve performance noticeably.

Near-optimal detectors performs better than sub-optimal linear or non-linear detectors with practical computational complexity. However this trade-off mainly depends on algorithm used for their exhaustive search. The main focus of this thesis work, the Real domain SE based K-Best and Complex domain SE based K-Best algorithm along with their enhancements, fall into category of breadth first search detection algorithms with near-optimal performance fixed throughput and are independent of channel SNR. Sphere decoding is well-known example of depth first search detection, which has capability to achieve ML performance, if it is executed without termination. However, since this is not practically applicable, they are classified for near-optimal performance and their execution time is dependent on channel conditions, noise interference and resultant SNR of wireless medium. For rest of this chapter, I have briefly elucidated sub-optimal linear and non-linear, and ML detectors, for making this thesis work, self-explanatory.

2.5.1 Maximum Likelihood Detection

The MIMO problem defined in (2.13) describes that fundamental solution to find symbol with minimum argument value $|| \bar{Y} - \tilde{R}\,\tilde{s} \,||^{\,2}$, is to traverse through all possible constellation symbols Ω for modulation order 'Q', used for transmitting them. Maximum Likelihood detection algorithm exactly shadows that logic and thus resulting in optimal bit error rate performance. At each antenna level, ML detector searches all possible constellation points (|Ω| = 'Q'), and chooses closest possible solution to transmitted complex symbols [2]. For $N_T \times N_R$ MIMO system, considering possible symbols at all antenna levels, total number of computations for ML detector is $Q^{\,N_T}$, where N_T is number of transmit antenna levels and 'Q' is modulation order. In real domain, number of computations for ML detector is $Q^{\,2N_T}$, since there are twice as many antenna levels to estimate, virtually.

Hence though it provides optimal bit error rate performance, the complexity of ML detector exponentially increases with number of transmit antennas and constellation order. ML detector

has high power requirements, especially for massive MIMO systems with high modulation order, and thus not considered a practical solution to (2.13). However, the optimal performance defined by ML detection simulations is considered as reference to other low power MIMO detectors, to categorize them as sub-optimal and near-optimal based on their bit error rate performances.

2.5.2 Linear MIMO Detectors

Zero Forcing (ZF) and Minimum Mean Square Error (MMSE) detection algorithms are well-known detection models for sub-optimal linear MIMO detectors. Their linear complexity provides linear estimation of transmitted symbols based on (2.13) by cancelling noise interference and effect induced by transmission medium [14]. All linear MIMO detectors aim at building channel reversal matrix '$\tilde{L}$' based on their respective least square version. This is later used to achieve linear estimation of transmitted symbol vector '$\tilde{x}$' by multiplying received complex vector '$\tilde{Y}$' with channel reversal matrix, as shown in (2.15) below.

$$\bar{z} = \Gamma(\tilde{L} \times \tilde{Y}) \tag{2.15}$$

where $\bar{z}$ is linear estimate of transmitted complex vector $\tilde{x}$ as defined in (2.1). Since resultant output vector may not contain values restricting to constellation points $|\Omega|$, additional slicing operator Γ should be used to extract meaningful estimate, from resultant vector. The slicing operator Γ maps each resultant value to nearest constellation symbol. The linear detector solving equation as defined in (2.15) aims at processing all antenna level concurrently, decreasing comprehensive computational complexity and also detection performance, especially for symmetric MIMO systems ($N_T = N_R$). In the next couple of sub-sections, I have briefly introduced ZF and MMSE detectors for making this thesis work, self-explanatory.

2.5.2.1 Zero Forcing Detection

Zero Forcing detector uses Moore-Penrose inverse [15] of channel response matrix to determine channel reversal matrix ($\tilde{L}$) as described previously, using least squares solution. ZF detector exhibits extremely poor performance for asymmetric MIMO systems with low SNR regions. How-

ever, it filters out complete interference in high SNR regions where $N_T \geq N_R$, due to its extremely low computational complexity. The channel response matrix ($\tilde{H} \in C^{N_T \times N_R}$), with possibility of being an asymmetric matrix, is multiplied with its conjugate transpose ($\tilde{H}^*$), to transform it to invertible symmetric matrix. Later $\tilde{H}\tilde{H}^*$ is multiplied with its inverse to form Moore-Penrose inverse of channel response matrix $\tilde{H}$. This computation extracts ZF estimate for transmitted symbol vector as shown in (2.16, 2.17) below.

$$\tilde{H}^* \ \tilde{Y} = \tilde{H}^*(\tilde{H}\tilde{x} + \tilde{n}) = \breve{H}\tilde{x} + \breve{n} \tag{2.16}$$

$$\bar{z}_{ZF} = \tilde{H}^* \ \tilde{Y}\breve{H}^{-1} = \tilde{x} + \tilde{n}_{ZF} \tag{2.17}$$

where $\tilde{n}_{ZF}$ represents ZF estimation error with error co-variance matrix $\boldsymbol{\sigma^2(\tilde{H}^* \ \tilde{H})^{-1}}$. It can de deduced that when $\tilde{H}$ is close to being singular, ZF detector showcases poor performance due to high noise amplification as per error co-variance defined above. Thus ZF detector is attractive model for practice in high SNR regions where noise doesn't effect transmitted symbols significantly.

2.5.2.2 Minimum Mean Square Estimation Detectors

ZF performs significantly poor in noise amplification conditions. The ZF construction of channel reversal matrix $\tilde{L}$ doesn't consider noise parameter, making it susceptible. As name suggests, the Minimum Mean Square Error estimation is calculated by taking mean square between transmitted complex symbols and output of MMSE detector $\bar{z}$. The channel reversal matrix for MMSE detector is similar to that of ZF detector, except that it also includes noise parameters making it prone to noise amplification. It can be derived using orthogonal principle, and final result of channel reversal matrix is defined in (2.18) below.

$$\tilde{L} = (\tilde{H}^* \ \tilde{H} + \sigma^2\mathcal{I})^{-1}\tilde{H}^* \tag{2.18}$$

where $\mathcal{I}$ is representation of identity matrix with dimension $N_T \times N_T$, for complex MIMO detectors. This channel reversal matrix, which represents trade-off between channel and noise interference, is multiplied with received complex vector $\tilde{Y}$ to get an MMSE estimate $\bar{z}_{ZF}$ of transmitted vector $\tilde{x}$, as defined in (2.19) below.

$$\bar{z}_{MMSE} = \tilde{L}\tilde{Y} = \tilde{Y}(\tilde{H}^* \ \tilde{H} + \sigma^2\mathcal{I})^{-1}\tilde{H}^* \tag{2.19}$$

The performance of MMSE detector is still considered as sub-optimal, even when their estimate is processed iteratively to arrive at a better estimate. Hence it can be deduced that they are not practically capable for usage in low SNR regions, irrespective of their lower computational complexity, due to their significant increment in bit error rate.

2.5.3 Non-Linear Detectors

Linear detectors solves for symbols from all antenna levels concurrently where as non-linear detectors estimate symbols going from easiest possible estimate and using that knowledge to estimate later signals at other antenna levels. Successive interference cancellation (SIC) and Bell-labs layered space time decoder (BLAST) are two well-known detection models for non-linear detectors, with sub-optimal performance.

2.5.3.1 Successive Interference Cancellation

As the name suggests, given nature of non-linear detectors, easier symbols are estimated initially and their interference contribution is removed from received vector, before moving to estimate symbol for next antenna level. This cancellation provides additional diversity at higher iterations, increasing by '1' for each iteration. After successively cancelling the interference caused by previous symbols, channel reversal matrix and slicing function Γ are used to provide best possible estimate for current level, similar to linear MIMO detectors.

However symbol ordering of cancellation is significant in determining their bit error rate performance. If the contribution of symbol with highest interference is processed and cancelled first, then remaining symbols are estimated with better bit error rate. Thus interference cancellation

order and its resultant error accumulation at each antenna level definitely influences estimation of following symbols.

2.5.3.2 Bell-Labs Layered Space Time

BLAST detector is based on successive interference cancellation algorithm, by dynamically cancelling interference at each antenna level under processing. This iterative algorithm assumes that interference from all symbols, except the symbol under estimation, must be nullified, by multiplying received vector with nullifying vector. Hence this detection model is combination of SIC and ZF algorithms, by locally generating linear nullifying vector by using Zero Forcing or Minimum Mean Square Estimation detection models. Similar to SIC, detection performance is significantly dependent on symbol ordering for processing and their interference cancellation, with quadratic complexity with respect to number to transmit antennas N_T. However, BLAST detector outperforms fundamental SIC and various linear detectors discussed above but still considered as sub-optimal detector, compared to performance of ML detector. Various near-optimal detectors including K-Best detectors, with better performance and lesser complexity have been elucidated in this chapter.

2.5.4 Lattice Detectors

Near-optimal detectors are capable of achieving best possible estimates, closer to ML detection performance, but with lesser complexity, which depends on algorithm of the MIMO detector. If each column in channel response matrix is considered as basis vector for any lattice under assumption, the MIMO problem defined in (2.6) can be considered as finding shortest lattice vector in given lattice [3]. And this gives rise to new kind of detectors called lattice detectors, which can achieve near-optimal performance. Moreover various pre-processing techniques such as lattice reduction can be used to increase orthogonality of basis vectors in channel matrix through which lattice points can be easily differentiated. The more orthogonal, basis vectors are, the more faster it is to find best possible estimate at each antenna level.

If we consider $\tilde{R}$ as defined in 2.13, since it's an upper triangular matrix, each row starting

from bottom of matrix can be re-constructed as one antenna level in tree search problem to find best possible estimate at each tree level, as there are N_T rows in $\tilde{R}$. In fundamental tree problem, each complex node in current level has 'Q' possible child nodes among which best estimate has to be calculated by minimum partial euclidean distance (PED). And since $\tilde{R}$ is an upper triangular matrix, PED estimate of i^{th} row depends on error accumulation based on symbols estimated in all post-processed rows ($(i+1)^{th}, (i+2)^{th}, (i+3)^{th}, ..., N_T^{th}$). The complexity of this tree search problem or closest lattice point problem at each tree level can be considered as NP-Hard, since arbitrary channel response lattice matrix is considered for calculating minimum PED. Accurately speaking, across lattice formed by basis vectors of channel response matrix, received symbol vector can be a point on it, if channel noise is assumed to be absent. Since noise is always present in MIMO problems, the lattice search gives us best possible estimate of transmitted symbols, by finding lattice point closest to received symbol vector with noise. This can be achieved by expanding all lattice points at each antenna level or intelligently choosing order for expanding or calculating PED of each lattice point.

The computational complexity of near-optimal lattice detectors depends on number of child nodes being expanded at each antenna level of tree search. Hence we should rationally decrease number of expanded child nodes or choose intelligent ordering for expansion to find best possible estimates at each tree level. At every node on each level, symbols which are farther from noiseless received vector or very unlikely can be pruned by introducing constraint for minimum acceptable PED, thereby reducing number of child nodes to be expanded and hence their complexity. Tree search can be performed by expanding complete path from root to leaf nodes or by expanding all child nodes at once in each level and going forward with selected bunch from current level to next tree level until leaf nodes are reached. This is referred to as depth first search and breadth first search respectively.

Depth First Search (DFS) algorithm expands all nodes along single path from root to leaf node at once, and move back and forth based on PED calculated at each level of that path. Sphere decoding (SD) is well-known detection model for DFS algorithm, which has been discussed in

next sub-section. Breadth First Search (BFS) expand all possible child nodes at current level and considers selected bunch of nodes with minimum PED value for processing at next tree level. This algorithm doesn't move back once nodes are selected at previous levels in tree search. Fundamental K-Best algorithm is well-known example for BFS algorithm. In this thesis work, I have focused on exploring different modified versions of K-Best algorithm for massive MIMO systems with high modulation order, and implemented possible enhancements to further decrease computational complexity or increase detector performance.

2.5.4.1 Sphere Decoder

Sphere decoder is based on limited depth expansion of Depth First Search algorithm. As name suggests, the radius of sphere 'r' is used as constraint upon which all symbols which are inside such sphere with received vector as origin, are expanded [16]. For complex MIMO system, this can be defined as shown in (2.20) below.

$$r^{\,2} > ||\tilde{Y} - \tilde{H}\ \tilde{s}||^{\,2},\ \ \tilde{s} \in \Omega^{\,N_T} \tag{2.20}$$

where $\tilde{s}$ represents all possible constellation lattice points in Ω. Since PED values of all child nodes depend on error accumulation based on symbols estimated previously, if any node at current level exceeds sphere radius constraint, all child nodes within its depth search can also be expected to violate radius constraint. Hence eligible nodes can be easily identified and inadmissible nodes can be pruned without expanding majority of search tree, based on radius constraint. This significantly reduces comprehensive computational complexity of MIMO system, which depends on radius constraint. Due to this reasoning, it is also referred to as least sphere decoder (LSD). Sphere decoder can also be implementing using BFS algorithm. The choice of radius constraint may lead to best possible estimate of transmitted symbols or no estimate at all, if radius is smaller than necessary. It is difficult to predict initial sphere radius constraint, in BFS sphere decoder as all eligible nodes inside radius constraint may suddenly become inadmissible, when moved to it next tree level, without giving any estimate for transmitted vector. However DFS sphere decoder gives bet-

ter prediction of initial sphere radius constraint, leading to considerable reduction in computational complexity. However if noise amplification is higher or received signal is weaker, the required initial sphere radius constraint may need to be larger. This leads to expansion on majority of leaf nodes and hence all their parent nodes, influencing complexity reduction to no effect. However if any sphere decoder is executed without ever terminating, it can lead to optimal performance, matching bit error rate of ML detector. Since throughput of this algorithm depends on many factors like channel interference, noise amplification, received signal, it's performance is varying and may need extra hardware overhead to make it reliable.

From next chapters, our focus is shifted towards K-Best MIMO detectors, which is well-known detection model for Breadth First Search traversal algorithms. I have explored various existing modified K-Best algorithms and presented their implementation results. I have also presented possible enhancements to increase performance or reduce computational complexity of K-Best detectors.

3. DESIGN EXPLORATION OF EXISTING LOW COMPLEX DETECTION ALGORITHMS

3.1 Introduction

Breadth First Search based detectors expands all potential nodes on current tree level, and progresses to expand child nodes of only selected bundle of nodes, from current level. Unlike depth first search based detectors, this is non-recursive scheme, meaning that they progresses in forward direction only without re-visiting levels that have already been processed. In general BFS based algorithms, Partial Euclidean Distance is considered as measuring criteria for constructing selective bundle of nodes from current level. Fundamentally, it can be elucidated that all nodes with PED values less than distance constraint can be added to admissible set of nodes, whose child nodes are to be expanded in next tree level. As traversal reaches to bottom of tree search and once admissible leaf nodes are selected based on minimum PED criteria, traversal from root node to each leaf node represents one of best possible estimate solution for transmitted complex vector, based on detection algorithm being used.

Any version of K-Best detector is considered a breadth first search based algorithm and fundamental K-Best detector is well-known among them. Unlike sphere decoder, the bit error rate performance from K-Best algorithm is independent of channel SNR. Their algorithmic flow is feasible to design pipelined hardware architecture giving them edge over other MIMO detectors. This chapter is organized as follows: Initially I have included brief introduction about theory of conventional K-Best algorithm along with possible pre-processing techniques like Lattice Reduction and QR Decomposition on channel response matrix. Later I have elucidated real domain SE based K-Best algorithm with its advantages and drawbacks. I have implemented floating point and fixed point versions of corresponding MIMO detector, from scratch, suing MATLAB and presented behaviour evaluation results. I have introduced complex domain SE based K-Best algorithm and followed the same organization for its improved version, with reduced complexity. At end of this chapter, I have briefly introduced possible enhancements that can be made, to explored detectors,

to increase their performance or decrease their complexity, even further.

3.2 Conventional K-Best Detection Algorithm

The MIMO problem defined in (2.13) can be interpreted as tree search problem with complex parent and child nodes, where each tree level represents one row of $\tilde{R}$ or best possible estimates for one transmitted symbol. In (2.1), We assumed complex MIMO system with antenna dimensions $N_T \times N_R$, thus resulting in dimensions of $N_R \times N_T$ for $\tilde{H}$. After processing channel response matrix with QR Decomposition using Given's rotation, the resultant MIMO system has been transformed to (2.10), and upper triangular matrix $\tilde{R}$, with dimensions of $N_T \times N_T$. Thus for MIMO system with N_T transmit antennas, there exists N_T number of rows in upper triangular matrix $\tilde{R}$. Considering we should solve for best possible estimate for transmitted vector $\tilde{x}$ of dimensions $N_T \times 1$, each estimated symbol corresponds to solving each row in $\tilde{R}$.

Considering dependency of current estimate on earlier computed estimates and intrinsic property of error accumulation, Solving for N_T symbols can be assumed as tree search problem with mapping last row of $\tilde{R}$ mapped with root node, until first row of $\tilde{R}$ is mapped with processing leaf nodes. Each parent node at any level has to expand or perform computations of Partial Euclidean Distances as defined in (2.13), on all complex constellation points 'Q', as per modulation order Q-QAM. Thus as conventional tree search, each complex parent node has to expand all 'Q' child nodes at each tree level, to finally arrive at estimated vector of dimensions N_T with minimum comprehensive error accumulation. Expanding all child nodes from root level to leaf results in exponential increase in computational complexity, which is similar to ML detection complexity.

Conventional K-Best algorithm aims at reducing computational complexity by expanding only selected bundle of nodes at each tree level. Starting from root node, it expands all child nodes to compute their PED values, and selects only K-Best children after sorting them based on PED criterion. The child nodes present in K-Best set are considered for further expansion, pruning all other child nodes which had high PED value, than first K-Best child nodes. Thus computational complexity for estimating transmitted symbol at level $'e'$ in search tree, has been reduced from expanding $Q^{\,e}$ nodes to expanding $Q \times K$ nodes. The expanded nodes at level $'e'$ are sorted to

extract K-Best possible candidates for next level. For MIMO system with N_T transmit antennas and modulation order 'Q', complex PED computation for tree level $'e'$ can be performed as defined in (3.1) below.

$$PED_{[e]}^{\tilde{s}_e} = \tilde{Y}_{[e]} - \tilde{R}_{ee}\tilde{s}_e - \sum_{i=(e+1)}^{N_T} \tilde{R}_{ei}\hat{s}_i \ , \quad \tilde{s}_e \in \Omega^{[e]} \ , \quad |\Omega| = Q \tag{3.1}$$

where $\hat{s}_i$ represents earlier processed complex parent nodes for this particular K-Best path, $\tilde{s}_e$ represents one of all possible child nodes from constellation Ω.

Conventional K-Best algorithm for real domain works in identical way, except that there are $2N_T$ number of tree levels to solve for, as defined in (2.14) for any real MIMO system model, assumed in (2.12), constructed from real value decomposition of original complex MIMO system model, defined in (2.10). The double order increase in number of search levels increase comprehensive latency for hardware implementation. However number of possible child nodes per parent node is reduced from 'Q' to '$\sqrt{Q}$'. Moreover unlike complex tree search, all PED values are to be computed with real numbers thereby reducing computational and sorting complexity. Using conventional K-Best algorithm further reduces this complexity from expanding $\sqrt{Q}^{\,e}$ nodes to expanding $\sqrt{Q} \times K$ nodes, at tree level $'e'$. Processing with higher number of K-Best possible candidates per tree level increases computational complexity and also leads to optimal performance, and vice versa. For any complex MIMO system with modulation order 'Q', as number of possible candidates 'K' at each tree level reaches modulation order value 'Q', K-Best algorithm reaches optimal performance of ML detector, along with it computational complexity. However choosing extremely low K-Best possible candidates per tree level drastically effects bit error rate performance. Therefore, it is crucial to arrive at appropriate value of K-Best possible candidates taking into account of resultant computational complexity and detection performance. For MIMO system with N_T transmit antennas and modulation order 'Q', real PED computation for tree level $'e'$ can be performed as defined in (3.2) below.

$$PED_{[e]}^{s_e} = Y_{[e]} - R_{ee}s_e - \sum_{i=(e+1)}^{2N_T} R_{ei}\hat{s}_i \ , \quad s_e \in \omega^{[e]} \ , \quad |\omega| = \sqrt{Q} \tag{3.2}$$

where $\hat{s}_i$ represents earlier processed real parent nodes for this particular K-Best path, s_e represents one of all possible child nodes from constellation ω.

The resultant output of K-Best algorithm is K-Best estimate of paths from root node to leaves in search tree. The path or estimated vector with lowest accumulated PED can be considered as output for hard decision detector, where as all K-Best paths can be considered for computing their Log Likelihood Ratio values for soft decision detector. The LLR values can be transferred to decoding systems like LDPC, Turbo for iterative processing. However for massive MIMO systems with high modulation order, more number of K-Best possible candidates are required for achieving reasonable performance from MIMO detector. However this significantly increases computational complexity, which has been our major concern primitively. This can be solved by intelligently expanding child nodes starting from highest probable node to be included in K-Best set for current tree level. This can be continued till K-Best candidates are added to K-Best set of current level before progressing further. Later in this chapter, I have explored such modified versions of existing low complexity K-Best algorithms in real and complex domains.

3.3 Possible Pre-Processing Enhancements

Before processing each antenna level in search tree, few pre-processing enhancements like Lattice Reduction and QR Decomposition have to be made on channel response matrix and received signal vector. I have used CORDIC algorithm using Given's rotation [13] for performing QR decomposition on channel response matrix $\tilde{H}$. QR decomposition is well-known for its disadvantages with respect to its hardware latency and power requirements. An efficient hardware design of QR decomposition algorithm being used is crucial for taking advantage of its capability to dismantle complex MIMO problem into antenna level wise processing. This ultimately leads to pipelined hardware design and implementation of MIMO detectors.

K-Best algorithm is nothing but searching for lattice points on lattice generated from basis

column vectors of channel response matrix. Since channel response matrix is arbitrarily formed from channel estimation of previously transmitted pilot symbols, the lattice search problem can be categorized as NP-Hard problem. Hence, it would be efficient to increase orthogonality of lattice by changing basis vectors using Lattice Reduction technique. This makes searching for lattice points easier and quicker, thereby reducing latency of detection.

3.4 Schnorr Euchner Based Real Domain K-Best MIMO Detection

A $N_T \times N_R$ complex MIMO system as defined in (2.1) can re-defined as $2N_T \times 2N_R$ real MIMO system as defined in (2.4). This has been evidently declared in Table. 2.1, using real value decomposition of complex MIMO system. Hence real MIMO system can be solved according to problem equation defined in (2.7). The channel response matrix has been processed through QR decomposition (2.8) to dissolve $\tilde{H}$ into unitary matrix $\tilde{Q}$ and upper triangular matrix $\tilde{R}$. After necessary adjustments, we have arrived at (2.12) with problem equation of (2.14). The updated real MIMO system problem has upper triangular matrix $\tilde{R}$ with channel information, which is compatible for sequential antenna level wise estimation of transmitted symbols and hence, pipelined hardware design and implementation of MIMO detector. As defined in previous section, the equation defined in (2.14) can be re-organized as tree search problem, where each level of tree represents lattice point search problem locally, where lattice is formed by basis vectors of $\tilde{R}$.

Hence we have $2N_T \times 2N_R$ real domain MIMO system, with modulation order 'Q' and K-Best possible candidates to select on each tree level from available $\sqrt{Q}$ child nodes for each parent node, in real domain. In conventional K-Best algorithm, estimation starts from root node of tree, which represents bottom row of upper triangular matrix R and proceeds to top row, by estimating K-Best possible estimates at each row or tree level. At each antenna level, only K-Best child nodes with lowest PED values are considered as K-Best possible estimates for that level and their child nodes are expanded in next tree level, pruning possibilities of other child nodes in current level. Even though this modification reduces computational complexity of detector to certain extent, compared to typical tree search problem, this doesn't seem to be advantageous with massive MIMO systems or high modulation orders due to their requirements for larger value of K-Best candidates being

short-listed per antenna level, leading to increased computational complexity. This exhaustive exploration for K-Best candidates can be perceived by taking one of configuration model, defined in Table. 2.2. Let us assume 100×100 massive MIMO system, transmitted with 256-QAM order symbols. As tree search problem, each parent node has $\sqrt{256} = 16$ possible real nodes for computing their PED values and sorting them to find lowest K-Best candidates. Since there exists K-Best parent nodes from previous level, total number of child nodes expanded at any tree level is given by $16K$. Hence comprehensive computational complexity of real domain massive MIMO system using conventional K-Best algorithm is $3200K$, where number of symbols to be expanded is considered as basis for complexity. Since we are using high modulation order, there is a necessity for larger value of K-Best candidates at each antenna level, to achieve better performance from detector. In general complexity can be represented as $\sqrt{Q} \times K \times 2N_T$, for estimation of transmitted symbol vector. Hence complexity linearly increases with antenna dimensions of MIMO system, modulation order and K-Best possible estimates at each tree level.

The complexity can be significantly reduced by intelligently expanding child nodes, starting from node with highest probability of having lowest PED and being included into K-Best possible estimates for that level. Schnorr Euchner based K-Best algorithm, proposed in [17], reduces complexity of real domain MIMO system from $\sqrt{Q} \times K \times 2N_T$ to $(2K - 1) \times 2N_T$. The modulation order doesn't have any kind of impact either on number of K-Best candidate requirements at each tree level or on computational complexity, leading to stable performance of MIMO detector, even with lower K-Best values. In SE based K-Best algorithm, each row from upper triangular matrix R or each tree level is processed using SE row enumeration technique for estimation of K-Best possible candidates for that level. At any tree level $'e'$, symbol is estimated using lattice point search assuming noiseless received vector on given lattice, with channel interference alone. This is termed as Zero child and it may not represent one of lattice points due to various assumptions made during its calculation. Hence zero child is used as an measure for lowest possible PED and it is mapped to its closest lattice point or constellation symbol. Hence nearest lattice point to zero child, is estimated with lowest PED, and is termed as first child (FC) for that parent node in tree

level $'e'$. In other words, first child is one of the child nodes, with lowest PED and highest probability to be included as one of the K-Best possible candidates for level $'e'$. Hence there exists one first child for each parent node in tree level. For estimation of K-Best candidates on tree level $2N_T$ or root node, there exists only one parent node and hence only one first child. For tree levels $'e' \in (2N_T - 1, 2N_T - 2, ..., 3, 2, 1)$, there exists K-Best parent nodes and hence 'K' first child nodes need to be computed on each parent node, assuming noiseless received vector on lattice, using lattice search problem. All first child nodes are added to current sorter list for level $'e'$ and it is sorted based on their respective path accumulated PED value and the one with lowest will be first one to get added to K-Best list of next level. This is referred to as distributed sorting of first child nodes, unlike global sorting of all child nodes in conventional K-Best algorithm. That first child is replaced by its local next best child node in current sorter list and this process is repeated until there exists K-Best possible estimates for tree level $'e + 1'$.

3.4.1 Design Exploration

As defined before, estimation starts from bottom row of upper triangular matrix R in 2.12 system model. The single first child of tree level $2N_T$ is computed assuming noiseless channel interference only received vector and is added to K-Best list for current level. At every antenna level, length of current sorter list should be 'K', except for $2N_T$, where it should be one. Hence the single element sorter first, which currently holds first child is replaced by its local best child, calculated by Schnorr Euchner row enumeration technique [17]. When elements are placed along row or column, the Schnorr Euchner row enumeration traverses from first child to its adjacent best child nodes, alternatively on its either sides. In this way, current child which is about to replace one of its predecessor in current sorter list, is closest unexpanded node to zero child and is used only after all better child nodes have already been added to current sorter list and considered for sorting based on their respective path accumulated PED values.

At tree level $'e'$, first child of particular parent node, selected after sorting, is added to K-Best list of tree level $'e + 1'$. The next child, which has next lowest path accumulated PED locally, from same parent node, replaces its first child in current sorter list. The current sorter list is sorted again

Table 3.1: Real Domain General Complexity Analysis

MIMO Detection Algorithm	Complexity	256-QAM, K=5 (Model Example 1)	1024-QAM, K=5 (Model Example 2)
ML	$\sqrt{Q}^{2N_T}$	16^{200}	32^{200}
Conventional K-Best [18]	$\sqrt{Q} \times K \times 2N_T$	16000	32000
Real domain SE based K-Best [17]	$(2K-1) \times 2N_T$	**1800**	**1800**

Where 'Q' represents modulation order, N_T represents number of transmit antennas ($N_T = 100$) in Model examples 1 & 2), 'K' represents K-Best possible estimates at each tree level. Number of expanded nodes during detection is taken as basis for complexity factor since it is most computationally extensive and latency effecting portion of MIMO detector.

to find best child node with minimum respective path accumulated PED value, which is added to K-Best list for next level. The next child, for corresponding parent of best child, previously added to K-Best list of next level, replaces its predecessor in current sorter list. This procedure is iterated until there exists K-Best possible candidates, which turn into 'K' parent nodes for next level. This noiseless channel interference only lattice search problem with Schnorr Euchner row enumeration is iterated over all antenna levels, finally resulting in K-Best possible path estimates from root node to leaves, for transmitted symbol vector. This algorithmic flow corresponding to Schnorr Euchner row enumeration delivers similar performance for high modulation order, even with low number of K-Best possible estimates at each antenna level. As a result there exists linear dependency of computational complexity on antenna dimensions alone, leaving out effect of modulation orders, making it practicable for massive MIMO systems with high modulation order.

3.4.2 General Complexity Analysis

The general computational complexity analysis comparing Real domain SE based K-Best detector with ML detector and conventional K-Best detector has been provided in Table. 3.1.

3.4.3 Benefits & Drawbacks

The main advantage of real domain SE based K-Best algorithm is its computational complexity and its limited dependencies on other attributes, as elucidated. It increases linearly only with antenna dimensions of MIMO system, giving reliable performance on massive MIMO systems with high modulation order, provided reasonable number of K-Best possible candidates. As mentioned before, there is no dependency on modulation order, due to SE based row enumeration technique applied for defining expansion order of all child nodes of current tree level. As a result, it expands 2K-1 child nodes, compared to $K \times \sqrt{Q}$ child nodes in conventional K-Best algorithm. It is compatible with various pre-processing improvements like Lattice Reduction [18] and QR Decomposition techniques [13]. The detection latency is always independent of constellation size, and only varies with antenna dimensions [17]. Due to real value decomposition of complex MIMO system into real domain, all computations have to be performed only with real numbers, significantly reducing silicon complexity required. The algorithmic flow can be used to implement hardware design in pipelined manner, further reducing comprehensive latency of detector.

The real domain MIMO detectors are known for providing similar bit error rate performance compared to their complex domain counterparts. However due to their higher degrees of freedom related to compatibility, there are few instances where they have experimentally proven to be beneficial, than their complex counterparts. As discussed in Chapter II, performance of VBLAST MIMO detectors is significantly impacted by detection ordering and real domain VBLAST MIMO detector outshines its complex domain counterpart owing to its optimal ordering [19].

The main drawback of real domain SE based K-Best algorithm is real value decomposition of complex MIMO system $N_T \times N_R$ into real domain MIMO system $2N_T \times 2N_R$, with twice antenna dimensions at transmitting and receiving end. Therefore there exists, twice the number of tree search levels, compared to that of complex MIMO system. thereby increasing comprehensive hardware latency of system. Since all digital transmission modulation schemes like quadrature amplitude modulation, phase shift keying are composed of complex constellation symbols, complex domain MIMO detectors are succinct way to reverse effect of channel interference and noise ampli-

fications. As a result, real domain MIMO detectors are not effectively applicable for near Gaussian [20], differential [21] and non-rectangular constellations. Essentially, real domain MIMO detectors are effectively practical, if real and imaginary part are uncorrelated as defined in Chapter I (1.1). Therefore complex MIMO systems are flexible practical applications and since SE based K-Best algorithm can be easily expanded to complex domain, VLSI implementation of pipelined hardware architecture for complex domain MIMO system will prove to be highly efficient.

3.4.4 Fixed Point Iteration

The Real domain SE based K-Best MIMO detector was implemented using MATLAB and hence, all default variables required in algorithm are assigned floating point representation with bit width 64. Using default floating point representation for writing hardware description languages will result in excessive and wasteful utilization of hardware area and power consumption, due to higher number of flip flops or registers. The width of each variable can be reduced to a fixed point, without impacting the performance of detector. Hence it is mandatory to convert floating point representation to fixed point representation for efficient hardware implementation of design. However extremely smaller bit widths may result in unpredictable behaviour of detector, deteriorating its bit error rate performance. The bit widths of all intrinsic variables should be selected such that they are lowest possible bits required for each variable, without effecting performance of detector and resulting in desired precision.

It is conventional to use MATLAB fixed point arithmetic toolbox to integrate fixed point objects into all intrinsic variables in algorithm before running extensive simulations to select highest fixed point bit width for all variables and gradually decrease fractional bits to find lowest bit width, based on resulting performance and desired precision. This gives us dynamic range of fixed point values and the lowest bit width for each variable with desired performance can be selected as its optimized fixed point representation. But if there are significantly high number of fixed point objects going through iterative MATLAB extensive simulations for arriving at bit error rate performance curve, it requires substantial amount of memory and time to derive optimized fixed point representations for all concerned variables, using MATLAB fixed point iterative toolbox. Integrating fixed point

arithmetic manually into algorithmic flow decreases each simulation run time by approximately ten times. This has proven to be of great advantage, in case of simulating high number of frames, on massive MIMO systems, to derive detection performance curves.

Floating point variable 'P' can be converted to its fixed point representation 'Y' , with 'F' fractional bits, as defined in (3.3) below.

$$Y = \lfloor P \times 2^{F} \rceil \tag{3.3}$$

where $\lfloor . \rceil$ is rounding function to its nearest integer value. And corresponding real value representation 'K' that is consequence of length of fractional bits 'F', used in fixed point representation is defined in (3.4) below.

$$K = Y \times 2^{-F} \tag{3.4}$$

All fixed point arithmetic operations can be performed for estimating K-Best candidates and computing bit error rate, by first converting floating point variables to their fixed point representation as defined in (3.3) and performing arithmetic operations and finally deriving real value representation of fixed point result as defined in (3.4). I have followed this procedure to convert real domain SE based K-Best algorithm to its fixed point arithmetic representation and have achieved fixed point bit widths of key variables as shown in Table. (3.2).

Table 3.2: Fixed Point Bit Width Table for Real Domain

Attribute	**Fractional bit width**	**Fixed point bit width**
Received Vector ($\tilde{Y}$)	25	33
Channel Matrix ($\tilde{H}$)	25	33
Upper Triangular Matrix ($\tilde{R}$)	25	33
Noise (σ)	9	9
Modulation Order 'Q'	0	5
Noise vector ($\tilde{n}$)	25	33
K-Best value	0	5
LLR	7	15

where fractional bit width represents number of fractional bits assigned to fixed point bit width representation. Fixed point bit width is also referred to as Word Length.

3.4.5 Implementation Results

MIMO System model with configurations defined in Table. 2.2 were used to evaluate performance behaviour of Real domain SE based K-Best algorithm, described above. The presented results were generated from extensive simulations, by transmitted ten thousand randomly generated frames based on configured modulation order. In $N_T \times N_R$ complex MIMO system, each frame is composed of N_T randomly defined complex constellation symbols from quadrature amplitude modulation, which are decomposed into $2N_T$ real valued symbols for processing in detector, on receiver end. I have analysed dependency of bit error rate on antenna dimensions and channel SNR values, on different high modulation orders discreetly. Starting with first configuration of system models, I have studied performance of real domain K-Best algorithm, on different antenna dimensions, to define dependency of performance on conventional and massive MIMO systems. The second configuration of system models were utilized to evaluate behaviour of bit error rate in conventional MIMO systems, using different ranges of channel SNR values, from weak signal power to weak noise power. I have also reported this behaviour for different number of K-Best possible candidates on each tree search level. The third configuration was used to evaluate detection performance in massive MIMO systems, using different possible channel SNR values. I have analysed the same, using different number of K-Best estimates at each antenna level. One set of antenna dimensions was selected from first configuration to build conventional and massive MIMO system models respectively. All performance curves presented in this thesis work were generated from their respective MIMO detectors, without taking benefit of integrating Low Density Parity Check decoding system. I have calculated Log Likelihood values for all above configurations, which can serve as ingress for any potential iterative decoding systems, for achieving better performance. This is elucidated in detail, as possible extensions of this research work, in Chapter V.

The performance curves presented in Figure. 3.1, Figure. 3.2 and Figure. 3.3 defines behaviour of bit error rate, with respect to different antenna dimensions of complex MIMO system, configured

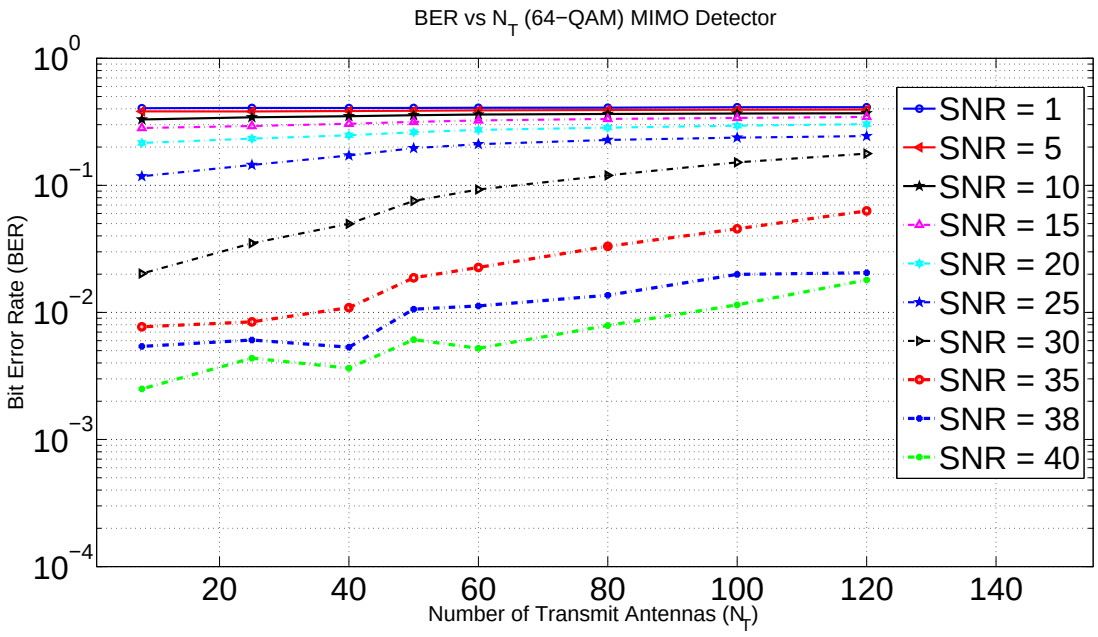

Figure 3.1: 64-QAM Dependency of BER Vs Antenna Dimensions, apropos of various channel SNR values.

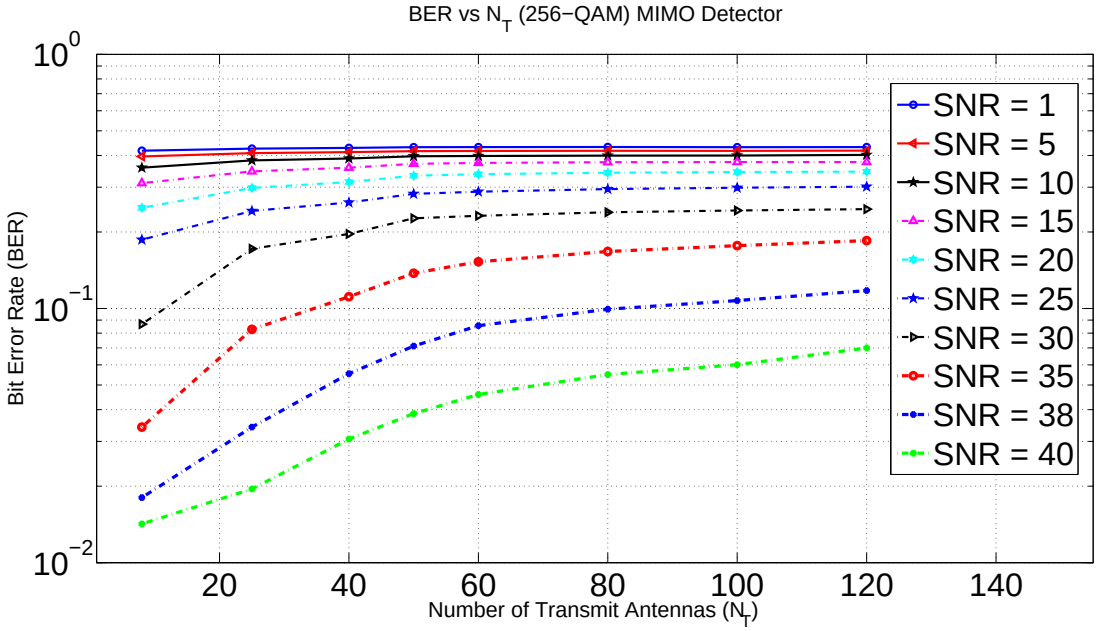

Figure 3.2: 256-QAM Dependency of BER Vs Antenna Dimensions, apropos of various channel SNR values.

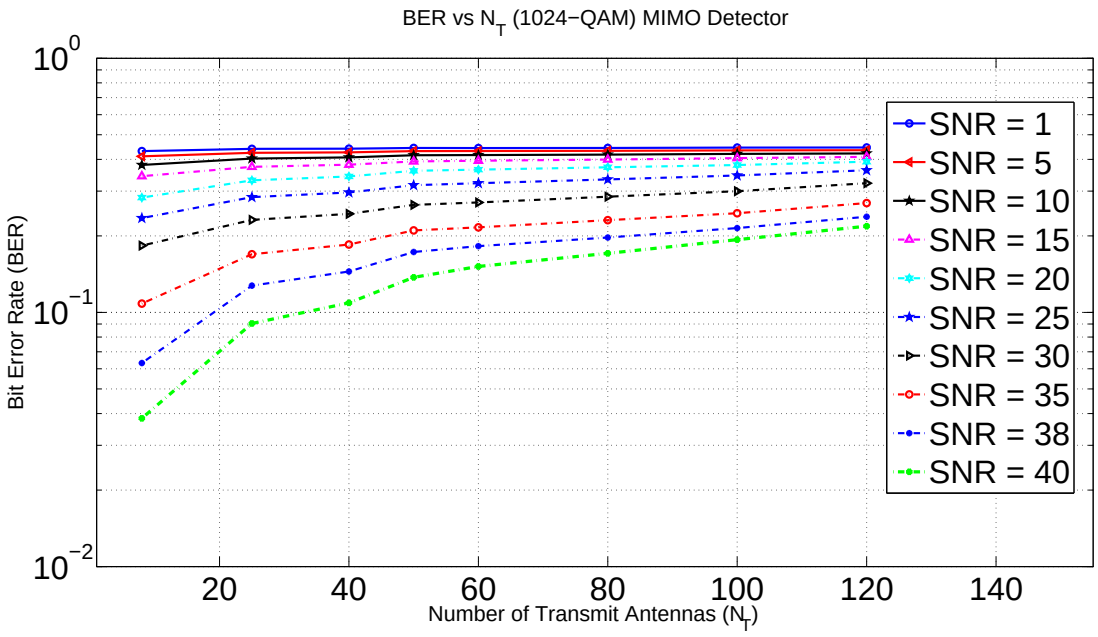

Figure 3.3: 1024-QAM Dependency of BER Vs Antenna Dimensions, apropos of various channel SNR values.

to transmit with Q-QAM {**Q =** 2^N**, N = 6,8,10**}, based on real domain SE based K-Best algorithm. All the graphs are on semi-log scale with bit error rates presented on logarithmic scale and antenna dimensions on linear scale. From Figures 3.1, 3.2 and 3.3, it can deduced that performance of current MIMO detector appears to be identical on lower channel SNR values $SNR \in [1, 10]$, irrespective of antenna dimensions of MIMO system model. In such regions, the transmitted complex symbol vectors are equally deteriorated by high noise amplifications. The weakened received bit stream provides resulting bit error rate values that appear to reach low asymptotic limit of current MIMO detection performance, irrespective of any antenna dimension. It can also be deduced that bit error rate is heavily dependent on antenna dimensions, across higher channel SNR values $SNR > 10$. It increases with increase in number of transmit and receiving antennas, which can be reasoned as follows. The number of transmitted symbols in each frame increases with antenna dimensions. The respective path accumulated PED and its corresponding error propagation plays a crucial role in estimating K-Best possible candidates at higher levels of upper triangular matrix $\tilde{R}$ or deeper levels of search tree. As accumulated error increases in deeper branches of search tree

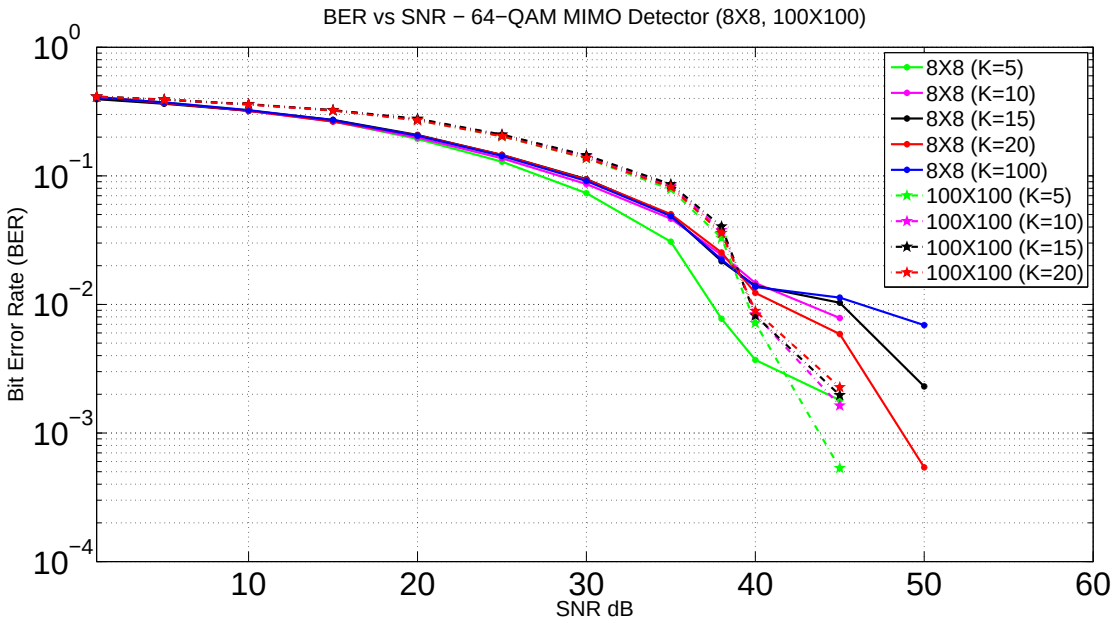

Figure 3.4: 64-QAM Dependency of BER Vs SNR, apropos different K-Best estimates.

or higher range of antenna levels, the capability of current MIMO detection algorithm to match its corresponding correct transmitted lattice point decreases, thus increasing comprehensive bit error rate of MIMO detector. This occurs at any high dimensional system model, irrespective of channel SNR value but at lower channel SNR, this effect is masked by high asymptotic limit of detector, as elucidated above. However, for higher channel SNR values, bit error rate doesn't reach such lower performance limits and this error accumulation effect at higher antenna levels can be clearly observed, as presented in Figure 3.1, Figure. 3.2 and Figure. 3.3.

The performance curves presented in Figure 3.4, Figure 3.5 and Figure 3.6 are related to second and third configurations in Table 2.2 respectively. It defines behaviour of bit error rate, with respect to different number of K-Best possible candidates on each antenna level, with each system model configured to transmit with Q-QAM **(Q = 64,256,1024)**, based on real domain SE based K-Best algorithm. Both of these graphs are on semi-log scale with bit error rates presented on logarithmic and channel SNR values on linear scales. From Figures 3.4, 3.5 and 3.6, it can be deduced that detector produces better performance as number of K-Best possible estimates per antenna level increases. It has been established previously that, in $2N_T \times 2N_R$ real valued MIMO

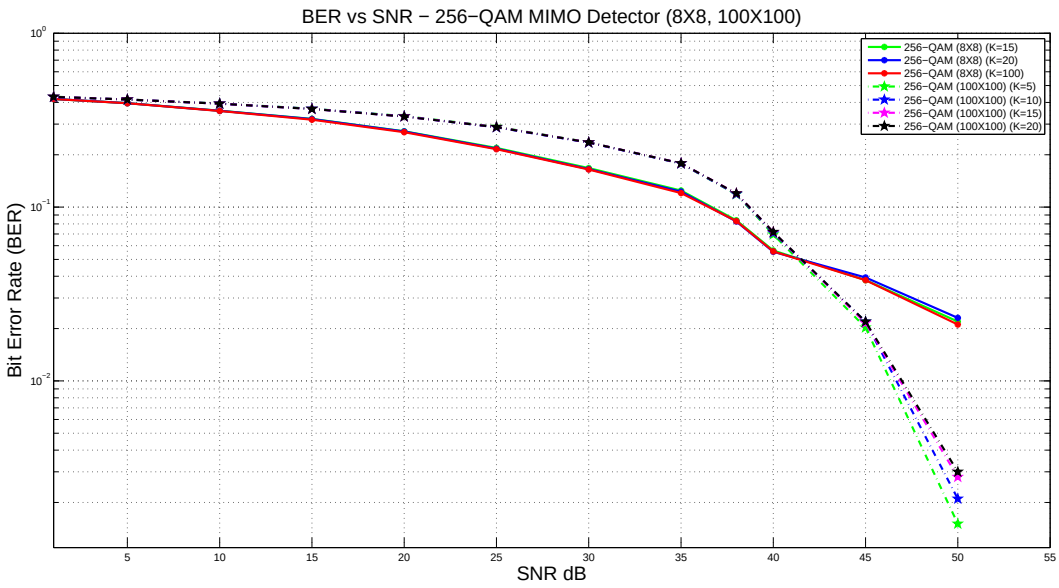

Figure 3.5: 256-QAM Dependency of BER Vs SNR, apropos different K-Best estimates.

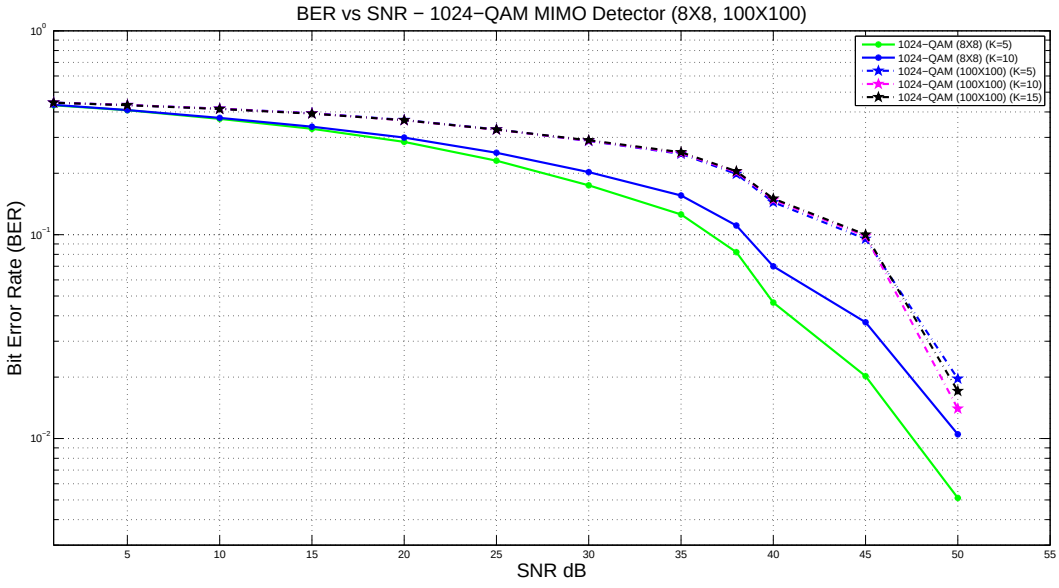

Figure 3.6: 1024-QAM Dependency of BER Vs SNR, apropos different K-Best estimates.

system, modulated with Q-QAM, if number of K-Best candidates on each tree level $'e'$ is equal to $\sqrt{Q}^{\,e}$, performance of this MIMO detector can reach to that of optimal ML detector. However

since is not practically feasible, appropriate number of K-Best candidates need to be selected to arrive at reasonable performance required by various applications. It can be observed that performance behaviour is significantly effected by K-Best value, only in low channel SNR values. The transmitted complex symbol vectors are possibly effected to high degree of deviation in response to increased noise amplification in the channel medium. Thus higher number of paths are needed to be considered to increase the probability of accurately estimating transmitted symbol on each tree search level. This can be achieved by increasing number of K-Best possible candidates to be propagated onto next search level, resulting in broadening of lattice point search problem locally, on each antenna level. It can also be deduced that this effect is not noticeable in behaviour of bit error rate in higher channel SNR values $SNR > 35$. The detection performance, in configurations related to high channel SNR values, appears to be unanticipated as it depends on randomized transmitted vectors and their ease of detection. However since transmitted vector can be accurately estimated from lower number of K-Best candidates due to less degree of deviation and weak noise amplification in wireless medium, detection performance is equally good and balanced for different number of K-Best candidates. Thus performance improvement with respect to increase in number of K-Best candidates per antenna level, is not noticeable.

The performance curves presented in Figure 3.7 and Figure 3.8 represents behaviour of bit error rate with respect to different modulation orders, **Q = 4,16,64,256,1024,4096** complex symbols per constellation, for real domain SE based K-Best algorithm. The presented graphs are on logarithmic scale with bit error rate values presented on vertical and modulation order on horizontal axis. The performance observed in Figures 3.7 and 3.8 can be correlated with that of Figures 3.1, 3.2 and 3.3. The probability of deviation for transmitted symbols in presence of noise, increases with modulation order. This generally occurs irrespective of channel SNR, as there exists $log_2 Q$ nodes which increases with modulation order. In low channel SNR $\in [1,\ 10]$, performance of MIMO detector is equally deteriorated by high noise amplification and weaker signal strength, irrespective of modulation order and antenna dimensions. Though performance can be improved by increasing K-Best possible candidates per antenna level, at significantly lower SNR values

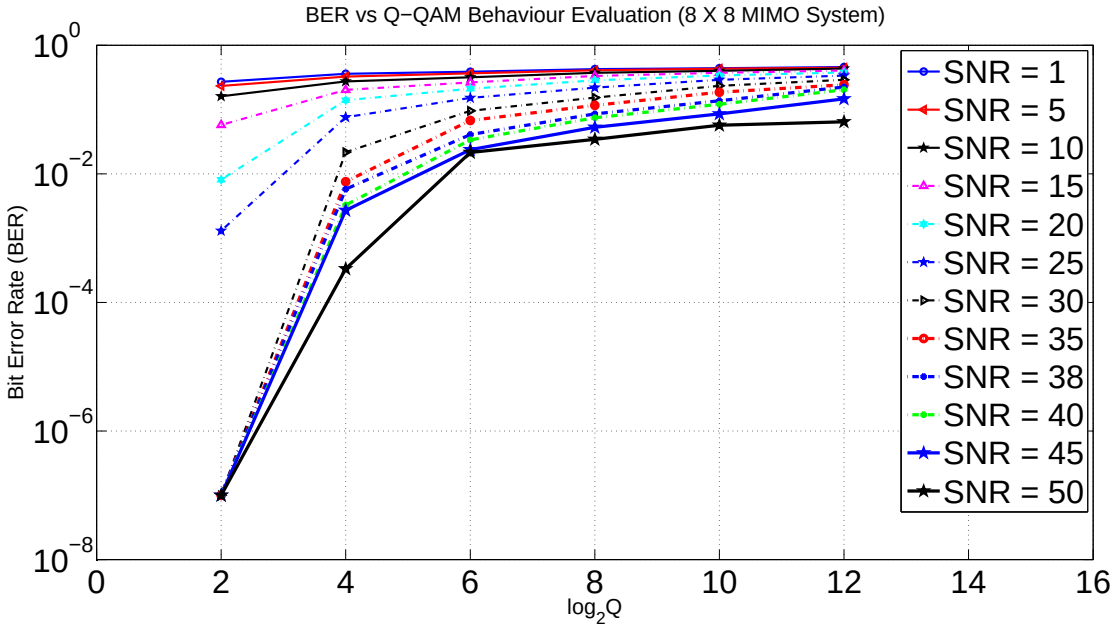

Figure 3.7: BER Vs Modulation Order (8×8 MIMO System), apropos different SNR channel values.

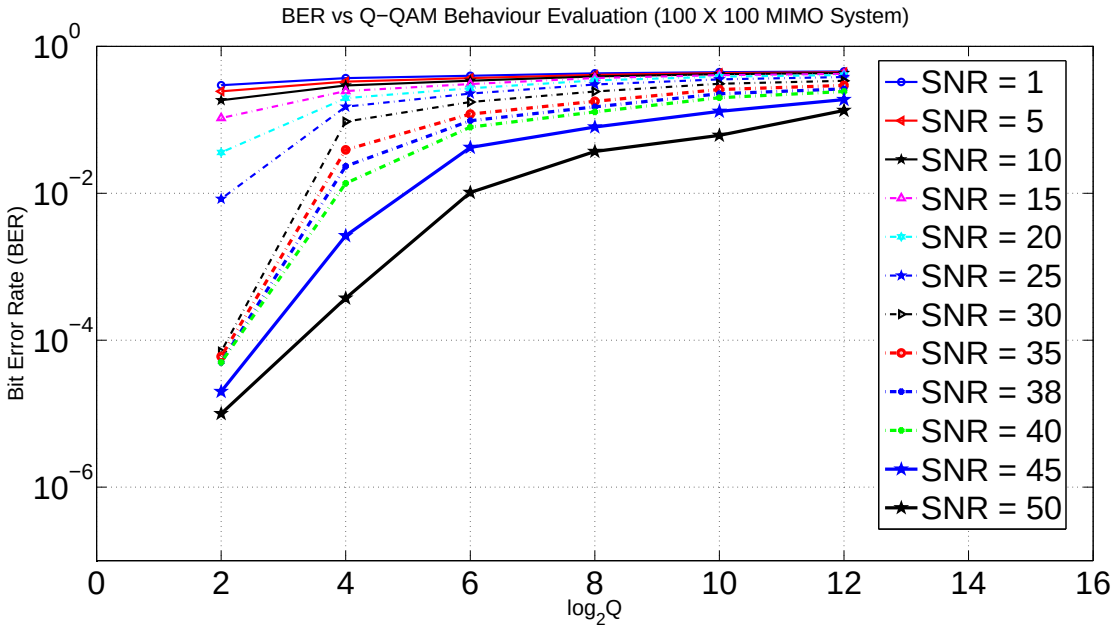

Figure 3.8: BER Vs Modulation Order (100×100 MIMO System), apropos different SNR channel values.

$\in [1,\ 10]$, this improvement and modulation order effect is concealed by lowest performance limit of MIMO detector. On the contrary, performance curve shows its dependency on modulation order or antenna dimensions across high channel SNR (> 10), which increases with either of configuration parameters. The bit error rate is not degraded to such extent, in higher channel SNR values. Hence performance curve can be observed with high estimation error on each antenna level, for high modulation order, due to high possibility of deviation. This results in higher path accumulated error propagation across deeper antenna levels, for high modulation orders.

3.4.6 Possible Enhancements

At initial levels of K-Best symbol estimation in tree search, fixed point precision is highly important. High error propagation at initial levels of tree will lead to massive fluctuations in detection at later antenna levels. If majority of K-Best candidates estimated at top levels of tree are incorrect, compared to corresponding transmitted symbols, the respective path accumulated error propagation will be significantly high. And estimation of K-Best candidates at level $'e'$ in real valued tree is dependent on all previously estimated symbols at levels ($i, i \in [e+1, 2N_T]$) and error accumulation of their resulting path from level $2N_T$ to $'e+1'$. Hence estimation of symbols at lower levels in tree are heavily dependent on accuracy of estimation for symbols at higher levels of tree. Let us assume lattice point search problem on tree level $'e'$ with inadequate number of fractional bits. This may lead to inaccurate or unpredictable behaviour of detector, resulting in incorrect estimation of symbols. When this path accumulated error propagates to tree level $'e+1'$, the updated path accumulated error corresponding to unerring symbols will appear to be higher, and detector selects its neighbourhood lattice points as one of K-Best candidates for level $'e+1'$. This effect further deteriorates estimation at lower tree levels leading to estimation of completely irrelevant symbols and as a result, rest of tree levels exhibit faulty detection of their corresponding transmitted symbols, with high bit error rate. Hence fixed point precision and its resulting performance should match corresponding default floating point performance, atleast during initial levels of tree search during lattice point detection.

However as we go down the search tree, fixed point precision or fractional bits of variables

can be gradually reduced without effecting performance of MIMO detector noticeably. This can be reasoned as follows. As symbols are estimated accurately at top levels of tree due to high fixed point precision, the respective path accumulated error propagation corresponding to estimated correct symbols would be lower, and it would be higher for symbols, surrounding them. Hence respective path accumulated error propagation for all K-Best estimated candidates from previous level will be lower, as required, leading to reasonable performance at lower levels of tree. After gradually decreasing fixed point bit width as we move down search tree, it needs to be maintained constant after certain levels due to minimum requirement limit for fractional bits in fixed point precision.

Though this slightly increases bit error rate of MIMO detector, decreasing number of variable bits per each level of detection can result in significant reduction of power consumption for massive MIMO systems, as there exists hundreds of antenna levels in search tree. This work has been explored further and implementation results have been presented in Chapter IV, to observe trade-off between bit varying fixed point precision and performance of MIMO detector.

3.4.7 Challenges

Real domain SE based K-Best algorithm is not practically applicable for star constellations, Gaussian and non-rectangular constellations, that have their broad scope of discrete industry applications. Modulation standards like quadrature amplitude modulation, phase or amplitude shift keying suffers performance loss in transmission rate, due to their uniform shaping and equidistant constellation structures [22], and this gap between Gaussian channel capacity and Shannon theoretical limit can be reduced by introducing non-uniformity in constellation shaping of symbols. However real domain detectors can't be used for such constellations as correlation exists between real and imaginary part of complex symbols. Typical complex domain MIMO detectors are reliable alternative as all digital transmissions naturally use complex symbol constellation standards for wireless communication. However either of them are inter-convertible to each other and original complex valued MIMO detectors are capable of achieving performance of real valued counterparts. I have explored original complex valued SE based K-Best algorithm later in this

Chapter. At the end of this Chapter, I have also explored modified version of complex domain SE based K-Best algorithm with reduced complexity [4], with lower complexity and presented its implementation results. Based on my exploration study and after observing reduced performance results of this modified version, I have proposed possible enhancements that can be assembled into it, in order to dynamically achieve trade-off between performance of original complex domain SE based K-Best MIMO detector and its computational complexity, to achieve reasonable bit error rate, based on application requirements.

3.5 Schnorr Euchner Based Complex Domain K-Best MIMO Detection

In this section, I have explored complex valued SE based K-Best MIMO detector and reported computational complexity and challenges related to its hardware implementation. A $N_T \times N_R$ complex MIMO system has been defined in 2.1 and its corresponding problem equation has been defined in 2.6. There is no need to utilize real value decomposition as all complex symbols are to be estimated as they were transmitted without disintegrating real and imaginary parts. Hence there exist N_T levels in search tree, half compared to real valued tree. However lattice point search with complex valued computations, on each antenna level results in higher local complexity in both computational and silicon implementations. Regardless of higher complexity, complex valued detectors are of more interest practically, due to their broadened scope of possible applications in various communication systems with different modulation techniques.

The channel response matrix $\tilde{H}$ as defined in 2.1 can be processed through CORDIC QR decomposition algorithm to disintegrate $\tilde{H}$ into unitary matrix $\tilde{Q}$ and upper triangular matrix $\tilde{R}$, as defined in 2.8. After further computations, we derive updated complex MIMO problem 2.13, that composes upper triangular matrix $\tilde{R} \in \mathbb{C}^{N_T \times N_T}$, with channel information. The updated structure of MIMO problem 2.13 induces compatibility for sequential estimation of transmitted symbols, starting from bottom row of $\tilde{R}$. This sequential iterative estimation with accumulated error propagation, can be utilized to design pipelined hardware architecture of complex valued MIMO detector. Hence MIMO problem defined in 2.13 can be re-structured as tree search problem with complex valued lattice point search problem locally, on each antenna level, where lattice is con-

structed from basis vectors of $\tilde{R}$. The orthogonality of basis vectors or lattice can be increased using Lattice reduction [12], resulting in efficient estimation of possible candidates on each level.

Let us assume $N_T \times N_R$ complex valued MIMO system, with modulation order 'Q' and K-Best possible estimates for each antenna level, from available Q child nodes on each parent node, in complex domain. The complex constellation with modulation order **Q = 64** has been presented in Figure 1.1, with $\sqrt{Q}$ complex symbols on each horizontal and vertical axes. In complex valued conventional K-Best algorithm, lattice point search starts from bottom row of upper triangular matrix $\tilde{R}$ and proceeds until estimation of leaf nodes in search tree, by expanding all child nodes of K-Best possible candidates from previous level. At each antenna level, all complex child nodes are expanded by computing their respective path accumulated PED values and only lowest K-Best child nodes are considered for next tree level. This reduces complexity, compared to ML detection, by pruning expansion of other child nodes and their respective paths at later tree levels. This algorithmic flow results in limited reduction of computational complexity, compared to typical tree search problem, which is not efficient with detection in massive MIMO systems with high modulation orders due to their high requirements for K-Best possible candidates to be progressed into next tree level, each time. Let us examine one configuration of complex MIMO system model, defined in Table 2.2 to understand exhaustiveness in its algorithmic expansion. In 100×100 massive MIMO system model, configured with 256-QAM, according to search tree, each complex parent node has **Q = 256** possible complex child nodes for computing and sorting their respective path accumulative PED value, to short-list lowest K-Best candidates, which are parent nodes for next level. Since each level has K-Best parent nodes from previous level, total number of child nodes expanded at any tree level according to conventional K-Best algorithm is given by $256\ K$. Hence comprehensive computational complexity for current complex valued massive MIMO system with conventional K-Best algorithm is given by $100 \times 256\ K = 25600\ K$, where number of complex symbols to be expanded is considered as basis for complexity. This is significantly higher than that of identical real valued MIMO system model, which turned out to be $3200K$.

With high modulation order, there is requirement for considering higher number of K-Best

possible candidates at each antenna level, to achieve reasonable detection performance. Hence in general computational complexity of complex valued conventional K-Best MIMO detector can be defined as $Q \times K \times N_T$, for detection of complete transmitted vector, which increases linearly with modulation order, antenna dimensions and K-Best candidates required at each antenna level. This complexity is resultant of number of expanded child nodes, in process of searching for best estimates of transmitted vector. Thus it can be greatly decreased by intelligently reducing number of expanded child nodes, by always starting expansion of child node with highest probability to get included in K-Best candidates for current level. Complex domain SE based K-Best algorithm, as proposed in [3] reduces complexity of complex valued MIMO system from $Q \times K \times N_T$ to $(3K-2) \times N_T$. The resultant computational complexity $(3K-2) \times N_T$ is lower than that of its real valued counter part $(2K-1) \times 2N_T$, irrespective of modulation order. It doesn't effect performance of MIMO detector, when transmission is configured with high channel SNR values, providing stable performance on lower K-Best candidates per antenna level.

The algorithmic flow of real valued and complex valued MIMO SE based K-Best detectors are similar, except building current sorter list and selecting first child, next child on each sorted iteration, for building K-Best candidates on each antenna level. Just to re-cap, estimation starts with root node in search tree, which corresponds to bottom row of upper triangular matrix $\tilde{R}$. Each row $'r' \in (N_T, N_T-1, ..., 3, 2, 1)$ in $\tilde{R}$ is processed using SE based row enumeration technique for short-listing K-Best candidates on each antenna level $'r'$. At any tree level $'r'$, zero child is computed by assuming noiseless received symbol $\tilde{Y_r}$ on any given lattice, constructed from basis vectors of $\tilde{R}$, using equation defined in 3.5 below.

$$ZC_r = Y_r - \sum_{i=r+1}^{N_T} (\tilde{R}_{r,i}\bar{z}_i) \tag{3.5}$$

where $\bar{z}_i$ represents processed estimates at corresponding levels in respective path in search tree and ZC_r represents of current parent node on tree level $'r'$. Since zero child is computed as lattice point without considering noise effects, resulting point may not be constellation point from configured modulation order. The nearest lattice point is defined as first child (FC) for

corresponding parent node on tree level $'r'$. Hence first child can be considered to one of child nodes with highest probability to get included as K-Best possible candidate for current tree level. There exists K-Best parent nodes and same number of first child nodes, on every tree level $'r' \in (N_T - 1, N_T - 2, ..., 3, 2, 1)$, except for tree level N_T, where there exists only one parent node and first child. On each antenna level, 'K' first child nodes are computed, sorting local child nodes on respective parents, and all first child nodes are included into current complex sorter list for current level $'r'$. Respective path accumulated PED values, calculated as defined in 3.6 are used for sorting first child list, and the one with lowest PED value, termed as best first child, is included into K-Best candidates for next level, and is removed from current complex sorter list. The local child node with next lowest PED value, computed from same parent of best first child, is included into current sorter list to next sorting iteration. This procedure is iterated until K-Best possible estimates are selected on current tree level $'r'$, which serves as parent nodes for tree level $'r+1'$.

$$PED_r^{FC_i} = \tilde{Y}_r - \tilde{R}_{r,r} FC_i - \sum_{j=r+1}^{N_T} \tilde{R}_{r,j}\, \bar{z}_j \ , \quad FC_i, i \in (1, 2, ..., K-1, K) \tag{3.6}$$

where $\bar{z}_i$ represents processed estimates at corresponding levels in respective path in search tree and $FC_i, i \in [1 \quad K]$ represents current complex sorter list. Later in this section, I have explored procedure of intelligently selecting and expanding child nodes with possibly next lowest PED, locally on each parent node, using complex SE row enumeration technique.

3.5.1 Design Exploration

Complex SE based K-Best algorithm differs from its real counterpart only in row enumeration techniques. The complex SE row enumeration should expand on both horizontal and vertical axes unlike real valued SE row enumeration, which expands only along horizontal or real axis. However zero child, first child are computed similar to that of real valued counterparts, except that complex PED computations are performed on respective complex matrix elements as defined in 3.6, unlike real matrix elements in real valued detectors. The estimation begins with bottom row of complex upper triangular matrix $\tilde{R}$ as defined in 2.10, after QR decomposition. The single **zero-child** of

tree level N_T is computed by ignoring noise amplification effect, and assuming noiseless channel interference only received vector. This leads to single **first child**, that is the first candidate to get added to K-Best list of current level. The length of current sorter list on any antenna level is not constant and varies between 'K' and '2K-1' as elucidated. The complex SE row enumeration expands in two directions - horizontally and vertically, using real valued SE row enumerations on either of them. In horizontal direction, one of the next expanded nodes will be computed by using real valued SE based row enumeration on real part of complex first child, and is termed as **real best node**. In vertical direction, other of the next expanded nodes is computed by using real valued SE based row enumeration on imaginary part of complex first child, and is termed as **imaginary best node**. This is visualized in Figure 1.1. Hence if first child has to be replaced in current sorter list, two expanded nodes, each from horizontal and vertical axes are added to current sorter list, increasing its length by one. If such replacement occurs in every iteration, when best node from current sorter list is added to K-Best candidates, in K^{th} iteration on same level, length of current sorter list will increase to '2K-1' child nodes. However, on any iteration, if best node that is added to K-Best candidates doesn't have same imaginary value as first child of its corresponding parent node, then the complex SE based row enumeration occurs only along vertical axes. This results in expansion along vertical axis alone, and only one next expanded node is calculated by performing real valued SE row enumeration on imaginary part of best node, that was added to K-Best candidates in this iteration. This replaces best node in current sorter list without changing its length for this iteration. Hence it's length can vary between 'K' in 1^{st} iteration to '2K-1' in K^{th} iteration on same antenna level.

For antenna level N_T, single first child node is added to K-Best list and is replaced by corresponding real and imaginary best nodes in current sorter list. Current sorter list is sorted on each iteration and child node with lowest respective path accumulated PED values, as computed in 3.6 and termed as **best next-child**, is selected as one of K-Best candidates in current level. If imaginary part of any best next child is equal to that of first child, on corresponding parent, it is replaced by real and imaginary best nodes in current sorter list. However if imaginary part is different than

that of first child on same parent, then it is replaced by only its imaginary best node, in current sorter list. The real and imaginary best nodes are selected for any best next child, by performing real valued SE based row enumeration technique on real and imaginary axes respectively. Hence depending on which element of current sorter list is best next child and is added to K-Best candidates, it is updated accordingly by replacing best next child with successive nodes as discussed above. This occurs at end of each iteration, and current sorter list is sorted again for best next child in next iteration.

At any tree level $'r' \in (N_T - 1, N_T - 2, ..., 3, 2, 1)$, there exists 'K' parent nodes and hence 'K' first child nodes initially. The complex first child of particular complex parent node, with minimum respective path accumulated PED value, as computed in 3.6, termed as **best first-child** is selected after sorting, and is added to K-Best list of tree level $'r + 1'$. The current sorter list is updated accordingly as elucidated above, and is sorted again to find best next child node with minimum respective path accumulated PED value. The best next child is added to K-Best candidates in current level, and it is replaced by successive real and imaginary best nodes or only the latter, depending on imaginary part of best next child. After $K^{\,th}$ iteration, K-Best possible candidates are selected from current level, which serves as 'K' parent nodes for next tree level $'r + 1'$. The initial noiseless channel interference only lattice search problem, followed by complex valued SE based row enumeration is iterated over N_T antenna levels, resulting in K-Best possible path estimates from root node to leaves in search tree. This algorithmic flow of original complex domain SE based K-Best MIMO detector has potential to reach stable performance of real valued counterpart, for massive MIMO systems with high modulation order. There exists linear dependency on antenna dimensions alone, as reasonable performance can be achieved with lower number of K-Best possible estimates irrespective of any modulation order, making it attractive for detection in massive MIMO systems with high modulation order. However, it has high silicon complexity on account of numerous complex PED computations and their sorting for 'K' iterations, on each antenna level. Various challenges associated with it have been elucidated later in this section.

Table 3.3: Complex Valued SE Based K-Best General Complexity Analysis

MIMO Detection Algorithm	Worst Case Complexity	256-QAM, K=5 (Model Example 1)	1024-QAM, K=5 (Model Example 2)
ML	Q^{N_T}	256^{100}	1024^{100}
Conventional K-Best [18]	$Q \times K \times N_T$	128000	512000
Complex domain SE based K-Best [17]	$(3K-2) \times N_T$	**1300**	**1300**

Where 'Q' represents modulation order, N_T represents number of transmit antennas ($N_T = 100$) in Model examples 1 & 2, 'K' represents K-Best possible estimates at each tree level. Number of expanded nodes during detection is taken as basis for complexity factor since it is most computationally extensive and latency effecting portion of MIMO detector.

3.5.2 General Complexity Analysis

The general computational complexity analysis comparing complex valued SE based K-Best detector with ML detector and complex valued conventional K-Best detector has been provided in Table. 3.3.

3.5.3 Challenges

For any tree search detectors with error propagation, performance is significantly effected by accuracy of estimation on top levels of tree. The real valued detectors are capable of achieving better performance than complex counterparts due to redundant channel information, in decomposed real channel response matrix 'H', compared to original complex channel matrix $'\tilde{H}'$. However complex valued detectors are capable of achieving better performance if real and imaginary parts of constellation points are not completely uncorrelated. Designing efficient pipelined hardware architecture for complex valued SE based K-Best algorithm can be demanding due to silicon complexity associated with complex computations and sorted involved at every iteration, and dynamic nature of current sorter list in complex valued SE based row enumeration. As a result, there is no detailed design of such pipelined architecture till date, for complex valued SE based K-Best

algorithm.

In the next section, I have explored modified version of complex valued SE based K-Best MIMO detector with reduced complexity in original complex valued row enumeration [4], and presented its implementation results using MATLAB. Though silicon complexity associated with row enumeration was reduced, the performance observed to be drastically effected by modification in original complex valued SE row enumeration. Since majority of potential lattice points were not even considered for expansion and not being included in current sorter list on each antenna level, I have proposed enhancements that can be integrated into this modified version, which can dynamically control the broadening of lattice point search to required number of complex layers. This proposed enhancement has been defined in detail, in Chapter IV, and implementation results have been presented to dynamically observe improvement in performance with broadening of search along complex layers or their imaginary axes.

3.6 Modified Complex Domain K-Best MIMO Detection

In this section, I have explored modified version of complex valued SE based K-Best MIMO detector with reduced complexity and evaluated bit error rate performance and various benefits and drawbacks associated with it. Let us assume $N_T \times N_R$ MIMO system with Q-QAM modulation order as defined in 2.1. After performing QR decomposition on channel response matrix $\tilde{H}$, the resultant upper triangular matrix $\tilde{R}$ can be correlated with tree search problem with N_T levels and leaves, and each row equation starting from N_T level to top level, can be solved as lattice point search problem. Hence iterative application of lattice point search problem over N_T levels can lead to estimation of $N_T \times 1$ transmitted vector $\tilde{x}$. Lattice point search on respective levels, was distinctly performed using different enumeration algorithms, followed by sorting and resulting in one of K-Best possible estimate, in each iteration, for each level $i, i \in (N_T, N_T - 1, ..., 3, 2, 1)$. In real valued MIMO detector explored in Section 3.4, real SE based row enumeration was utilized to intelligently expand limited number of child nodes on each antenna level, resulting in reduced complexity as defined in Table 3.1. In complex valued MIMO detector, explored in Section 3.5, original complex SE based row enumeration was used to expand best successive child nodes for

expanding. For any complex symbol $\tilde{s} = s_r + js_i, \quad \tilde{s} \in \Omega^{N_T}$, real valued SE based row enumeration is performed individually on real and imaginary part of $\tilde{s}$, s_r and s_i respectively, to derive next best real and imaginary child nodes, on horizontal and vertical axes of constellation diagram respectively, as shown in Figure 1.1. Both next best real and imaginary child nodes are added to current sorter list, if imaginary part of its predecessor is identical to that of their first child node, from same parent. If not, only the latter is considered into current sorter list, for processing through next iteration.

The small modification in enumeration technique being used, can significantly impact both computational complexity and performance of MIMO detector as it is iteratively used 'K' times to construct K-Best possible estimates, for N_T levels, on $N_T \times N_R$ MIMO system, leading in $N_T \times K$ modifications in the detection algorithm. One such modification was proposed in [4], that reduces silicon complexity associated with complex enumeration. Also computational complexity can be dynamically controlled by using parameter termed as **Rlimit**, which controls horizontal width for estimation of first child on each parent in current level. However computation with respect to zero-child and first-child is performed similar to original complex domain SE based K-Best MIMO detector, by using noiseless channel interference adjusted lattice problem and respective path accumulated error propagation problem, as defined in 3.5 and 3.6 respectively. This modified algorithm differs from previous version, in selecting next best successive child nodes, when a child from same parent node is included as one of K-Best possible candidates in current iteration, on any tree level $i, i \in (N_T, N_T - 1, N_T - 2, ..., 2, 1)$. In this section, I have elucidated the reasoning and theory behind modification of complex SE based row enumeration, presented in [4] along with its effect on general complexity analysis and performance evaluation across different system model configurations, defined in Table 2.2. The trade-off associated with its performance and possible flexible variations of computational complexity has been discussed.

3.6.1 Design Exploration

Modified segment in complex valued SE based K-Best algorithm is the row enumeration technique used for determining best next child nodes on each respective parent node, for estimating

K-Best possible candidates on any antenna level $i, i \in (N_T, N_T - 1, ..., 3, 2, 1)$. Although computational complexity depends on additional parameter **Rlimit**, modified complex valued SE based row enumeration significantly reduces silicon complexity associated with it. The parameter Rlimit refers to horizontal width across zero-child, to estimate first-child within expanded child nodes, with identical imaginary parts s_i but different real parts s_r, in complex constellation symbol $\tilde{s} \in \Omega$. Let us assume $N_T \times N_R$ complex MIMO system with Q-QAM modulation order. The corresponding complex constellation is composed of 'Q' complex symbols with $\sqrt{Q}$ complex symbols on each row and column individually. All complex symbols that belong to same row have equal imaginary parts s_i and that belong to same column are equally real-valued s_r. Hence range of additional parameter **Rlimit** is $[1, \sqrt{Q}]$, which defines complexity as defined in Table 3.4.

The zero-child is computed similar to original complex valued row enumeration as defined in 3.5. After zero-child is computed, all child nodes around zero-child within horizontal width of **Rlimit** are expanded and their respective path accumulated PED values are computed as defined in 3.6. The child node with minimum PED value is selected as first-child, unlike original complex valued row enumeration in which closest child node to zero-child as first child. Hence increasing horizontal width broadens the estimation search for first-child by expanding more child nodes that belong to same row, thus increasing both detection performance and computational complexity. However the resulting edge with respect to trade-off between bit error rate and horizontal width, depends on degree of noise amplification and randomly generated transmit vector $\tilde{x}$.

Starting with bottom row of upper triangular matrix $\tilde{R}$, which corresponds to N_T antenna level in estimation search tree, zero-child is computed by assuming noiseless channel interference only received vector, as represented mathematically in 3.5. The first-child for each corresponding zero-child is computed by expanding child nodes across zero-child, till pre-determined horizontal width, and selecting child node with minimum respective path accumulated PED value. At level N_T, length of current sorter list is **Rlimit** at any K-Best candidates iteration. However at any antenna level $r, r \in (N_T - 1, N_T - 2, ..., 3, 2, 1)$, length of sorter list is given by $K \times Rlimit$ since there exists 'K' parent nodes on any antenna level r and each parent node initially expands 'Rlimit' child

nodes locally.

After determining first-child of parent node on any antenna level $i, i \in (N_T, N_T - 1, ..., 1)$, modified complex row enumeration expands only in vertical direction of constellation diagram. The 64-QAM constellation is presented in Figure 1.1. All child nodes that replaces their preceding first-child are generally termed as **next-child** and immediate next-child is termed as **imaginary best node**. In vertical direction next child nodes are computed by using real-valued SE based row enumeration on imaginary part of complex first child, and current next-child that is about to replace its predecessor is termed as **imaginary best node**. After sorting all first-child nodes, the first-child node with minimum PED value, termed as **best first-child** is added to K-Best possible candidates for current level i. Imaginary best node is computed along complex vertical layer of local first child using expanding child nodes across it, alternatively on either side. The best first child is replaced by its corresponding local imaginary best node, in current sorter list of length $K \times Rlimit$.

For antenna level N_T, single zero-child is computed using 3.5 and its corresponding first-child is determined by computing respective path accumulated PED value 3.6 of child nodes across zero-child, with horizontal width of **Rlimit**, and selecting child node with minimum PED value. The Rlimit child nodes comprises sorter list for first K-Best candidate iteration. Since on level N_T there exists only one parent node, its corresponding first-child is added as one of K-Best candidates, and it is replaced by imaginary best node, in current sorter list. In second K-Best candidate iteration, current sorter list, with imaginary best node or next child node and remaining 'Rlimit-1' child nodes, is sorted and the child with minimum PED value, termed as **best next child** is added as one of K-Best possible candidates for this iteration. Hence the current sorter list is updated by replacing best next child with successive imaginary best nodes for remaining iterations and sorted for best next child till K-Best candidates are selected from level N_T. At the end of processing for level N_T, one best first child and 'K-1' best next child nodes comprises K-Best possible estimates, which serves as parent nodes for next level $N_T - 1$.

From tree level $N_T - 1$, there exists 'K' parent nodes unlike level N_T, that had only one parent node. Hence there exists 'K' zero-child nodes. Considering 'Rlimit' expanded nodes across

zero-child on each parent node, current sorter list with $K \times Rlimit$ child nodes with different respective level paths, are sorted to determine best first-child for current K-Best candidate iteration. Using modified complex valued row enumeration, imaginary best node is computed for parent node of best first-child. It replaces best first-child in current sorter list, and $K \times Rlimit$ nodes with one updated child, are again sorted to determine best next-child, for current K-Best candidate iteration. After K^{th} iteration, K-Best possible estimates for level $N_T - 1$ are determined and they serve as 'K' parent nodes for level $N_T - 2$. The noiseless lattice point search or zero-child computation, followed by modified complex row enumeration is iterated over antenna levels $i, i \in (N_T, N_T - 1, ..., 1)$, resulting in K-Best estimates of $N_T \times 1$ transmitted symbol vector. The modified complex SE based row enumeration significantly reduces silicon complexity due to uncomplicated expansion technique used for updating current sorter list. However it also effects detection performance due to inadequate expansion of child nodes along vertical layers other than that of best first-child, determined on each antenna level. Various enhancements and challenges associated with it have been elucidated in this section.

3.6.2 General Complexity Analysis

The modification in complex valued SE based row enumeration, reduces computational complexity to $(Rlimit + 1) \times K \times N_T$, compared to worst-case complexity $(3K - 2) \times N_T$, exhibited by original complex valued detector. It introduces new parameter **Rlimit**, that can be accessed by user to tune the trade-off between performance and computational complexity. However silicon complexity is reduced significantly due to simpler complex valued enumeration being integrated in modified version. The general complexity analysis comparing modified complex valued SE based K-Best algorithm with Maximum Likelihood and complex valued conventional K-Best algorithms has been provided in Table 3.4.

3.6.3 Benefits & Drawbacks

The major benefit of modified complex valued SE based K-Best algorithm is lower silicon complexity for building current sorter list in each K-Best candidate iteration. The computational

Table 3.4: Modified Complex Valued SE Based K-Best General Complexity Analysis

MIMO Detection Algorithm	Worst Case Complexity	256-QAM, K=5 (Model 1)	1024-QAM, K=5 (Model 2)
ML	Q^{N_T}	256^{100}	1024^{100}
Conventional K-Best [18]	$Q \times K \times N_T$	128000	512000
Modified Complex domain SE based K-Best [4]	$(Rlimit + 1) \times K \times N_T$	**3000**	**3000**

Where 'Q' represents modulation order, $N_T = 100$ in Model examples 1 & 2, 'K' represents K-Best possible estimates at each tree level and **Rlimit = 5** represents horizontal width for first child estimation

complexity is dynamically programmable due to additional parameter **Rlimit** that refers to horizontal width expansion for first-child, as elucidated in Section 3.6.1. As a result, maximum child nodes that should be expanded, for selecting K-Best estimates on each antenna level can be given by $Rlimit + K - 1$ per antenna level, compared to $K \times \sqrt{Q}$ child nodes in real valued conventional K-Best and $K \times Q$ in complex valued conventional K-Best algorithm. Complex row enumeration technique is utilized to expand next-child nodes, resulting in non-dependency of complexity and detection latency on modulation order. It can be integrated with various pre-processing techniques such as low latency QR Decomposition using CORDIC algorithm [13], Lattice Reduction [12]. The complex-valued SE based row enumeration can be designed with pipelined hardware implementation, implementing each pipeline stage with antenna level, spitting out K-Best candidates immediately without waiting for complete K-Best possible estimates on each level. This ensures reduced comprehensive detection latency of MIMO detector. This is also practically compatible with MIMO system models configured with Gaussian, star and non-rectangular constellations [19].

The major drawback would be the inability of algorithmic flow to perform broadened expansion in searching for K-Best candidates on each level. As discussed in Section 3.6.1, only the vertical layer corresponding to first-child on each parent is expanded to determine next child nodes. If

noise amplification and channel interference disturbs both real and imaginary part of transmitted complex symbol during wireless transmission, corresponding detection at receiver end becomes out of reach of modified row enumeration, which can be elucidated as follows. Let us assume complex symbol $\tilde{s} = s_r + js_i$ has been transmitted through wireless medium. If only real part of transmitted complex symbol is altered due to channel and noise response, the resulting zero-child computed using 3.5, points to $s_r + js_i,\ \ s_r = s_r \pm 2 \times i,\ \ i \in \mathbb{Z}$ as first-child. The original transmitted real part can be reached by expanding child nodes along horizontal axes using additional parameter **Rlimit** until $s_r + js_i$ is added to current sorter list, as one of next child nodes. If only imaginary part of transmitted complex symbol is altered due to channel and noise response, the resulting zero-child computed using 3.5, points to $s_r + js_i,\ \ s_i = s_i \pm 2 \times i,\ \ i \in \mathbb{Z}$ as first-child. As vertical layer along first-child is expanded, the original transmitted imaginary part can be reached by expanding child nodes along vertical layer, in successive iterations, until $s_r + js_i$ is added to current sorter list, as one of next child nodes. However if both real and imaginary parts are altered by channel interference and noise amplification, the resulting zero-child points to $s_r + js_i,\ \ s_r = s_r \pm 2 \times i,\ \ s_i = s_r \pm 2 \times k,\ \ i, k \in \mathbb{Z}$ as first-child. As only horizontal and first-child related vertical child nodes are expanded, the transmitted symbol $s_r + js_i$ can never be reached and expanded, for it to be added to current sorter list. Hence it can be deduced that $\tilde{s}$ constellation point is not even in consideration for selecting K-Best possible candidates for current level. This significantly degrades bit error rate performance of MIMO detector, as observed in implementation results presented in this section.

3.6.4 Fixed Point Iteration

The modified complex domain SE based K-Best detector was implemented using MATLAB with default floating point representation for all variables. As elucidated in Section 3.4.4, to avoid wasteful utilization of hardware area and power consumption, the width of each variable can be reduced to fixed point representation, thus reducing register width required for that particular variable. The fixed point representation can be defined as least possible width that each intrinsic variable should have, to mimic performance of floating point representation. As MATLAB fixed

point arithmetic toolbox requires substantial amount of memory and time, to perform extensive simulations on complex domain K-Best algorithm, I have integrated fixed point arithmetic directly into algorithmic flow, to achieve bit error rate performance curves, with significantly smaller simulation time. This exhibited appreciable impact, especially for simulation large number of frames on massive MIMO systems with high modulation order.

The conversion of floating point into fixed point representation has been defined in 3.3 and 3.4. All fixed point arithmetic required for implementing enumeration and detection logic can be performed, by converting into fixed point representation and performing required arithmetic operations, and finally deriving real value representation of fixed point result with corresponding precision. This procedure was implemented to convert modified complex domain SE Based K-Best algorithm into fixed point iteration and observed fractional bit width and word lengths of major variables as defined in Table 3.5.

Table 3.5: Fixed Point Bit Width Table for Modified Complex Domain

Attribute	**Fractional bit width**	**Word Length**
Received Vector ($\tilde{Y}$)	25	30
Channel Matrix ($\tilde{H}$)	25	30
Upper Triangular Matrix ($\tilde{R}$)	25	30
Noise (σ)	9	9
Modulation Order 'Q'	0	5
Noise vector ($\tilde{n}$)	25	30
K-Best value	0	3
LLR	7	12

where fractional bit width represents number of fractional bits assigned to fixed point bit width representation.

3.6.5 Implementation Results

The performance of modified complex domain SE based K-Best MIMO detector was evaluated using MIMO system model configurations defined in Table 2.2. As elucidated in Section 3.4.5,

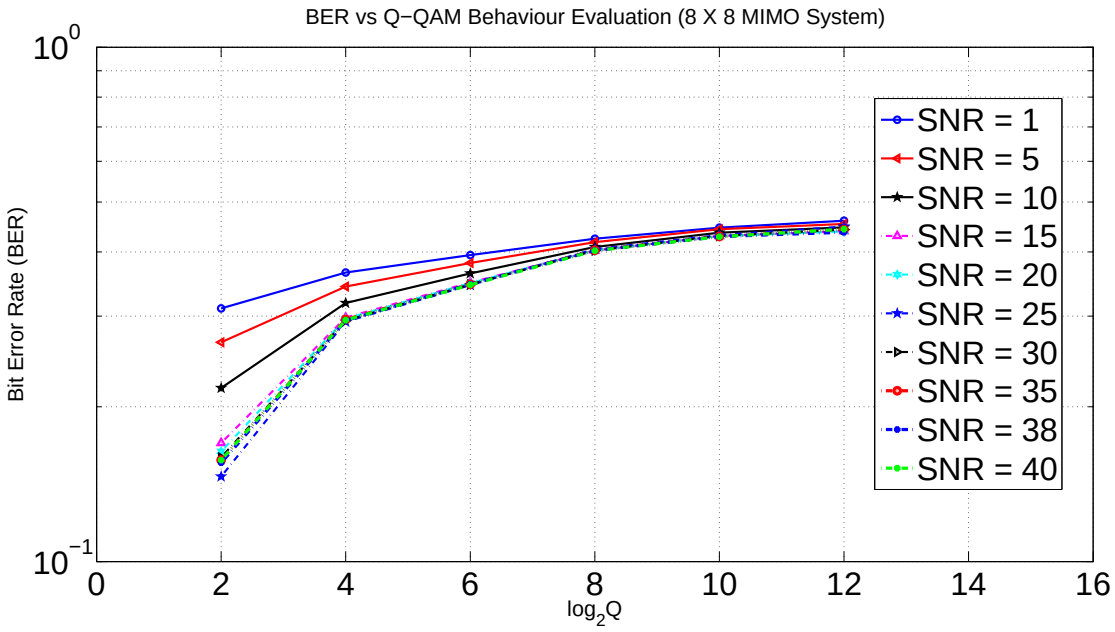

Figure 3.9: BER Vs Modulation Order (8×8 MIMO System), apropos different SNR channel values.

each frame in $N_T \times N_R$ MIMO system transmits N_T complex symbols, modulated with configured constellation order. The behaviour and dependency of bit error rate in regard to different modulation orders has been studied and analysed in this section. The performance graphs presented in this section were generated from standalone MIMO detector without taking advantage of iterative decoding systems. However soft output resulting from MIMO detector were sequentially used to calculate Log Likelihood values. They serve as ingress into potential iterative decoders such as LDPC decoding system introduced in Section 1.5. The graphs presented in 3.9 and 3.10 represents dependency of bit error rate in regard to different modulation orders, {**Q =** 2^N**, N = 2, 4, 6, 8, 10, 12**} on modified complex domain algorithm elucidated in Section 3.6.1 [4]. To maintain consistency with other explored algorithms, the graphs are on logarithmic scale with bit error rate and modulation order on vertical and horizontal axis respectively.

The bit error rate is expected to increase with modulation order or antenna dimensions, due to gradual rise in path accumulated error propagation, for broader lattice search or deeper tree levels respectively. From 3.9, 3.10, it can be deduced that in low channel SNR $\in [1,\ 10]$, bit error rate

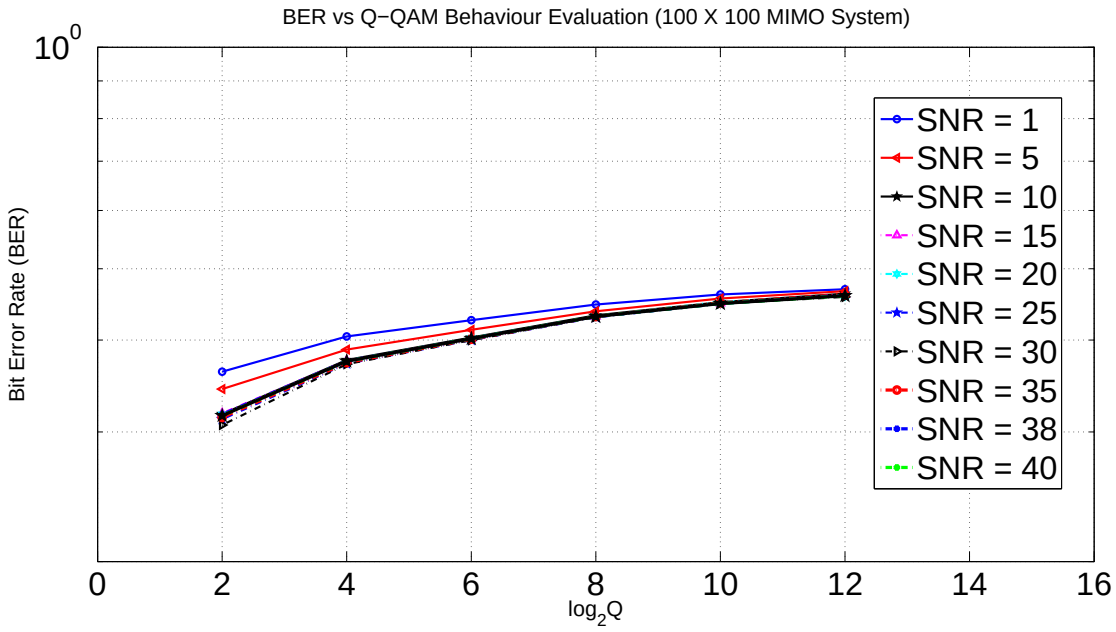

Figure 3.10: BER Vs Modulation Order (100×100 MIMO System), apropos different SNR channel values.

has been equally deteriorated due to high noise amplification and weaker signal strength in the transmission medium. Irrespective of system configuration, the resulting bit error rate from SNR $\in [1,\ 10]$ represents low asymptotic limit of modified complex domain MIMO detector and hence it can be observed to be near-equivalent among all modulation orders and antenna dimensions, in their respective graphs. Across high channel SNR values $SNR > 10$, bit error rate is dependent on system configuration. However juxtaposing Figures (3.7, 3.8) with Figures (3.9, 3.10) respectively, it can be observed that modified complex domain detector exhibits inferior performance compared to real domain detector, which was explored in Section 3.4. By examining through extensive simulations and debugging of modified complex domain algorithm, it was perceived that substandard performance is resultant of complex row enumeration to determine next child nodes in subsequent K-Best iterations on each antenna level.

To understand defect in modified complex row enumeration, let us consider 8×8 MIMO system, configured with 16-QAM modulation order. Hence constellation is composed of $\sqrt{16} = 4$ complex symbols along each horizontal and vertical axis. Let us assume a frame with $8^{\,th}$

antenna transmitting $\tilde{s}^{\,8} = 1 - j3$ complex symbol. The binary code bit symbol mapping for 16-QAM modulation order has been defined in Table 3.6. Based on bit symbol mapping, each complex symbol can be constructed from $log_2\,16 = 4$ bits, where first half bits contribute to real mapping and later half bits contribute to imaginary mapping. Using channel information, zero-child can be computed by assuming noiseless channel interference only received vector, using 3.5 and nearest lattice point is determined as first-child node. Let us assume first-child is determined to be $\tilde{s}^{8}_{FC} = 3 - j3$ complex signal, that is just adjacent to transmitted symbol $\tilde{s}^{\,8} = 1 - j3$. As elucidated in Section 3.6.1, modified complex row enumeration selects only the **imaginary best nodes** along vertical layer of first-child node $\tilde{s}^{8}_{FC}$ and **Rlimit real best nodes** across zero-child, along horizontal axis, as successive next-child nodes for building current sorter list in each K-Best iteration, if child node from same parent has been added to K-Best possible candidates for next tree level. The expansion order has been mentioned thoroughly in Section 3.6.1. From analysis of corresponding expansion of nodes with respect to modified complex row enumeration, it has been determined that expansion order is favourable towards selecting imaginary best child nodes $(3 - j3, 3 - j1, 3 + j1, 3 + j3)$ of first-child $\tilde{s}^{8}_{FC} = 3 - j3$, than **Rlimit** horizontal child-nodes $(1 - j3, -1 - j3, -3 - j3)$. Hence based on PED values computed by 3.1, enumeration tends to expand majority of existing **imaginary best nodes** on vertical layer, before considering **real best nodes** of first-child. It was observed that original transmitted symbol $\tilde{s}^{\,8} = 1 - j3$ was expanded only after selecting all **imaginary best nodes** $(3 - j3, 3 - j1, 3 + j1, 3 + j3)$. Hence higher K-Best candidates are required to expand **real best nodes**, especially with high modulation order. The resultant performance of modified complex domain detector relies heavily on accuracy of estimating first-child node and was determined to be inferior than its real domain counterpart, especially for high channel SNR values $SNR > 10$. Moreover modified complex row enumeration doesn't explore diagonal children to first-child. The theoretical analysis behind this major drawback has been elucidated in Section (3.6.3, 4.2.1.1) and corresponding enhancements have been proposed in Section (4.2.1.1 and 4.2.1.2) in detail.

Table 3.6: 16-QAM Binary Code Bit Symbol Mapping

Bit	Real Mapping	Imaginary Mapping	Complex symbol
00	-3	+3	$-3 + j3$ (0000)
01	-1	+1	$-1 + j1$ (0101)
10	+1	-1	$+1 - j1$ (1010)
11	+3	-3	$+3 - j3$ (1111)

3.6.6 Possible Enhancements

Modified complex row enumeration expands only vertical layer corresponding to first-child node, that was determined by sorting nodes across zero-child with horizontal width **Rlimit**. As elucidated in Section 3.6.3, if both real and imaginary part of transmitted complex symbol are effected by channel inteference and noise amplification to the extent that zero-child doesn't relate to either of them, the modified row enumeration doesn't even consider original transmitted constellation point for building K-Best possible candidates. This inadequate expansion along vertical layers significantly degrades detection performance for high modulation orders. Besides considering first-child vertical layer, expanding vertical layers corresponding to other child nodes within **Rlimit** horizontal width can increase possibility of expanding original transmitted complex symbol. Selecting that child node as one of K-Best possible estimates for that level, decreases bit error rate accordingly. This enhancement has been elucidated in Chapter IV of this thesis work.

The Dynamic Fixed Point enhancement that has been integrated into Real domain SE based K-Best MIMO detector can also be implemented in Complex domain detectors. Fixed point precision is significant especially in higher levels of search tree. Also in modified complex row enumeration, since initial K-Best iteration determines first-child node and expansion of only corresponding vertical layer, precision computation of first-child impacts comprehensive performance of detection for that antenna level. Inadequate number of fractional bits at initial stages of estimation may result in high error propagation and unpredictable behaviour of detector by causing broad fluctuations at deeper antenna levels. However fixed point bit widths with respect to each variable can be gradually reduced as each antenna level is processed. This has been elucidated in Section

3.4.6. It can drastically reduce power consumption for massive MIMO systems, by turning off inactive register bits using clock gating technique, at deeper tree levels. This enhancement has been elucidated in Chapter IV where observed fractional bit widths & word lengths of variables and corresponding implementation results have been presented in Chapter IV, only for real domain SE based K-Best MIMO detector. The similar enhancement can be easily extended towards modified complex valued SE based K-Best MIMO detectors.

3.6.7 Challenges

Complex valued detections are outperformed by their real valued counterparts, if transmission is configured with rectangular constellation orders and if real and imaginary parts of corresponding constellation symbols are uncorrelated. Due to redundancy of channel information from real value decomposition of complex channel response matrix $\tilde{H}$, real valued detections are known to achieve better performance. The major challenge for implementing modified complex row enumeration is determining efficient values for additional parameter **Rlimit**, that controls performance and computational complexity. Selecting higher than required width unnecessarily explores additional number of child nodes, and selecting smaller horizontal width may result in missing out consideration of original transmitted complex symbol. The similar explanation stands for requirement of determining efficient number of K-Best possible candidates per each antenna level. Hence defining appropriate **Rlimit** and **K** values for different configurations of system model is quite challenging and may require additional learning algorithms integrated into MIMO detector.

Complex valued detectors have less freedom of manipulation, compatibility of integrating additional features and degree of flexibility in selecting optimum detection ordering [19], than corresponding real valued counterparts, results in better performance from the latter. Though complex valued detectors have edge with broad range of practical applications using Gaussian, star or non-rectangular constellations, design of pipelined hardware architecture for various complex signal processing techniques, that are required to characterize such improper, non-circular or unsymmetrical complex constellation symbols [23] is very challenging. However due to existing correlation between real and imaginary parts of unsymmetrical complex symbols, complex valued detectors

outperform their real valued counterparts. For such applications, real valued detectors need to assume absence of correlation, for performing real value decomposition of unsymmetrical complex symbols, to process them for detection. As this uncorrelated assumption violates intrinsic properties of unsymmetrical constellation symbols, the performance of real valued detectors are degraded, compared to that of complex valued counterparts, defining significance of the latter.

3.7 Summary

In this chapter, I have explored real domain SE based K-Best MIMO algorithm [17] and its modified complex counterpart [4]. I have presented general complexity analysis and implementation results associated with them, using various configurations of system model, described in Table 2.2. Additionally, I have also explored original complex valued row enumeration technique for utilizing it to elucidate about the modifications performed in complex valued row enumeration technique. The analysis of performance behaviour has been reported in Section 3.4.5 and 3.6.5. Real domain detectors can perform comparatively better than their complex domain counterparts, if transmission is configured using rectangular and symmetric modulation techniques. This can be mostly observed in detection ordered based algorithms like VBLAST, LSD, K-Best MIMO detectors and is due to their high degree of compatibility, manipulation and extra redundancy in channel information attained using real value decomposition of complex MIMO system. However complex valued detectors can be utilized over broader range of constellations like Gaussian, non-rectangular and star with unsymmetrical and improper complex symbols [19]

3.7.1 A Peep into Possible Enhancements

In the next chapter, I have proposed two major enhancements that can be integrated into detection algorithms that have been explored in this section. First is the dynamic fixed point iteration through which involves progressive decrement of fractional width of each variable as tree levels are processed. Each bit reduction can be correlated to increase in unused flip-flops or register bits on each antenna iteration. Modern power reduction techniques like clock gating can be utilized to turn off such unused register bits while designing pipelined hardware architecture for the detection

algorithms. I have presented simulation implementation results of dynamic fixed point iterative real domain SE based K-Best MIMO algorithm and compared performance with that of its floating point representation. This can be easily extended to any sequential ordering detection algorithms like complex valued K-Best detectors. Second involves possible enhancement to modified complex valued row enumeration [4] elucidated in 3.6.1. This has already been briefly introduced in Section 3.6.6.

4. DESIGN ENHANCEMENT OF EXISTING LOW COMPLEX DETECTION ALGORITHMS

4.1 Dynamic Fixed Point Arithmetic Variation

Every variable in algorithm used for simulations is defined with floating point representation by default. For floating point variable, the default word length is 64 bits among which majority corresponds to fractional bits. The word length of any variable can be correlated to width of register, instantiated for that variable, in hardware. If floating point representation is used to directly design RTL for any algorithm, each variable corresponds to 64-Bit register, leading to high consumption of area and power. However similar performance can be achieved by fixing word length and fractional length of all internal variables in algorithm. Such fixed width can be determined by performing extensive simulations on algorithm, by decreasing length of variables gradually and observing the resultant performance from algorithm.

In real domain SE based K-Best algorithm, efficient fixed point conversion can be utilized to significantly reduce comprehensive power and area consumption of corresponding hardware design, especially for massive MIMO system with high modulation order. The floating point representation from MATLAB was converted to fixed point counterpart, using procedure defined in Section 3.4.4 by manually integrating fixed point logic into algorithm and using extensive simulations to determine efficient widths of internal variables. The resulted fixed point bit widths of each major variables have been presented in Table 3.2. The fractional bit widths listed in Table 3.2 represents minimum width of respective variable, to achieve performance of floating point representation, on any system model configuration of MIMO system. For any algorithm, there exists critical segments that can determine its final performance and requires high precision in fixed point performance. However, there also exists non-critical segments where bit width can be varied in circumstances where slight degradation in internal computations doesn't effect local estimation or lattice point search and the resulting comprehensive performance of detector. This phenomenon

can be utilized effectively to reduce power consumption at deeper level of tree search, in massive MIMO systems with high modulation order.

In this section, I have elucidated **Dynamic Fixed Point Iteration** in real valued SE based K-Best MIMO detector and presented its implementation results by juxtaposing it with original floating point performance. Finally various challenges and limitations in regard to affixing this design enhancement have been discussed.

4.1.1 Fixed Point Design Enhancements

The critical segment of real domain SE based K-Best detector is estimation of K-Best possible candidates at initial levels of search tree, where fixed point precision is extremely significant. Since calculation of partial euclidean distance of any node at tree level is based on respective path accumulated error propagation, high resulting error at initial antenna levels can lead to high fluctuations in selecting best possible estimates at later level. Hence at any tree level $'r'$, estimation of K-Best possible candidates is highly dependent on all earlier processed levels $i, i \in (r+1, r+2, ..., 2N_T-1, 2N_T)$ and their resultant propagated errors. Hence as we go down search tree, lattice point search at lower levels gradually increases its dependency factor on fixed point precision of algorithm. If fractional bit width is lower than minimum required as computed from extensive simulations, it may result in unpredictable nature of detector, from significant degradation of its performance to detecting lattice points irrelevant to transmitted possible constellation symbols. If current tree level $'r'$ is effected due to lower fixed point precision, all antenna levels after current level, $i, i \in (r-1, r-2, ..., 3, 2, 1)$ results in faulty detection of their corresponding transmitted symbols, due to respective path accumulated error propagation on all of them. This defines significance of precision at initial iterations of any sequential or ordered detection algorithms and their resulting performance should be identical to that of floating point representation during local lattice point search. The non-critical segments of real domain SE based K-Best detector can be defined as lower levels of search tree. Fixed point precision or fractional bits of variables can be gradually reduced without effecting estimation of K-Best candidates on each antenna level. If estimation occurs with high precision at critical segments of detection, the

resulting path accumulated error doesn't fluctuate or impact estimation of K-Best candidates often. The corresponding PED values of unerring symbols would be lower and it would be higher for all neighbourhood symbols surrounding it. This further results in propagation of lower accumulated error, resulting in reasonable comprehensive performance of detector.

As part of this enhancement, I have gradually reduced minimum fixed point bit widths defined in Table 3.2, for important variables in design. For processing K-Best candidates on tree level $2N_T$, the bit width was set accordingly to Table 3.2. As we move down the search tree, I have started gradually reducing width of fixed point variables by one bit, until number of fractional bits reach to lower minimum, termed as **Bit Width Limit**. The bit width limit is defined as minimum number of fractional bits required by particular variable, to achieve reasonable comprehensive performance of detector on any configuration of MIMO system model. Let us assume 25×25 MIMO system configuration as defined in Table 2.2. The Table 4.1 presents dynamic variation of fixed point iterations, with bit width limit 8, on 25×25 MIMO system.

Table 4.1: Dynamic Fixed Point Bit Width Table for Real Domain

Attribute	**OFBW**	**50** ($2N_T$)	**49**	**48**	**34**	**33**	**32**	**31**
Received Vector ($\tilde{Y}$)	25	25	24	23	9	8	8	8
Channel Matrix ($\tilde{H}$)	25	25	24	23	9	8	8	8
Upper Triangular Matrix ($\tilde{R}$)	25	25	24	23	9	8	8	8
Noise (σ)	9	9	8	8	8	8	8	8
Modulation Order 'Q'	0	0	0	0	0	0	0	0
Noise vector ($\tilde{n}$)	25	25	24	23	9	8	8	8
K-Best value	0	0	0	0	0	0	0	0
LLR	7	7	7	7	7	7	7	7

Where **Original Fractional Bit Width (OFBW)** represents minimum fixed point fractional bits required to achieve performance of floating point representation. **Dynamic Bit Width (DBW)** represents dynamically adjusted fractional bit widths on respective antenna levels starting from $2N_T = 50$.

where original fractional bit width represents minimum fixed point fractional bits required to achieve performance of floating point representation. Dynamic Bit Width represents dynamically adjusted fractional bit widths on respective antenna levels.

In Table 4.1, **Dynamic Fixed Point Iteration** for 25×25 MIMO system with Bit Width Limit 12, has been studied. The fixed point precision of first tree level $2N_T = 50$, is derived from Original Fractional Bit Width, from Table 3.2. It represents minimum bit width required by each variable to achieve performance of floating point representation. As we move down tree level, fractional bit width is decreased by one bit gradually, until Bit Width Limit is reached. Once fractional bit width reaches its Limit, all antenna levels after will have constant fixed point width, equal to Bit Width Limit. The Bit Width Limit can be adjusted based on configuration of MIMO system model. It can be deduced from implementation results that Bit Width Limit may need to be higher with massive MIMO systems or high modulation order, to achieve similar performance as floating point representation. However, the maximum value of Bit Width Limit that is sufficient for any configuration of MIMO system model, to achieve floating point detection performance, is 15 Bits.

Since bit width of simulation variables correlate with register width, when designing RTL, decreasing bit width dynamically on each iteration reduces active flip-flops gradually as shown in Table 4.1. This can be effectively implemented using power reduction techniques such as clock gating to completely switch off inactive register at deeper levels of search tree. From theoretical perspective, this provides significant reduction in comprehensive power consumption, for massive MIMO systems. This research work presents implementation results, generated by simulation of dynamic fixed point iterative real domain SE based K-Best algorithm. **Dynamic Fixed Point Bit Variation** can be used on any sequential or ordered detection algorithm and has significant impact in reduction of comprehensive power consumed by MIMO detector.

4.1.2 Implementation Results

MIMO System model with configurations defined in Table 2.2 were used to evaluate performance of dynamic fixed point iterative version of Real valued SE based K-Best algorithm, elu-

cidated above. The implementation results has been presented to compare resultant performance of dynamic fixed point version with their corresponding floating point representation. Table 4.2, comprises of **Dynamic bit width variations** used for 100×100 massive MIMO system, with respect to each antenna level, starting from root node to leaves in search tree, that have been used to generate performance comparison graphs between bit error rate and channel SNR values for 100×100 massive MIMO system. The Bit Width Limit of 15 fractional bits has been decided after observing derived performances of various bit widths, from extensive simulations. The behaviour evaluation for each performance curve has been elucidated in Section 3.4.5. Similar reasons can be assumed here because of identical performance curves observed as shown in this section. This section is mainly focused on juxtaposing performance of dynamic fixed point bit width varying real domain SE based K-Best algorithm and its floating point counterpart.

Table 4.2: Dynamic Fixed Point Bit Width (100×100 MIMO System)

Attribute	**200** ($2N_T$)	**199**	**191**	**190**	**189**	**100**	**50**	**1**
Received Vector ($\tilde{Y}$)	25	24	16	15	15	15	15	15
Channel Matrix ($\tilde{H}$)	25	24	16	15	15	15	15	15
Upper Triangular Matrix ($\tilde{R}$)	25	24	16	15	15	15	15	15
Noise (σ)	9	9	9	9	9	9	9	9
Modulation Order 'Q'	0	0	0	0	0	0	0	0
Noise vector ($\tilde{n}$)	25	24	16	15	15	15	15	15
K-Best value	0	0	0	0	0	0	0	0
LLR	7	7	7	7	7	7	7	7

Each column represents dynamically adjusted fractional bit widths on respective antenna levels starting from $2N_T = 200$.

The performance curves presented in Figure 4.1 have been generated utilizing varying fixed point bit width from Table 4.2. It represents behaviour of bit error rate for different modulation

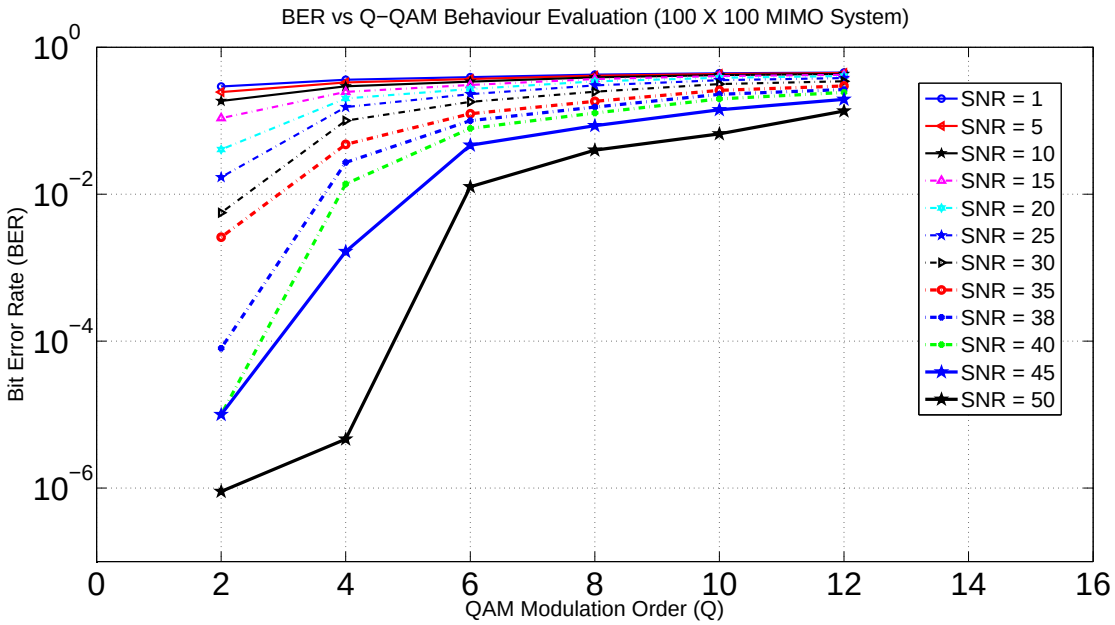

Figure 4.1: Dynamic Bit Width Varying BER Vs Modulation Order (100×100 MIMO System), apropos different SNR channel values.

orders, **Q=4,16,64,256,1024,4096** constellations. The presented graphs are on logarithmic scale with bit error rate and modulation order on vertical and horizontal axes respectively. It can be observed that performance of dynamic bit width variation algorithm over different modulation orders for massive MIMO systems, as presented in Figure 4.1, is almost identical to that of its floating point counterpart in Figure 3.8, over different channel SNR values. This can also be proved by computing average mean square difference between $BER_{dynamic}$ and $BER_{floatingpoint}$, as defined in 4.1.

Table 4.3, comprises of **Dynamic bit width variations** used for 8×8 MIMO system model, configured with 64-QAM modulation order, to generate performance curves between bit error rate and channel SNR values. Ten Fractional Bits (lower than 100×100 MIMO system) were adequate in achieving detection performance, equivalent to that of its floating point representation.

Similar analysis has been performed for conventional MIMO systems with 8×8 antenna configuration as system model. The performance curves presented in Figure 4.2 have been generated utilizing dynamic fixed point bit width variation, from Table 4.3. The behaviour of bit error rate

Table 4.3: Dynamic Fixed Point Bit Width (8×8 MIMO System)

Attribute	**16** ($2N_T$)	**15**	**10**	**9**	**8**	**3**	**2**	**1**
Received Vector ($\tilde{Y}$)	25	24	23	19	18	17	11	10
Channel Matrix ($\tilde{H}$)	25	24	23	19	18	17	11	10
Upper Triangular Matrix ($\tilde{R}$)	25	24	23	19	18	17	11	10
Noise (σ)	9	9	9	9	9	9	9	9
Modulation Order 'Q'	0	0	0	0	0	0	0	0
Noise vector ($\tilde{n}$)	25	24	23	19	18	17	11	10
K-Best value	0	0	0	0	0	0	0	0
LLR	7	7	7	7	7	7	7	7

Each column represents dynamically adjusted fractional bit widths on respective antenna levels starting from $2N_T = 16$.

for different modulation orders, {**Q =** 2^N**, N = 2,4,6,8,10,12**} constellations has been evaluated by using logarithmic scale in Figure 4.2, with bit error rate and modulation order on vertical and horizontal axes respectively. The performance of dynamic bit width variation algorithm over different modulation orders for conventional MIMO systems, as presented in Figure 4.2, is within reasonable deviation from performance of its floating point counterpart, as presented in Figure 3.7, over different channel SNR values. This can also be proved mathematically by computing average of squared euclidean distance between $BER_{dynamic}$ and $BER_{floatingpoint}$, as defined in 4.1.

The dynamic fixed point performance curves 4.1 and 4.2 has been juxtaposed with floating point counterparts 3.8 and 3.7 respectively, to compute resultant average performance degradation. Each numerical value listed in Table 4.4 has been computed using 4.1. For each model configuration, corresponding numerical value represents average of absolute difference between bit error rate achieved from dynamic fixed point algorithm and floating point version, over channel SNR values listed in 4.2. It can be observed that all numerical values in Table 4.4 are reported in order of 10^{-2}, thereby establishing integrity of proposed fixed point enhancement.

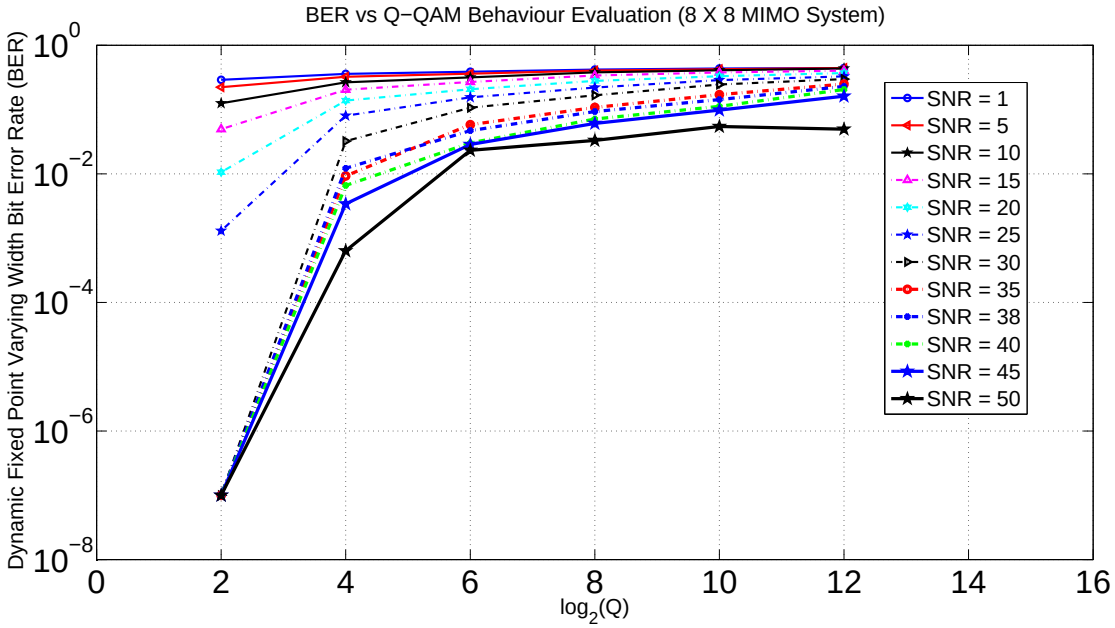

Figure 4.2: Dynamic Bit Width Varying BER Vs Modulation Order (8×8 MIMO System), apropos different SNR channel values.

$$\Delta = \frac{\sum_{snr=1}^{50} |BER_{snr}^{dynamic} - BER_{snr}^{floatingpoint}|^{2}}{N}, \tag{4.1}$$

$$SNR^{N \times 1} = \{1, 5, 10, 15, 20, 25, 30, 35, 38, 40, 45, 50\} \tag{4.2}$$

The performance curves presented in Figure 4.3, 4.4 and 4.5 represents bit error rate, for system models of different antenna dimensions $N_T \times N_T$, configured with modulation order **Q=64,256,1024** respectively. All graphs are on semi-logarithmic scale with bit error rates on vertical logarithmic axis and N_T on horizontal linear axis. Table 4.5 presents degree of deviation for performance of dynamic fixed point version with respect to its floating point counterpart, described in Section 3.4. Each numerical value is defined as average of squared euclidean distance 4.1 and they can be observed to be in orders of 10^{-3} for each system configuration, that may have been resulted from inconsistency of transmitted vectors used in either simulations. This mathematically proves integrity of dynamic fixed point bit width varying algorithm, as it is capable of achieving

Table 4.4: Performance Comparison Table over Modulation Orders

M / N_T	4	16	64	256	1024	4096
8×8	0.0064	0.0025	0.0105	0.0094	0.0148	0.0075
100×100	0.0024	0.0040	0.0065	0.0050	0.0035	0.0023

Where each numerical value represents Δ, the mean square difference over SNR $\in [1,\ 50]$, between bit error rate performance, achieved from Dynamic Fixed Point Varying MIMO Detector and Floating Point MIMO Detector for $N_T \times N_T$ MIMO system, configured with corresponding modulation order, as defined in 4.1.

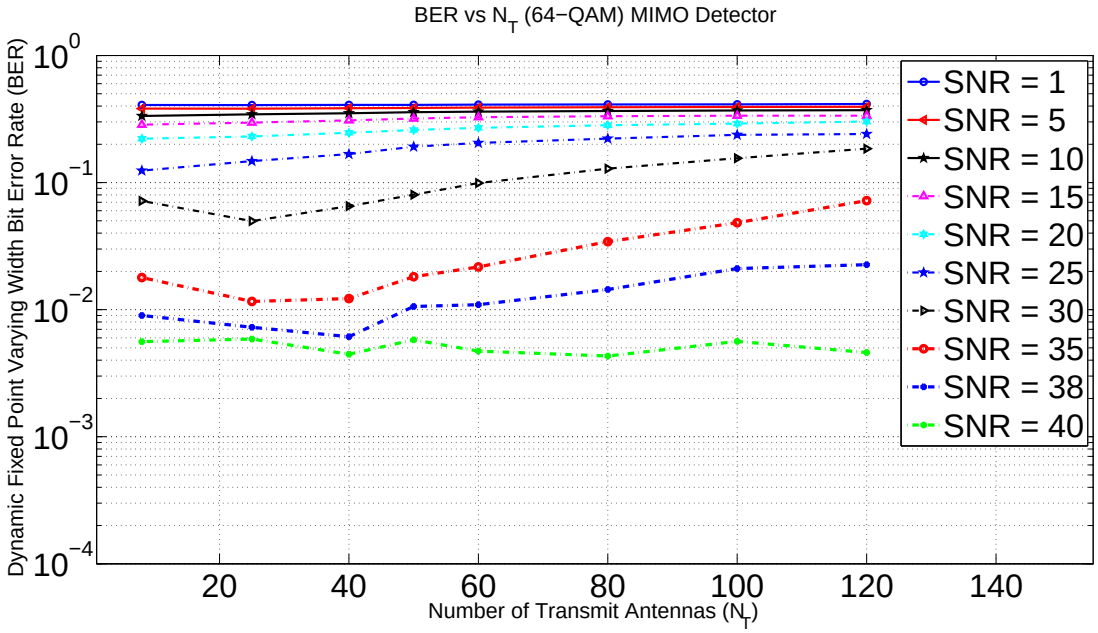

Figure 4.3: 64-QAM Dependency of Dynamic Bit Width Varying BER Vs Antenna Dimensions, apropos of various channel SNR values.

performance in proximity of their corresponding floating point MIMO detectors. Hence analysis of performance behaviour elucidated in Section 3.4.5 can be extended to these graphs as well.

The performance curves presented in Figure 4.6 and 4.7 defines behaviour of bit error rates over second and third system model configurations defined in Table 2.2. Dynamic fixed point version of real domain SE based K-Best algorithm has been evaluated using different K-Best possible

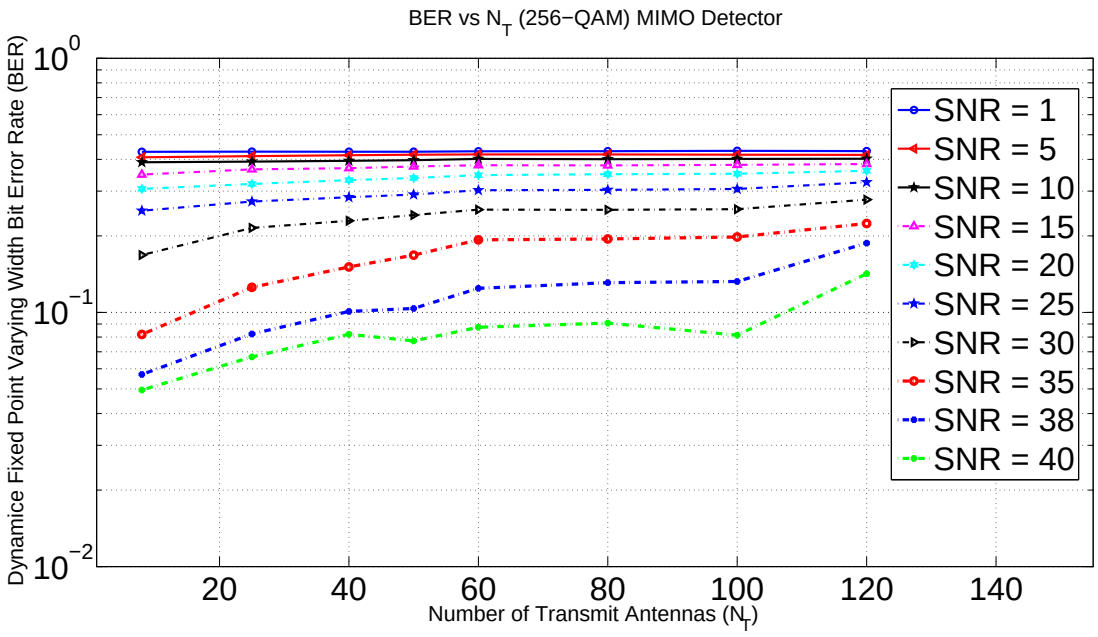

Figure 4.4: 256-QAM Dependency of Dynamic Bit Width Varying BER Vs Antenna Dimensions, apropos of various channel SNR values.

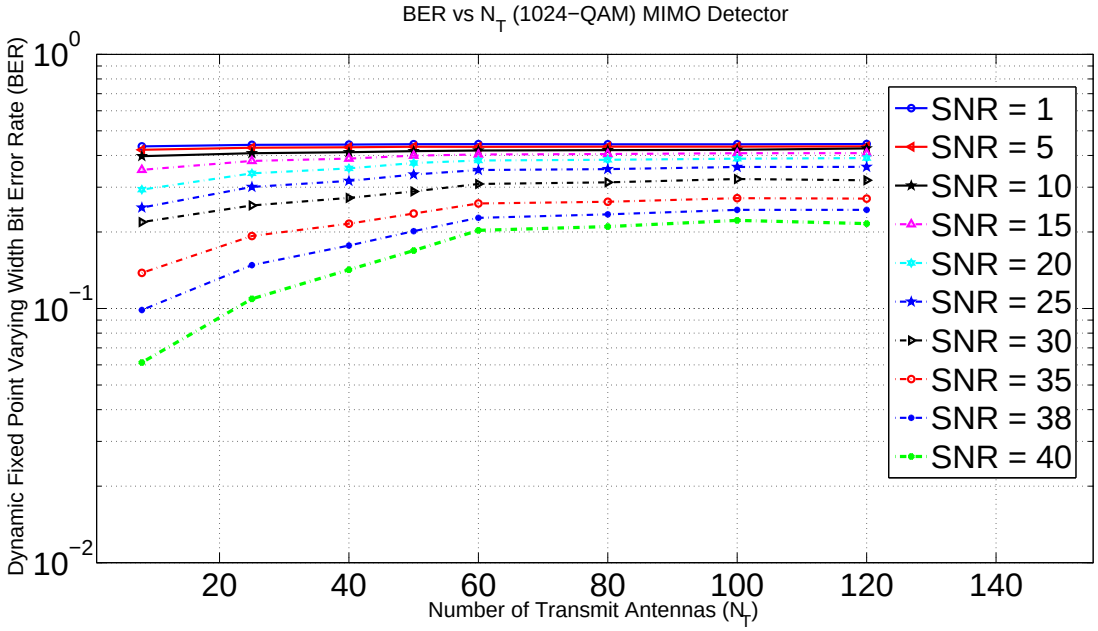

Figure 4.5: 1024-QAM Dependency of Dynamic Bit Width Varying BER Vs Antenna Dimensions, apropos of various channel SNR values.

Table 4.5: Performance Comparison Table over Antenna Dimensions

QAM \ N_T	8	25	40	50	60	80	100	120
64	0.0091	0.0024	0.0029	0.0046	0.0064	0.0021	0.0025	0.0051
256	0.0416	0.0113	0.0497	0.0107	0.0382	0.0080	0.0114	0.0260
1024	0.0187	0.0094	0.0289	0.0253	0.0239	0.0084	0.0333	0.0023

Where each numerical value represents Δ, the mean square difference over SNR $\in [1,\ 50]$, between bit error rate performance, achieved from Dynamic Fixed Point Varying MIMO Detector and Floating Point MIMO Detector for $N_T \times N_T$ MIMO system, configured with corresponding modulation order, as defined in 4.1.

candidates per antenna level. This has been analysed on conventional and massive MIMO systems by utilizing 8×8 and 100×100 system models respectively. Semi-logarithmic scale was used to present these graphs with bit error rate of vertical logarithmic axis and channel SNR values on horizontal linear axis, over different K-Best candidates. Juxtaposing performance curve in Figure 4.6 and 4.7 with Figure 3.4 and (3.5, 3.6) respectively, it can be deduced that dynamic fixed point achieves identical bit error rates with respect to its floating point algorithm. This has also been observed in earlier comparisons between behavioural analysis of bit error rate with different antenna dimensions and modulation orders, over various channel SNR values, defined in 4.2. This clearly determines integrity in detection performance, for integrating dynamic fixed point enhancement to any sequential ordered or tree based MIMO detectors. Thus various benefits of this enhancement defined in Section 4.1.3 can be derived, along with achieving near-equivalent performance, compared to their floating point counterparts.

4.1.3 Benefits & Prevailing Challenges

The main benefit of dynamic fixed point version of real valued SE based K-Best MIMO detector is reduction in number of active registers which gradually increase as we move down estimation tree. This enhancement is scalable to any system model configuration depending on performance requirements and it provides significant impact with respect to its benefits, on high end system

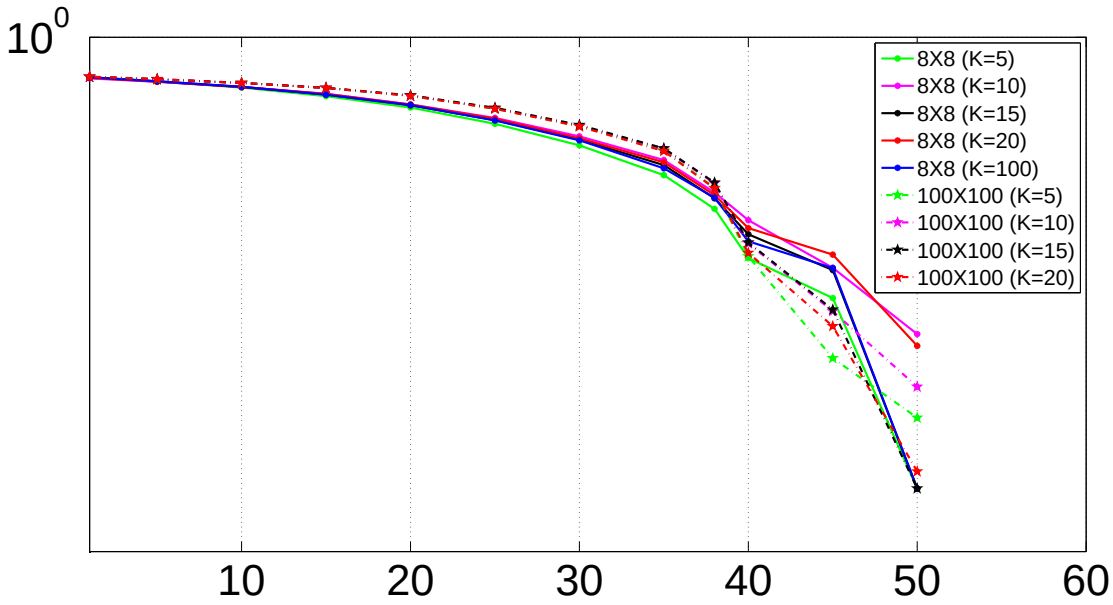

Figure 4.6: 64-QAM Dependency of Dynamic Bit Width Varying BER Vs SNR, apropos different K-Best estimates.

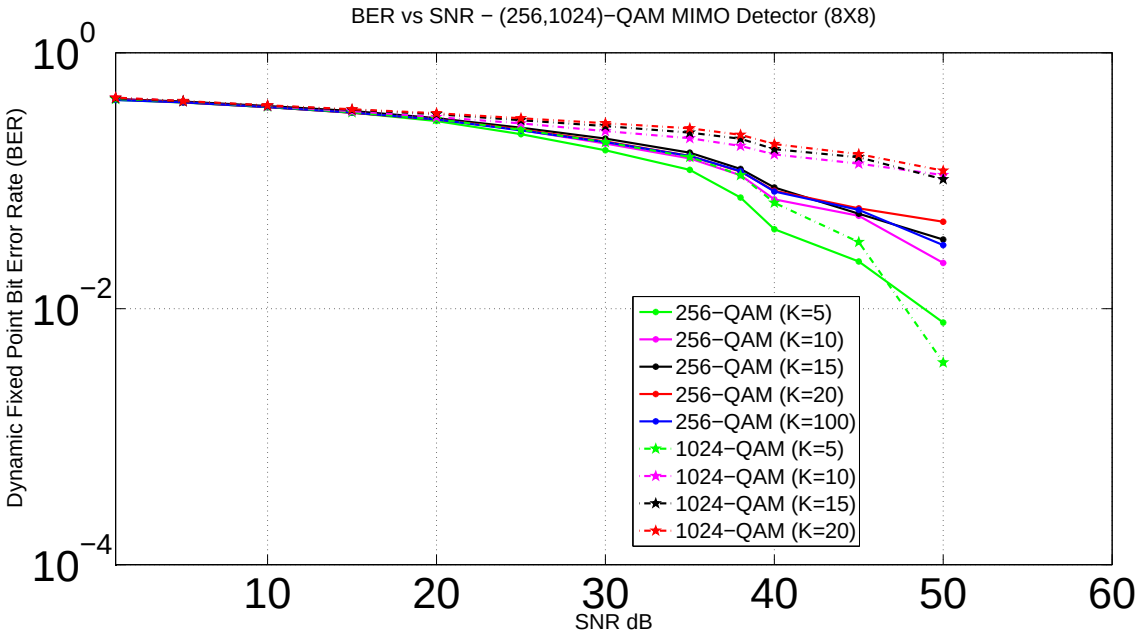

Figure 4.7: 256-QAM & 1024-QAM Dependency of Dynamic Bit Width Varying BER Vs SNR, apropos different K-Best estimates.

models like massive MIMO systems with high modulation order. It can be integrated into any sequential or ordered MIMO detectors, especially with simple clock gating management logic for feed-forward detectors like breadth first search algorithms. It presents high degree of freedom and compatibility due to its capability of dynamic adjustment in bit width limit and custom fixed point bit width, for critical antenna levels.

The main challenge for effectively integration of dynamic nature into fixed point iteration, is to determine least possible bit width limit, that can be scalable for any system model configuration. As presented in previous sub-section, 100×100 massive MIMO system possessed requirement of atleast **15** fractional bits on majority of longest variables in detection algorithm. However, 8×8 supported Bit Width Limit of **10**, to derive performance that can be related to floating point counterpart. Each bit reduction in any fixed point variable can be correlated with turning off flip-flop in register, corresponding to that variable in hardware design. This can be achieved with various modern power reduction techniques such as clock gating. Additional circuitry is required to manage clock gating of registers on various tree levels. The complexity of clock gating circuitry can be higher for non feed-forward MIMO detectors like depth first search sphere decoders, which can be reasoned as follows. High precision is required at initial tree levels of estimation, due to delicate and critical path accumulated error propagation nature of tree algorithms. Huge variations in performance may be observed if such critical segments of algorithm are processed with inadequate precision. Due to additional clock gating circuitry, dynamic fixed point iteration may not be effective for low end system model configurations like 2×2 or 4×4 MIMO systems. Hence reasonable trade-off should be considered between comprehensive power reduction with respect to clock gating and additional complexity introduced with it, besides gaining reasonable performance from dynamic fixed point iteration.

4.2 Design Enhancements in Modified Complex Domain K-Best MIMO Detection Algorithm

In this section, I have described potential enhancements that can be integrated in modified complex valued SE based K-Best algorithm, defined in Section 3.6.1. Two different versions of

enhancements with respect to their complex row enumeration have been proposed and have been elucidated later in this Section. The changes made in enumeration technique can significantly alter detection latency, performance and in few cases, computational complexity of MIMO detector as the same algorithm is iteratively implemented for $K \times N_T$ times, assuming $N_T \times N_R$ MIMO system with K-Best possible candidates on each antenna level. The algorithmic flow of original complex-valued SE based row enumeration is known for its high silicon complexity and hence, modification was proposed in [4], to simplify the procedure associated with complex row enumeration. Computational complexity can be dynamically altered with additional parameter **Rlimit** that corresponds to horizontal width of expansion for determining first child of each parent node in current level. This has been elucidated in Section 3.6.1, along with general computational complexity analysis in Table 3.4.

However, the modification in complex row enumeration introduced constraints in regard to expanding vertical layers within horizontal width **Rlimit**. As elucidated in Section 3.6.3, child nodes on vertical layer that doesn't correspond to first-child are not considered for updating current sorter list. If both real and imaginary parts of transmitted complex symbol are altered in wireless medium, by channel interference and noise amplification, in the manner that neither of them is determined in first-child node of any parent, algorithmic flow of modified row enumeration makes sure that the original transmitted symbol is not expanded or considered into current sorter level for any value of K-Best possible candidates. This occurs because only nodes that exist on perpendicular layers with first-child as intersection node, are expanded with **Rlimit** as width for horizontal layer and **K** for vertical layer. This has been symbolically explained in Section 3.6.3. This inadequate consideration of constellation symbols degrades performance of lattice point search and detection performance for high modulation orders. I have proposed two different enhancements in complex row enumeration that increases probability of expanding transmitted complex symbol in lattice point search. Both versions explore multiple vertical layers across horizontal width **Rlimit**. Additional parameter **LayerLen** indicates number of vertical layers across first-child, that should be considered to build or update current sorter list. The first enhancement explores **LayerLen**

vertical layers, retaining computational complexity. The second enhancement also explores **LayerLen** but it is further instrumental in improving detection performance with moderately higher computational complexity. However the complexity can be dynamically controlled using parameters **LayerLen** and **Rlimit** based on performance requirements. In this section, I have elucidated theory behind either enhancements proposed in this thesis work and presented general complexity analysis along with their implementation results with system model configurations defined in Table 2.2.

4.2.1 Enumeration Design Enhancements

Both enhancements are induced in algorithmic flow of complex valued row enumeration used for determining next child nodes of each parent, for updating current sorter list in K-Best iterations on each antenna level. It introduces additional parameter **LayerLen** that corresponds to expanded vertical layers with respect to nodes across horizontal width **Rlimit**. As elucidated in Section 3.6.1, at initial K-Best iteration for determining first-child of each parent, **Rlimit** nodes are expanded across zero-child. All nodes exist on horizontal axis, implying that they have different real parts s_r and identical imaginary parts s_i of complex constellation symbol $\tilde{s} \in \Omega^{N_T}$.

A $N_T \times N_R$ MIMO system, configured with Q-QAM modulation order transmits N_T complex symbols per frame, where each symbol is modulated using 'Q' constellation points. For every complex symbol $\tilde{s} = s_r + js_i$, there exists exactly $\sqrt{Q} - 1$ complex symbols with either identical real part s_r or imaginary part s_i in constellation. Hence for every zero-child computed, range of possible values of **Rlimit** can be given by $[1,\ \sqrt{Q}]$ and of **LayerLen** is [1, Rlimit]. The computational complexity associated with either enhancements can be dynamically controlled using these additional parameters, as presented in Table 4.6. For any parent node, zero-child and its resulting first-child are computed similar to modified row enumeration defined in Section 3.6.1. However algorithmic flow for selecting next-child nodes and building current sorter list has been enhanced by broadening search along vertical layers, as described below.

4.2.1.1 First Enhancement

Let us assume that complex symbol $\tilde{s}^{\,m} = {s_r}^m + j{s_i}^m$ has been transmitted using any antenna level $m \in (N_T, N_T - 1, ..., 1)$ and using channel information, zero-child $\tilde{zc} = zc_r + jzc_i$ has been computed as defined in 3.5, for any parent node $P_i, i \in (1, 2, ..., K)$. According to initial expansion of child-nodes across zero-child $\tilde{zc}$, **Rlimit** lattice points are expanded by computing their respective path accumulated PED values using 3.6. $\mathbb{S}$ = $\{\tilde{s}^{\,n}, n \in (1, 2, ..., Rlimit)\}$ child-nodes are sorted and corresponding node with lowest PED value, $\tilde{s}^{\,FC} \in \mathbb{S} = \{{s_r}^{FC} + j{s_i}^{FC}\}$ is selected as first-child in initial K-Best iteration. Let us assume $\mathbb{L}$ = $\{\tilde{s}^{\,t} \in \mathbb{S}, t \in (1, 2, ..., LayerLen)\}$ are **LayerLen** child-nodes with lowest PED from $\mathbb{S}$, after sorting. Hence it can also be deduced that $\{\tilde{s}^{\,FC} = \tilde{s}^{\,t}, t = 1\} \in \mathbb{S}, \mathbb{L}$. In modified row enumeration 3.6.1, only, the child nodes on vertical layer $\mathbb{M}^{\,FC}$ corresponding to $\tilde{s}^{\,FC}$ is considered for updating current sorter list. And in successive K-Best iterations, child nodes $\tilde{s} \in \mathbb{M}^{\,FC} = \{{s_r}^{FC} + js_i\}$ that have same real part as first-child node $\tilde{s}^{\,FC}$, are added to current sorter list using row enumeration, defined in Section 3.4.1 for sorting in next iteration, if any predecessor nodes are added to K-Best possible candidates, in that iteration. This enumeration doesn't explore vertical layers $\mathbb{V}^{\,t} \neq \mathbb{V}^{\,FC}, \{t \in (2, ..., LayerLen)\}$ and as a result if first-child $\tilde{s}^{\,FC}$ has both different real and imaginary parts, compared to original transmitted symbol $\tilde{s}^{\,m}$, i.e. if ${s_r}^{FC} \neq {s_r}^m$ and ${s_i}^{FC} \neq {s_i}^m$, then corresponding transmitted point $\tilde{s}^{\,m}$ is not considered into current sorter list and hence not selected as one of K-Best possible candidates for antenna level m.

In first enhancement, in lieu of always expanding the vertical layer $\mathbb{V}^{\,FC}$ in every iteration, vertical layers $\mathbb{V}^{\,t}, t \in (1, 2, ..., LayerLen)$ corresponding to child nodes, that were added to K-Best possible candidates in successive K-Best iterations, are expanded for next iteration for updating current sorter list. Also it is not effective to expand vertical layers for complex symbols, with large PED values that exist over large distance from first-child node $\tilde{s}^{\,FC}$. The limit of vertical layers considered for expansion, is defined by additional parameter **LayerLen**. Hence if $\mathbb{S}$ = $\{\tilde{s}^{\,n}, n \in (1, 2, ..., Rlimit)\}$ are initially expanded for defining first-child node, vertical layers are expanded for $\mathbb{L}$ = $\{\tilde{s}^{\,t} \in \mathbb{S}, t \in (1, 2, ..., LayerLen)\}$ and if any child node from remaining nodes,

$\tilde{s} \in \mathbb{S}, \notin \mathbb{L}$, is added to K-Best candidates, child node from $\mathbb{V}^{FC}$ are expanded. Let us assume $\tilde{s}^{\bar{t}} \in \mathbb{L}, \{\bar{t} \in t = (1, 2, ..., LayerLen)\}$ is added to K-Best possible candidates in second iteration, vertical layer corresponding to $\bar{t}$, i.e. $\mathbb{V}^{\bar{t}}$ is expanded instead of $\mathbb{V}^{FC}$ and next-child computed on that vertical layer, using row enumeration 3.4.1 is added to current sorter list, for next iteration.

The proposed first enhancement broadens the scope of search for original transmitted symbol $\tilde{s}^{m}$, thus increasing detection performance. This also increases probability of detecting complex symbols where ${s_r}^{FC} \neq {s_r}^{m}$ and ${s_i}^{FC} \neq {s_i}^{m}$, by expanding vertical layers $\mathbb{V}^{t}, t \in (1, 2, ..., LayerLen)$. It can de deduced that number of expanded child nodes for selecting K-Best possible candidates on antenna level m, are exactly identical to that of modified complex row enumeration 3.6.1. Hence the proposed first enhancement possibly provides better performance with identical computational complexity and with similarly reduced silicon complexity, compared to original complex SE based row enumeration, as defined in Section 3.5.1.

4.2.1.2 Second Enhancement

The second enhancement constantly fluctuates size of current sorter list by adding one next-child node from all vertical layers $\mathbb{V}^{t}, t \in (1, 2, ..., LayerLen)$, in few K-Best iterations. No vertical layer is expanded till all **Real best nodes** within horizontal width of **LayerLen** are selected as K-Best candidates for that tree level. Once all **LayerLen** nodes are selected, imaginary best node corresponding to each real best node is computed and **LayerLen** nodes are replaced by their successive next child nodes. This increases the probability of selecting more number of real best nodes, compared to imaginary best nodes along vertical layers, resolving the condition in relation to favourable expansion of imaginary nodes, observed in modified complex enumeration. Let us assume $\mathbb{S}$ = $\{\tilde{s}^{n}, n \in (1, 2, ..., Rlimit)\}$ are initially expanded for defining first-child node, and $\tilde{s}^{\bar{t}} \in \mathbb{L}, \{\bar{t} \in t = (1, 2, ..., LayerLen)\}$ is added to K-Best possible candidates in any successive iteration, then all vertical layers $\mathbb{V}^{t}, \{t \in (1, 2, ..., LayerLen)\}$ corresponding to $\mathbb{L}$ = $\{\tilde{s}^{t}, t \in (1, 2, ..., LayerLen)\}$ are expanded instead of only $\mathbb{V}^{FC}$ as in modified complex row enumeration 3.6.1 or $\mathbb{V}^{\bar{t}}$ as in the first enhancement, elucidated above. As a result, for each predecessor node that is added to K-Best possible candidates, next-child is individually computed on all vertical

layers, using row enumeration 3.4.1 and **LayerLen** child nodes are added to current sorter list, for next iteration. This enhancement has the potential to resolve conditions related to expansion of child nodes, diagonal to FC and favourable expansion of imaginary best nodes, than real best nodes.

The proposed second enhancement also broadens the scope of search along all vertical layers $\mathbb{V}^t, t \in (1, 2, ..., LayerLen)$ uniformly, intelligently expanding reasonable number of child nodes with similar silicon complexity as 3.6.1 and 4.2.1.1. Uniform enumeration across all vertical layers further increases detection performance, compared to proposed first enhancement, at the expense of higher computational complexity in the former. The general complexity analysis of either enhancements and the implementation results for first enhancement, have been presented in this section.

4.2.2 General Complexity Analysis

Computational complexity can be dynamically controlled by additional parameters introduced with the modifications **Rlimit** and **LayerLen**, that corresponds to horizontal width and vertical layers respectively. The first proposed enhancement retains computational complexity of modified complex row enumeration $(Rlimit + 1) \times K) \times N_T$ and corresponding general complexity analysis has been given in Table 3.4. However the second proposed enhancement for modified complex row enumeration, utilizes **LayerLen** to tune trade-off between computational complexity and detection performance, and corresponding complexity can be given by $\{[(Rlimit + 1) \times K] + [\left\lceil \frac{K - LayerLen}{LayerLen} \right\rceil \times LayerLen]\} \times N_T$. The general complexity analysis of either enhancements, comparing Maximum Likelihood and original complex valued conventional K-Best algorithms have been provided in Table 4.6

4.2.3 Fixed Point Iteration

Either of proposed enhancements were implemented using MATLAB with variables using default floating point representation with word length of 64 bits. Fixed point iteration has been utilized, as defined in Section 3.4.4, to avoid unnecessary area and power consumption, associated

Table 4.6: Enhanced Complex Valued SE Based K-Best General Complexity Analysis

MIMO Detection Algorithm	Worst Case Complexity	256-QAM, K=5 (Model 1)	1024-QAM, K=5 (Model 2)
ML	Q^{N_T}	256^{100}	1024^{100}
Conventional K-Best [18]	$Q \times K \times N_T$	128000	512000
First Version of Enhancement	$(Rlimit + 1) \times K \times N_T$	**3000**	**3000**
Second Version of Enhancement	$\{[(Rlimit+1) \times K] + [\lceil \frac{K-LayerLen}{LayerLen} \rceil \times LayerLen]\} \times N_T$	**3000**	**3000**

Where 'Q' represents modulation order, $N_T = 100$ in Model examples 1 & 2, 'K' represents K-Best possible estimates at each tree level and **Rlimit = 5**, **LayerLen = 5** represents horizontal width for first child estimation and vertical layers expanded respectively.

with corresponding hardware design implementation. Fixed point arithmetic has been integrated to algorithmic flow of MIMO detector using 3.3 and 3.4. After extensive simulations, the fractional bit width of each intrinsic variable was placed at least possible width, to imitate performance of floating point representation. Dynamic fixed point iteration, defined in Section 4.1.1 has been implemented for real domain detector. It can be easily extended to either enhanced versions, defined in 4.2.1.1 and 4.2.1.2, to further reduce power consumption, as elucidated in 4.1.1.

Both enhanced versions of modified complex domain SE based K-Best MIMO detectors were extensively simulated and selected fractional bit width and word lengths of major variables have been defined in Table 4.7

4.2.4 Implementation Results

The drawbacks of modified complex row enumeration were addressed and enhancements have been proposed in Section 4.2.1.1 and 4.2.1.2. Complex MIMO detector described in Section 4.2.1.1 has been evaluated and corresponding performance results have been presented in this section. The behaviour of bit error rate with respect to different modulation orders have been stud-

Table 4.7: Fixed Point Bit Width for Enhanced Complex Domain

Attribute	**Fractional Bit Width**	**Fixed Point Bit Width**
Received Vector ($\tilde{Y}$)	25	30
Channel Matrix ($\tilde{H}$)	25	30
Upper Triangular Matrix ($\tilde{R}$)	25	30
Noise (σ)	9	9
Modulation Order 'Q'	0	5
Noise vector ($\tilde{n}$)	25	30
K-Best value	0	0
LLR	7	12

Where **Fixed Point Bit Width** represents word length of each variable and **Fractional Bit Width** represents number of fractional bits assigned.

ied and their resultant curves have been presented for different channel SNR values as shown in Figure 4.8 and Figure 4.9. The bit error rate was derived by standalone MIMO detector. However the Log Likelihood ratio values of each bit in soft output can be computed sequentially and can be processed with iterative decoders to significantly improve the resultant bit error rate.

The first enhancement considers incomplete expansion of child nodes into account and selects child nodes from all vertical layers as elucidated in Section 4.2.1.1. While the performance behaviour with respect to each modulation order is identical to previously explored algorithms and slightly better than modified complex detector, it derives higher bit error rate at higher channel SNR values, compared to real domain detector. This can be correlated to pre-existing complication that has been discussed in Section 3.6.5, pertaining to inclination of expanding most of the **imaginary best nodes** before expanding atleast one **real best node** of the first child corresponding to any parent node. This defect in complex row enumeration blocks detection algorithm to achieve much lower bit error ratio during transmission through high SNR channel. Hence further enhancements are required to halt expansion of unnecessary **imaginary best nodes**, thereby forcing atleast surrounding **real best nodes** around first child, to get selected into current sorter list. This analysis determines that ideal complex row enumeration would imitate expansion nature of original complex domain row enumeration [3], but with lower silicon complexity.

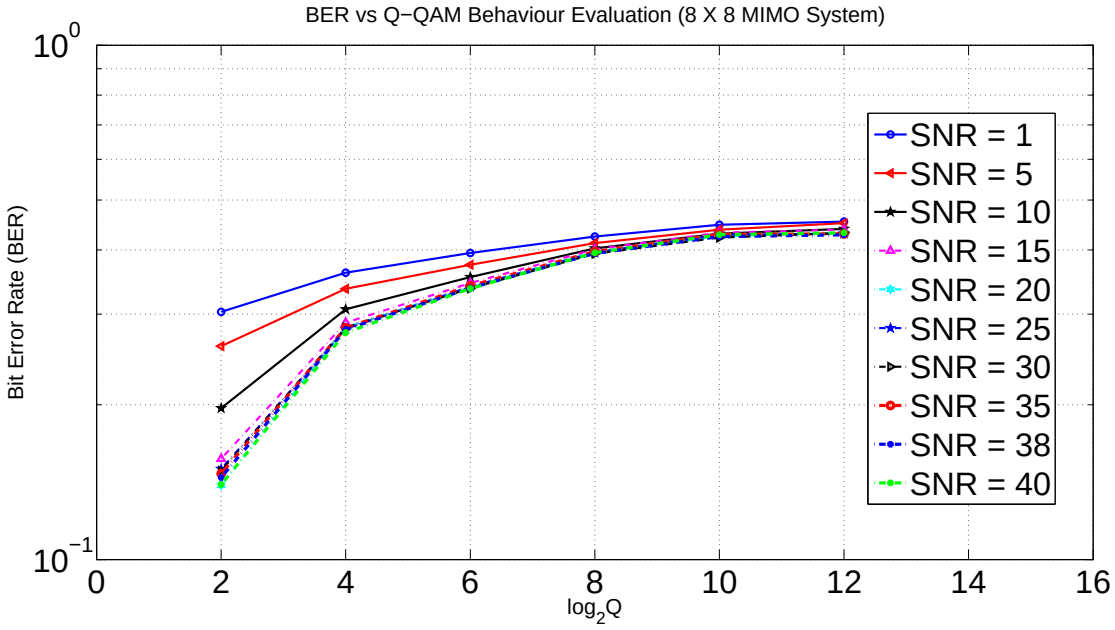

Figure 4.8: BER Vs Modulation Order (8×8 MIMO System), apropos different SNR channel values.

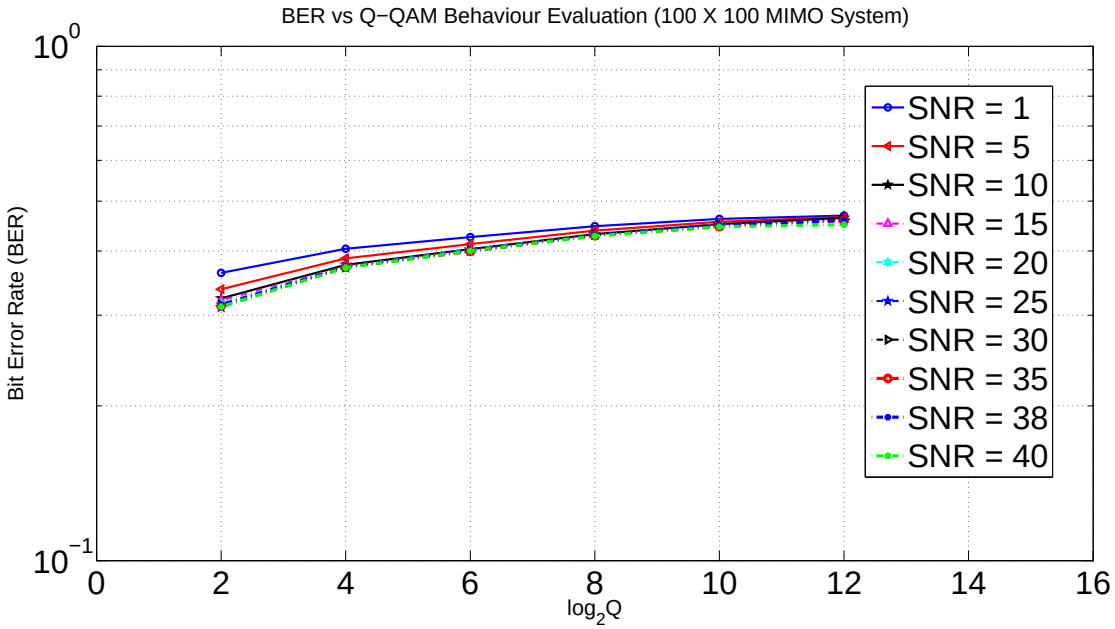

Figure 4.9: BER Vs Modulation Order (100×100 MIMO System), apropos different SNR channel values.

4.2.5 Benefits & Prevailing Challenges

All benefits of modified complex valued SE based K-Best algorithm, defined in Section 3.6.3 can be extended to either enhancements, besides those, elucidated in this section. The proposed enhancements broadens the intelligent expansion of child nodes during lattice point search, increasing probability of estimating transmitted symbol, accurately, on each antenna level. The major benefit of either enhancements would be reduced silicon complexity for estimated best next child nodes on each antenna tree level. Moreover computational complexity can be dynamically controlled using **LayerLen**, **Rlimit** depending on complexity of system model configuration. Massive MIMO systems with high modulation order {**Q =** 2^N**, N = 8, 10, 12**} may require higher values of these additional parameters to achieve detection performance required by communication systems. However Massive MIMO systems with lower modulation order {**Q =** 2^N**, N = 2, 4, 6**} and conventional MIMO systems can exhibit appreciable performance with lower parameter values, thus reducing computational complexity and resulting power consumption. MIMO detectors corresponding to either of enhancements, can be integrated with pre-processing techniques such as QR Decomposition [13], Lattice Reduction [12] as elucidated in Section 2.1.1. Sequential processing of tree levels can be utilized to design pipelined hardware architecture, representing each antenna level into one pipeline stage. The overall detection latency of MIMO detector can be decreased by processing and forwarding of each K-Best candidate on any tree level, without waiting for estimating all K-Best candidates on current level. Complex detectors are compatible with broad range of constellations like Gaussian, star, rectangular and non-rectangular [19], thus making them promising alternative for above constellation dependent practical communication systems, especially for Line Of Sight applications. Most importantly, due to sequential ordering detection, dynamic fixed point iterative technique, defined in Section 4.1.1 can be integrated into MIMO detectors with either enhancements, for efficient hardware design in regard to corresponding area and power consumption.

If real and imaginary parts of constellation symbols are completely uncorrelated, real valued detectors outperform complex valued counterparts due to redundant channel information from real value decomposition of complex channel matrix $\tilde{H}$. Though modified and enhanced complex

valued MIMO detectors relatively have low silicon complexity than original complex valued algorithms, it is possible at expense of degraded performance for massive MIMO systems with high modulation order. The major challenge would be to determine efficient and least possible values for additional parameters **LayerLen**, **Rlimit** and **K**, to decrease computational complexity and also to achieve detection performance required by applications. Selection of larger values unnecessarily expands higher number of child nodes, and selecting smaller values may result in inadequate expansion of child nodes, for estimating transmitted symbol vector. As described in Section 3.6.7, determining appropriate values for such parameters, on various system model configurations can be achieved with Lookup Tables (LUT) or additional pre-processing learning algorithms, integrated into detector. Though complex detectors are applicable for non-rectangular constellation configured MIMO system models, designing pipelined hardware architecture is very challenging due to necessity of various advanced signal processing techniques, for processing transmitted unsymmetrical symbols.

5. CONCLUSION

Different low power MIMO detectors, efficacious on massive MIMO systems with/or high modulation order have been explored in this research work. Initially mandatory technological introductions have been discussed, presenting the thesis outline. Different elementary MIMO detectors with performance categorization has been studied along with simulation tools and experimental framework utilized in this work. Section 3.4 explored Real domain SE based K-Best algorithm [17] and corresponding results were generated using various system models, defined in Table 2.2. Dynamic fixed point bit width varying version of real domain detector was proposed in Section 4.1.1 and resultant performance was juxtaposed with original floating point counterpart, by presenting implementation graphs and by computing average squared euclidean distance between $BER_{dynamic}$ and $BER_{floatingpoint}$ over different channel SNR values, defined in 4.2. The possible benefits for dynamic fixed point enhancement has been clearly elucidated in Section 4.1.3. The proposed dynamic fixed point enhancement can be extended to any sequential processing detection algorithm including all versions of Complex Domain SE based K-Best algorithms explored and proposed in this research.

Section 3.5 explored theory for original work on Complex Domain SE based K-Best algorithm [17]. Advantages and possible modifications have been reported in Section 3.5.3, that have been explored in Section 3.6.1. Based on enumeration design analysis, enhancements have been proposed in Section 4.2.1.1 and 4.2.1.2 and their implementational results have been presented. For any MIMO system model configuration, performance of all detectors explored and proposed in this research work are ordering based on their bit error rate performance in Table 5.1. The general complexity analysis of all explored and proposed algorithms have been discussed in their corresponding sections.

Table 5.1: MIMO Detection Algorithms Performance Ordering

ML	$>$	Original Real Domain K-Best SE Based MIMO Detector [17] [5]
	$\geq$	Dynamic Fixed Point Real Domain MIMO Detector (Proposed in Section 4.1.1)
	$\geq$	Original Complex Domain MIMO Detector [3] [5]
	$\geq$	Improved Complex Domain MIMO Detector (Proposed in 4.2.1.1 and $4.2.1.2^{\star}$)
	$\geq$	Modified Complex Domain MIMO Detector [4]

Where ML represents maximum likelihood optimal detection performance and $\star$ refers to detection algorithms that have been proposed in this research work but their performance hasn't been evaluated yet. They have been included in this ordering based on theoretical analysis of their detection algorithms

5.1 Comprehensive Analysis

All sequentially processed MIMO detectors that have been explored, can be designed with pipelined architecture, resulting in reduced comprehensive latency. In the event of transmission with rectangular constellation systems, Real domain detectors are expected to outperform their Complex domain counterparts, due to availability of extra redundancy in channel response matrix H, generated from real value decomposition of complex channel response matrix $\tilde{H}$. This can be observed only if real and imaginary part of complex constellation symbols are completely uncorrelated. It has been reflected in implementation results presented for Real domain SE based K-Best algorithm and its corresponding complex counterpart. However Complex domain detectors establishes their authority in flexibility of selecting different constellations like Gaussian, star or non-rectangular systems with unsymmetrical and non circular complex symbols [19], where real and imaginary parts are correlated. But it requires complex valued computations intricate signal processing techniques, that results in high computational complexity for designing efficient hardware architecture. The analysis behind performance curves have been presented in their respective sections and possible enhancements for improving bit error rate has also been discussed.

Dynamic fixed point Real domain SE based K-Best MIMO detector, proposed in this work, achieves near-equivalent performance to that of floating point version [17], but with reduced comprehensive active register count. Hence inactive registers can be turned off using modern power

reduction techniques such as clock gating, that has been discussed briefly in Section 5.2.1. The proposed real domain pipelined architecture can be extended to dynamic fixed point bit width varying version by integrating additional clock gating enable signals, to turn off corresponding flip-flops, as processing goes into deeper pipelined levels in MIMO detector architecture. Also certain sub-blocks used for designing real domain architecture in [17] and [5] can be extended, with minimal modifications, to implement original complex domain MIMO detector as it differs only in Complex row enumeration technique, compared to Real domain counterpart. Since there exists no detailed design and study of efficient pipelined hardware architecture for original Complex domain SE based K-Best algorithm, explored in Section 3.5, it can be explored as potential and interesting extension to this research. The pipelined architecture for Real domain SE based K-Best algorithm, explored in Section 3.4 has been proposed all inclusive, in [5] and [17].

5.2 Possible Future Work

The performance evaluation in this research was performed assuming MIMO detector as a standalone algorithm. The bit error rate can be significantly decreased if MIMO detector is connected to decoding system such as LDPC decoder. As elucidated in Section 1.5, each of K-Best possible estimate vectors $\tilde{Z}_i, \in \mathbb{C}^{N_T \times 1}$ $\{i = 1, 2, ..., K\}$ are taken into account, one at a time, for computing Log Likelihood Ratio values and forwarding them sequentially to decoding systems. Hence LLR values corresponding to each estimated soft output $\tilde{Z}_i$ is processed through iterations between variable nodes and check nodes until parity check equation utilized to construct the transmitted LDPC codewords is satisfied. The elaborated functionality of decoding iterations in Section 1.5 provides fundamental knowledge of algorithmic flow for LDPC system. Standalone MIMO detection algorithms that were explored and proposed in this work, can be integrated with fully parallel LDPC decoding system, as potential developments of this research work. Finally in this section, from the perspective of hardware design, I have presented a brief outline of potential practical developments for implementing dynamic fixed point bit varying real domain algorithm, by using modern power reduction techniques such as clock gating that can be utilized to integrate with existing real domain SE based K-Best pipelined architecture, proposed in [17].

5.2.1 Clock Gating Enhancements

The theory of dynamic fixed point bit width varying technique has been proposed in Section 4.1.1 and corresponding results have been presented. The performance proved to be near-equivalent to that of floating point version, with difference in the orders of 10^{-3}, computed per 4.1. The average of squared euclidean distance across SNR values 4.2 has been presented in Table 4.4 and Table 4.5, evaluating this enhancement apropos modulation order and antenna dimension respectively. The ideal next development would be to integrate this technique into existing pipelined hardware architecture for real domain detector ([5], [17]).

Let us assume 100×100 massive MIMO system configured with modulation order Q-QAM. As presented in Table 4.2, bit width of major internal variables at level $2N_T = 200$ is experimentally determined to be 25, and it is gradually decreased as processing moves down the search tree. Variable $\tilde{H}$ is required to be stored in 25-Bit register, in hardware. All 25-Bits will be accessed for execution of instruction during processing of level $2N_T = 200$. In next pipelined stage, only 24 active bits are required as bit width. Starting from 190^{th} antenna level, 15 active bits are adequate, thereby reducing $[190 \times (25 - 15)] + \{\sum_{i=0}^{15} i \ \ \} = 2200$ Bits all-inclusive for each variable, thus decreasing significant hardware area and power consumption. For $N_T \times N_T$ MIMO system, if Original Fractional Bit Width, defined in Table 4.2 is determined to be 'K' and Bit Width Limit is defined as 'L', then corresponding area and power reduction can be associated with inactive bits and general expression for inactive bits N_A all-inclusive for each variable, throughout the MIMO detector can be given as 5.1.

$$N_A = [(N_T + L - K) \times (K - L)] + \sum_{i=0}^{L} i \tag{5.1}$$

Modern power techniques like clock gating or additional enable signals can be used to reduce dynamic power dissipation by pruning N_A inactive bits to avoid unnecessary switching activity. Increasing N_A can result in more power reduction than area, due to high number of lattice search processing iterations required to estimate K-Best candidates on each antenna level. Simple gating

controller can be integrated externally with MIMO detector to maintain an account of inactive bits on current level for each variable.

REFERENCES

[1] B. Halak, M. El-Hajjar, O. H. Toma, and Z. Cheng, "Energy-efficient hardware implementation of an lr-aided k-best mimo decoder for 5g networks," *Journal of Low Power Electronics and Applications*, vol. 6, no. 3, p. 12, 2016.

[2] M. Shabany, D. Patel, M. Milicevic, M. Mahdavi, and P. G. Gulak, "A 70 pj/b configurable 64-qam soft mimo detector," *Integration*, 2018.

[3] M. Shabany, *VLSI Implementation of Digital Signal Processing Algorithms for MIMO/SISO Systems*. PhD thesis, 2009.

[4] M. Rahman, E. Rohani, and G. S. Choi, "An iterative soft decision based adaptive k-best decoder without snr estimation," in *Signals, Systems and Computers, 2014 48th Asilomar Conference on*, pp. 1016–1020, IEEE, 2014.

[5] D. Patel, *VLSI Implementation of Digital Signal Processing Algorithms for MIMO Detection and Channel Pre-Processing*. PhD thesis, 2010.

[6] R. Dash, *VLSI Implementation of Low Power Reconfigurable MIMO Detector*. PhD thesis, 2009.

[7] A. Salvekar, S. Sandhu, Q. Li, M.-A. Vuong, and X. Qian, "Multiple-antenna technology in wimax systems.," *Intel Technology Journal*, vol. 8, no. 3, 2004.

[8] I. L. S. Committee *et al.*, "Ieee standard for local and metropolitan area networks part 16: Air interface for fixed broadband wireless access systems," *IEEE Std 802.16ˆ< TM>-2004*, 2004.

[9] L. Miles and S. Whitaker, "Low-density parity-check (ldpc) encoder," June 2 2009. US Patent 7,543,212.

[10] T. L. Narasimhan, P. Raviteja, and A. Chockalingam, "Large-scale multiuser sm-mimo versus massive mimo," in *2014 Information Theory and Applications Workshop (ITA)*, pp. 1–9, IEEE, 2014.

[11] S. Tanno, T. Nishimura, T. Ohgane, and Y. Ogawa, "A comparison of serial and parallel llr updates for ldpc coded massive mimo detection with belief propagation," in *Information Theory and Its Applications (ISITA), 2016 International Symposium on*, pp. 473–477, IEEE, 2016.

[12] H. Yao and G. W. Wornell, "Lattice-reduction-aided detectors for mimo communication systems," in *Global Telecommunications Conference, 2002. GLOBECOM'02. IEEE*, vol. 1, pp. 424–428, IEEE, 2002.

[13] H. Lee, H. Kim, M. Cho, and J. Kim, "Low-latency implementation of cordic-based sorted qr decomposition for high-speed mimo-ofdm system," in *Radioelektronika (RADIOELEKTRONIKA), 2018 28th International Conference*, pp. 1–4, IEEE, 2018.

[14] M. Rahman and G. S. Choi, *K-Best Decoders for 5G+ Wireless Communication*. Springer, 2017.

[15] R. Penrose, "A generalized inverse for matrices," in *Mathematical proceedings of the Cambridge philosophical society*, vol. 51, pp. 406–413, Cambridge University Press, 1955.

[16] U. Fincke and M. Pohst, "Improved methods for calculating vectors of short length in a lattice, including a complexity analysis," *Mathematics of computation*, vol. 44, no. 170, pp. 463–471, 1985.

[17] M. Shabany and P. G. Gulak, "A 675 mbps, 4×4 64-qam k-best mimo detector in 0.13 μm cmos," *IEEE transactions on very large scale integration (VLSI) systems*, vol. 20, no. 1, pp. 135–147, 2012.

[18] M. Shabany and P. G. Gulak, "The application of lattice-reduction to the k-best algorithm for near-optimal mimo detection," in *Circuits and Systems, 2008. ISCAS 2008. IEEE International Symposium on*, pp. 316–319, IEEE, 2008.

[19] S. Yang and L. Hanzo, "Fifty years of mimo detection: The road to large-scale mimos," *IEEE Communications Surveys & Tutorials*, vol. 17, no. 4, pp. 1941–1988, 2015.

[20] I. Nevat, G. W. Peters, and J. Yuan, "Detection of gaussian constellations in mimo systems under imperfect csi," *IEEE Transactions on Communications*, vol. 58, no. 4, 2010.

[21] X. Dong, T. T. Tjhung, and F. Adachi, "Error probability analysis for 16 star-qam in frequency-selective rician fading with diversity reception," *IEEE Trans. Veh. Technol*, vol. 47, no. 3, pp. 924–935, 1998.

[22] F. Steiner and G. Böcherer, "Comparison of geometric and probabilistic shaping with application to atsc 3.0," in *SCC 2017; 11th International ITG Conference on Systems, Communications and Coding; Proceedings of*, pp. 1–6, VDE, 2017.

[23] T. Adali, P. J. Schreier, and L. L. Scharf, "Complex-valued signal processing: The proper way to deal with impropriety," *IEEE Transactions on Signal Processing*, vol. 59, no. 11, pp. 5101–5125, 2011.